A Study of Ultraviolet Radiation Effects on Porcine Crystalline Lens and Development of a New Assay Methodology for UV Cataractogenesis Investigation

by

Olanrewaju Matthew Oriowo

A thesis

Presented to the University of Waterloo

in fulfillment of the

thesis requirement for the degree of

Doctor of Philosophy

in

Vision Science

Waterloo, Ontario, Canada, 2000

The University of Waterloo requires the signatures of all persons using or photocopying this thesis. Please sign below, and give address and date.

ABSTRACT

Four aspects of ultraviolet radiation (UVR) induced cataractogenesis were studied. Firstly, the suitability of porcine lens for organ culture study and the feasibility of using two fluorescent dyes (alamarBlue™ and 5-carboxyfluorescein diacetate-acetoxymethyl ester [CFDA-AM]) for *in vitro* UVR-lens study were examined. Secondly, because there were no available data for whole lens *in vitro* UVR threshold investigation, an experiment was conducted to determine the *in vitro* action spectrum for UVR-lens photodamage with a secondary purpose of assessing the recovery pattern in the exposed lenses. The third set of experiments investigated the efficacy of the two assay dyes (alamarBlue™ and CFDA-AM) to quantitatively determine the broadband UVB and UVA *in vitro* thresholds for impairing lens cellular function. Simulating environmental conditions, the fourth objective was to investigate the synergy of sub-solar low level UVB and UVA exposures in compromising lens integrity.

In all experiments, aseptically dissected porcine lenses were preincubated in organ culture for approximately one week. Addressing the first objective, the two dyes were assayed together. The lenses were immersed in the assay medium for fluorescence measurements at predetermined intervals over a period of 8 weeks. The assay results were validated with a scanning laser system that measured the optical quality of the same set of lenses. It was shown that porcine lenses can be cultured for at least 6 weeks without any compromise in cellular and optical integrity and that the two fluorescent indicator dyes are not toxic to the cultured lenses.

The *in vitro* action spectrum for UVR wavelengths from 270 nm to 370 nm was determined by subjecting cultured porcine lenses to varying UV radiant exposure levels at

defined wavelengths. The action spectrum was derived with probit analysis of the data using an ascending/descending staircase method for dose determination at each waveband. In terms of repair, the data indicate shorter latency periods and slower recovery for higher UV energy levels, while the reverse is the case for lower UV energy levels. However, this observation is wavelength dependent. The damage and repair data demonstrate that at twice the threshold levels, permanent damage occurs for both UVB and UVA wavelengths.

The results from exposures involving UVB alone, UVA alone, and UVA and UVB in combination, show that exposure to low levels of UVB and moderately high levels of UVA can cause metabolic stress in the crystalline lens by inhibiting the lens epithelial cells' mitochondrial function and disrupting membrane integrity. The synergism study shows that subthreshold levels of UVB and UVA exposures acting together can cause decreased lens cellular metabolism and increased permeabilisation of lens epithelial and fibre cell membranes, triggering glutathione (GSH) depletion in the lens. These UV phototoxic events would render the lens epithelium incapable of regulating ions and water homeostasis, thereby causing lens swelling and opacity. Evaluation of the morphological changes showed that UVB irradiation caused "spoke like" equatorial opacity while UVA irradiation caused reversible anterior subcapsular vacuoles at almost 100 times the UVB exposure level.

ACKNOWLEDGMENT

Now the "light" at the end of the tunnel is clearer. I thank God. I will ever remain grateful to my supervisors and mentors, Drs. Anthony P. Cullen and B. Ralph Chou, for their great insight, optimism, encouragement, confidence, advice and total support throughout this PhD research endeavour. It has been an adventure. Their enthusiasm and communication right from 1986 when I first wrote to Dr. Cullen expressing interest in graduate research training have been a great impetus to me. My humble and sincerest thanks to Dr. Jacob G. Sivak for his encouragement and valuable input and support, especially his generosity with laboratory facility, and as a member of my thesis advisory committee. He is also a key mentor in my research career. Heartfelt thanks to Dr. Niels C. Bols for granting me access to his laboratory facility and introducing me to cell biology, and to Dr. Kristin Schirmer (I say "Danke") for her help in my exploration of fluorometry and bioassay techniques as components of my PhD projects. Thanks also to Liz Hekkila and other members of the Bols' Lab. I am thankful to Drs. Paul O. Ogbuehi, Dan D. Sheni and Olalekan A. Oduntan who in the mid 1980s encouraged my interest and potential to pursue postgraduate studies. In my quest for research training, I was fortunate to spend a brief time with Distinguished Emeritus Professor Donald G. Pitts at the University of Houston College of Optometry, Texas, (USA) just before his retirement, and I sincerely thank him for his unflinching encouragement and advice throughout graduate school. He constantly communicated from his home in Tulsa, Oklahoma, USA, and expressed optimism about my research interest and pursuit. I thank Dr. John R. Trevithick for agreeing to be my thesis external examiner.

I am also thankful to Drs. William R. Bobier, Murchinson G. Callender, John G. Flanagan, Trefford L. Simpson and Jeffrey K Hovis. My deep appreciation also to Drs. William M. Lyle and Rodger Pace, Mrs. Debbie Clermont, Dr. Marlee Spafford, Mrs. Sharon Dahmer, Mrs Alison Zorian, Sue Morton, Liz Reidt, Marie Amodeo, and all School of Optometry administrative, library and clinic staff for their individual help. Thanks also to Ms. Erin Harvey, Dr. David Matthews of UW Statistics Consulting Services, for their help with statistical analyses, and Jack Cooper, Colin Campbell and Andrea Chappell of UW Information Systems and Technology for their individual help with mathematical and statistical softwares for my data analyses.

I would also like to express deep appreciation to the University of Waterloo for supporting me with Graduate Scholarships, the foreign student fee waivers (nine terms), and International Graduate Student Scholarships during this endeavour. I thank the School of Optometry Graduate and Research Committee for the several encouraging awards, particularly the 1997/98 H. Winston Algate graduate scholarship. I gratefully acknowledge the grant-in-aid-of research award from the USA National Academy of Sciences, through the Sigma Xi Scientific Research Society in 1997. Further financial support from the University of Waterloo and the Ontario Government in forms of the Ontario Graduate Scholarship for Science and Technology 1998/99, and the prestigious Ontario Graduate Scholarship 1999/2000 is gratefully appreciated. I also thank the Awards Committee of Canadian Optometric Education Trust Fund for the 1999 research grant, which was a significant boost to my research efforts.

Deepest appreciation to my wife OluMayowa Roseline, and my daughter Fogofoluwa Glory for their love, endurance and support through the course of this study.

Gratitude to my parents especially my mother Mrs. Adunola Rachel Oriowo, my uncle Mr. Olu Fatoyinbo, my late great aunt Madam Dorcas Oni, and my late grandmother madam Mariani Ajayi Fatoyinbo who all contributed their best for my early childhood education, particularly attending high school. My gratitude also to Mr. Olagunju Arowosegbe of Lagos; Mr. Dotun Okubajo of Houston, Texas; Mr. Barry Fox (Kitchener); Mr. James Mason (Waterloo); Drs. Peter Oyakhire (Atlanta), Glenn Holzman (Springdale, Arkansas), and George Campion (St. Catharines); Brad and Darlene Bell, John and Loron Pellowe, the Dobsons, the Bustards and many other members of the Waterloo Pentecostal Assembly too many to name.

My sincere thanks to Messrs. Robin Jones, Andrew Nowinski, Andy Lankin and Chris Mathers for their assistance in technical and computer matters. I am grateful to the staff of Heidelberg Meats & Deli Ltd (Mrs. Doris Hueftlein, Messrs. Heinze Hueftlein and Ron Weiland) for generously providing the pig eyes. I thank Corrine Motluk, a former lab mate in Dr. Cullen's lab, all my friends and all graduate student colleagues. Special thanks to Mrs. Kelley L. Moran (Dr. Sivak's Lab) for her kind assistance with time, advice and lab facility. Thanks also to Drs. Bruce Greenberg and Chris Marwood for the use of their spectroradiometer. Forever, I am most grateful to the almighty God, the alpha and omega who blessed me with so many kind people and with the grace to complete this greatly challenging PhD adventure. To God be all the glory and honour in Jesus name.

TABLES OF CONTENTS

LIST OF TABLES

LIST OF FIGURES

LIST OF ABBREVIATIONS

AB	alamarBlue™
ACGIH	American Conference of Governmental Industrial Hygienists
ATP	Adenosinetriphosphate
ATPase	Adenosinetriphosphatase
CFDA-AM	5-Carboxyfluoroscein diacetate-acetoxymethyl ester
CIE	Commission Internationale de l'Eclairage
DMSO	Dimethyl sulphoxide
ED_{50}	50% effective radiant energy (dose)
EMR	Electromagnetic radiation
GLM	General linear model
GSH	Glutathione
g/L	gram per litre
HEPES	N-2-hydroxyethyllpiperazine-N'-2-ethanesulfonic acid
L	litre
M	molarity
µL	microlitre
mL	millilitre
mM	millimolarity
µM	micromolarity
mW/cm^2	milliwatt per square centimetre
$\mu W/cm^2$	microwatt per square centimetre
nm	nanometre
SEM	Standard error of the mean
STD	Standard deviation
SLM	Scanning Laser Monitor
UVR	Ultraviolet radiation
v/v	volume per volume

Chapter 1

GENERAL INTRODUCTION

1.1 BACKGROUND OVERVIEW

Among the several risk factors for cataract formation, solar ultraviolet (UV) radiation has been implicated as a major environmental factor. The gradual depletion of stratospheric ozone due to chlorofluorocarbons (CFCs), aircraft pollutants and other major industrial pollutants substantially increases the levels of ultraviolet radiation (UVR), particularly ultraviolet radiation B (UVB) reaching the Earth's surface (Kerr and McElroy, 1993). The focus of this thesis is limited to environmental solar radiant energy in the 290-400 nm range, since shorter wavelength UV below approximately 290 nm, is absorbed by water, air, and ozone in the upper atmosphere (i.e. stratosphere). Between altitudes of 30,000 and 100,000 km, the atmospheric ozone absorbs all of the solar UVR in the 200 - 288 nm wavelength range (Pitts, 1993). This means that UVR wavelengths from 290 to 400 nm will reach the Earth's surface. UVR wavelengths from 100 to 400 nm may be referred to as UV energy, and according to Commission Internationale de l'Eclairage i.e. International Commission on Illumination (CIE, 1987), they are subdivided into short wavelength UV (UVC: 100-280 nm), middle wavelength UV (UVB: 280 - 315 nm), and long wavelength UV (UVA: 315 - 400 nm).

For atmospheric and environmental applications, it is sufficient to adopt the intervals from 290 to 320 nm, and 320 to 400 nm as working definitions of the UVB and UVA regions, respectively (Parrish et al., 1978; Cullen, 1980; Pitts, 1993). In most cases it is experimentally useful to consider the effects of UVB and UVA separately, but the natural environment always contains a mixture of both UVB and UVA (Zigman, 1993).

Thus UVA and UVB synergism is part of the focus of this thesis. According to Zigman (1993), the solar UVR in the environment is 97% UVA and 3% UVB, and from direct sun at an intermediate latitude, the eye would receive approximately 300 kJ/m^2 (30 J/cm^2) of UVA and 10 kJ/m^2 (1 J/cm^2) of UVB in 30 minutes.

The effect of solar UVR on cataract prevalence has been a major focus in epidemiologic and laboratory studies. Cataract in ocular terminology is the opacification or loss of transparency of the crystalline lens of the eye, which interferes with vision. The crystalline lens is a transparent, biconvex, and elliptically (round in some animals) shaped living intraocular tissue. Its transparency and ability to change shape in order to modulate ocular accommodation makes it an integral part of the optical system of the eye. The lens contributes approximately 1/3 of the optical power of the human eye, while the cornea contributes the remaining 2/3 (Moses, 1981). The attachment of the zonular fibres (suspensory ligaments), and the support provided by the vitreous posteriorly and the iris anteriorly maintain the position of the lens. This support facilitates changes in lens shape that are essential for accommodation, and to assist the cornea in the focusing of light on the retina. The lens cells have definite metabolic needs and require a balance in their plasma membrane integrity in order to maintain optical transparency of the lens. The crystalline lens is exposed to the UV, visible and infrared (IR) wavebands of the electromagnetic radiation (EMR) spectrum throughout life.

EMR is a form of energy which is emitted, transmitted or absorbed in wave or particulate form (Pitts, 1993). The term radiation is often referred to as radiant energy. Radiant energy is an EMR propagated through space, a vacuum or any medium to impinge on an object or a molecule. The medium might be isolated cells, intact tissues or

a whole organ. EMR, often considered as waves by physicists, is characterised by its wavelength and frequency of oscillation, and these are related by the formula $c = \lambda\nu$, where c is equal to the velocity of propagation in the medium, ν is the frequency, and λ is the wavelength. Although the frequency (ν) of a wave is its more fundamental characteristic, photobiologists most commonly use the wavelength (nm). EMR acts as small bundles of energy having many of the properties ascribed to particles. These are called photons or quanta. Ultraviolet radiation (UVR), which is the spectrum of focus of this thesis, constitutes the wavelengths between 400 nm and 100 nm of the EMR. The UVR is an important component of the EMR spectrum because of its abiotic effects, to which the human eye is constantly exposed environmentally and occupationally. The eye is the only organ or tissue in the body (aside from the skin) that is particularly sensitive to the non-ionizing wavelengths of the EMR, from 280 nm to 1400 nm, which is normally present in our environment (Sliney, 1986). The amount of UVR impinging on a unit area of surface is called irradiance (unit of measurement: W/m^2 or W/cm^2). The dose of UVR is the irradiance multiplied by the exposure duration in seconds (Pitts, 1993). The threshold dose refers to the least radiant energy (Unit: J/cm^2) needed to cause an adverse biological effect. The most damaging UVR waveband to the lens is from 290 nm to 315 nm (Pitts, 1993). The mechanisms by which UV radiation causes cataracts are still not clear. Several possible mechanisms have been suggested, including tryptophan degradation leading to decreased levels of ATPase and increased levels of free radicals, and UVB damage to the lens epithelium leading to a calcium imbalance in the membrane (Zigman, 1985; Hightower and McCready, 1992a, 1992b). It is agreed that UVB can cause cataract, but the role of UVA is still controversial (West et al., 1998; Dillon, 1999).

For cataract studies, experimental methods have involved *in vivo* and *in vitro* approaches. However, concerns for animal welfare have led to a need to reduce the use of live animals in research. Therefore, scientists now concentrate on *in vitro* studies to understand the cellular, molecular, biochemical and biophysical mechanisms of UV induced human cataracts.

1.2 REVIEW OF LITERATURE

1.2.1 Cataractogenesis and UV Radiation

The rate of blindness is an increasing concern worldwide. Cataract is the commonest cause of blindness (acuity less than 3/60) in the world, and the second leading cause of visual impairment (acuity less than 6/18 to 3/60) after uncorrected refractive error (Al Farran, 1990; Badr, 1993; West and Valmadrid, 1995). It has been stated that communities in developing countries have enhanced morbidity due to cataract when compared to developed countries (Steele, 1990; West and Valmadrid, 1995). Part of this has been attributed to environmental factors, physical agents such as UVR or genetic and/or disease conditions such as diabetes, diarrhea or malnutrition (Taylor et al., 1988; Harding, 1991; Taylor, 1995; West and Valmadrid, 1995). Improvements in healthcare, welfare and diet over the last 3 to 5 decades have resulted in more people living longer. The process of ageing affects the eye just as any other part of the body. In the United Kingdom, a study (with a response rate of 71.5%) of people over 75 years living in the Melton Mowbray area for sight threatening conditions showed the prevalence rates to be 46.1% for age related cataracts and 41.5% for macular degeneration (Gibson et al., 1985). Although visual loss due to cataract might be remedied surgically, its surgical

management would continue to cause increasing demands on healthcare and human resources, and this is currently a major concern worldwide. In the United States, eye problems will grow as the presently estimated 76 million baby boomers age. Cataracts are expected to increase from 12.2 million cases in 1995 to 23 million in the year 2030 (this is an 89% rise, according to Prevent Blindness America, 1996). The US National Society to Prevent Blindness states that the prevention and slowing of cataract development is one of their major goals for future vision research projects (Prevent Blindness America, 1996).

In many countries, particularly developing nations, cataract surgical treatment is not easily attainable. Cataract has been, and still is a major healthcare problem in both developed and developing countries such as the United States (Kahn et al., 1977a & b; Hiller et al., 1983; Young, 1991), Canada (Seidman-Ripley and Huang, 1993), Australia (Livingston et al, 1994), India (Thylefors, 1995; Chartterjee et al., 1982), Nepal (Mitchell and Lepowski, 1986), Africa (Thylefors, 1995; Zerihun, 1994), England and Wales, and China and Hong Kong (Yap and Wong, 1992). A report from the United Kingdom in 1998 also supports the implication of cataract as a major cause of blindness with the data showing a backlog of 16-20 million unoperated cases globally per year (Thylefors, 1998). A waiting period for cataract surgery has been estimated to be approximately 18 months in the United Kingdom (Harding, 1999), with most patients likely spending more than a tenth of their remaining life expectancy visually impaired on the list. This information will probably apply to some developed and most developing countries with longer waiting periods. Also, the cost of cataract surgery is a concern to some authorities, accounting for 12% of the Medicare budget in the United States (Harding, 1999). This

underscores the significance of UV cataract studies. Although cataract is believed to be a multifactorial ocular pathology, the UVR aetiologic component, environmentally and occupationally, is critical. Therefore it is necessary to continue investigation on the effects of UVR exposure on the eye (lens in particular), in order to increase the existing knowledge base.

That exposure of the human eyes to the UVR wavelengths of sunlight may be a factor in the formation of cataracts has been known for many years (Verhoeff et al., 1916; Duke-Elder, 1926; Clark, 1935; Pitts et al., 1977b; Zigman, 1977; West et al., 1998). Duke-Elder and Duke-Elder, (1929) cited that the first series of scientific work on the production of cataract from UV exposure was carried out by Widmark between 1889 and 1903. Widmark (1889, 1892, 1893, and 1901) found that 2 to 4 hours *in vivo* exposure of rabbit eyes to the UV portion of experimental radiation, from a powerful carbon arc, caused lenticular opacification. Widmark (1892 and 1893) described the morphological changes to the lens following acute UVR dose and observed that anterior cortical opacities occurred after irradiation with broad spectrum UVR. He described the opacities as diffuse milky opalescence and a radial stripe at the anterior lens surface. Also in 1901, Widmark found that 18 hours or more post-UVR exposure in rabbits showed an increase in the number of epithelial cells, and damage in the anterior subcapsular zone. This zone had swollen lens fibres, granular spaces between lens fibres, and sometimes epithelial cells buried in the anterior cortex. In the early part of the 20th century, Hess (1907), Martin (1912), Verhoeff et al., (1916), and Duke-Elder and Duke-Elder (1929) performed experiments with high doses of UVR to lenses *in vivo*, and found the same microscopic alterations described by Widmark (1892, 1893, and 1901). Pitts et al., (1977a) described

the appearance of the lens using slit-lamp biomicroscopy following acute *in vivo* exposure to 5 nm bandwith in the 300 nm wavelength region. They found that reversible changes occurred if the UVR dose was near a threshold level (0.15 J/cm^2 UVB): the anterior lens capsule orange-peel appearance was enhanced; the anterior suture line increased in prominence; and small discrete white dots appeared in the anterior subcapsular region of the lens epithelium. Permanent damage to the lens occurred at radiant exposure levels approximately twice the threshold level with coalescence and migration of the small white dots posteriorly into the anterior cortex, cortical haze increase, and appearance of vacuoles. Verhoeff et al., (1916) found that crystalline lenses were maximally sensitive to exposure in the 300 nm wavelength region. Using a double monochromator with a 5 nm band pass and rabbit eyes *in vivo*, Pitts et al., (1977a) confirmed Verhoef et al's (1916) initial discovery that the lens is maximally sensitive to UVR in the 300 nm region.

The association of cataract prevalence with UVR from sunlight has been supported with more recent scientific data (Grover and Zigman, 1972; Pitts et al., 1977a; Zigman, 1977; Zigman et al., 1977; 1979; Brilliant et al., 1983; Frederick et al, 1989; The Italian-American Cataract Study Group, 1991; Schein et al., 1994; West et al., 1998). However, the mechanisms for the development of discrete light scattering cortical and subcapsular opacities (cataracts) by UVB, require further investigation (Pitts et al., 1977b; Thomas and Schepler, 1980; Cullen et al., 1994; Stuart and Doughty, 1996).

The current belief amongst some epidemiologic and laboratory investigators is that only the UVB component of the solar radiation could cause UV induced cortical cataracts in humans (Taylor et al., 1988; West et al., 1998). However, since the vast

majority of the environmental UV radiation absorbed by the lens is UVA, we may not exclude its involvement in the formation of cortical cataracts in humans (Dillon, 1999). Experimental evidence shows that UV radiation with wavelengths below 300 nm is absorbed by the cornea, and that of wavelengths between 300 nm and 400 nm reach the lens, and are absorbed, causing abiotic effects (Pitts, 1993). It has been suggested that the dose of UVR required to induce cataracts would have to be so great that corneal and iris damage would occur first (Duke-Elder and McFaul, 1972). But experiments by Pitts et al., (1977a and b), and Jose (1986) have shown that lenticular opacities may occur in *in vivo* experiments, without causing observable macroscopic changes to the cornea. As mentioned earlier, Zigman (1995) calculated that only approximately 3% of the total UVR wavelengths reaching the surface of the lens are UVB, and it is believed that the 3% UVB could still be very potent in causing lenticular damage without appropriate protection (Taylor et al., 1988; West et al., 1998). Supporting the UVA theory, Barron et al. (1987) and Giblin (1998) showed that UVA causes nuclear light scattering in the guinea pig and GSHPx knockout mouse, respectively. Linetsky and Orthwerth (1995) have shown that UVA irradiation of older yellow human lens protein causes the formation of a number of reactive oxygen species.

Burge et al. (1937) explained that the ionization of phosphate by solar UV is followed by the formation of insoluble calcium phosphate deposits, which could be a mechanism underlying senile cataract formation. In addition, Zigman (1985) mentioned that solar UV would cause tryptophan degradation and calcium imbalance in the lens membrane. Van Hehningen (1972) compared cataracts removed from patients in Pakistan to those in England and found more elevated calcium phosphate deposits in brunescent

cataracts removed from patients in Pakistan, thereby supporting Burge et al. (1937)'s theory. Hightower and McCready (1994a) following in vitro UVB irradiation of cultured rabbit lens epithelial cells have reported loss of ion homeostasis in the lens epithelium. In another theory, Vérétout et al., (1989) mentioned that the "short range" order of the protein molecules in the crystalline lens is sufficient to ensure transparency, and that any disruption of the short-range order would cause opacification. Addressing the issue of mechanisms further, in this thesis, it is hypothesised that both moderately high levels of UVB and UVA would reduce lens cellular metabolism (particularly mitochondrial cytochrome activity) and destabilize cell plasma membrane, which might invariably disrupt the "short range" order of lens protein molecules.

1.2.2 Spectral Transmission of the Anterior Eye Segment

Due to filtering by the cornea, the UVR normally reaching the lens ranges from 290 nm to 420 nm (Kinsey, 1948). The amount of radiation that reaches the ocular lens from a light source is determined by the transmittance of the cornea and aqueous humour anterior to the lens. For visible and near infrared, there is little difference between the spectral transmittance of the individual ocular media (Boettner and Wolter, 1962; Barker, 1979; Chou and Cullen, 1984). The near-UV radiation is strongly absorbed in the anterior segment of the eye by the cornea, aqueous humour and lens. The exception to this is that in aphakic eyes (i.e. eyes in which the crystalline lens has been removed), the posterior eye segment can also receive sufficient near-UV energy to be damaged by it (Zigman, 1993; Oriowo, 1996). Since the lens acts as a UV filter, the greatest damage to the retina in intact eyes is from blue light. The blue retinal photoreceptors absorb blue light for

vision, but they can also be damaged by intense exposure to it. Blue light and near-UV radiation induced cellular damage is often enhanced by natural photosensitizers present in all living cells and body fluids, for example riboflavin (Zigman, 1993). A quantitative determination of UV radiation absorption by the cornea and aqueous humour is important to study its effect on the lens. Lembares and co-workers (1997) studied the absorption spectra of porcine and human corneas from 190 to 350 nm. They found that corneal UV absorption increases significantly with wavelength decreasing from 240 to 220 both in porcine and human corneas (Lembares et al., (1997). It should be remembered that it is not (exclusively) the transmittance amount that determines damage but rather the matching of the tissue receptor to the wavelength of radiation. When this happens one photon can produce UV biochemical damage (personal communication with Dr. D. G. Pitts, 1998).

1.2.3 UV Radiation Sources

Sunlight is the chief source of natural UVR. Sunlight is such a common experience for humans, animals and plants, that sometimes its contribution to our lives and importance to our environment is not appreciated (Pitts, 1993). UV radiation was discovered in 1801, when Ritter found that silver chloride was blackened, just as it is by light, if placed at the violet end of the spectrum where there seems to be no light at all (cited by Tousey, 1961). The sun is essentially a sphere of gas around which the Earth and other planets revolve. It is heated by the nuclear reaction derived from its centre and it provides heat, light, and energy for the entire solar system.

All life forms including humans are constantly exposed to solar UVR from the solar sphere, directly from the sky, and indirectly by diffuse and specular reflection from various surfaces of the earth. Each of these factors continuously varies with the time of day, zenith angle of the sun, the cloud cover and changes in reflecting surfaces (Pitts, 1988). These variables make the determination of solar UVR available for exposure very difficult (Scotto et al., 1976; Fröhlich and Brusa, 1981; Rosenthal et al., 1985; 1988). Considering the albedo (i.e. reflected rays) from surfaces, the total UV radiation reflected from grass has been reported to be about 3%, 20 to 30% from sand, and 3 to 5% from fresh water, but reaches 85 to 95% from fresh snow (Sliney, 1986; Pitts, 1988). This information indicates that the total amount of environmental UVR reaching the eye is greatly enhanced by the reflectance of the surroundings such as concrete sidewalk, white house paint, dull aluminum, open water, sea surf, sand and snow.

The solar radiation received on the Earth's surface from sunlight is called direct while the scattered solar rays as the result of water vapour, turbidity and Rayleigh and other scatter is called indirect solar radiation. The combination of both direct and indirect is called sunlight total or global spectral radiation. The solar UVR in the environment exceeds that directly from sunlight, because the total UVR in the environment includes both the direct and indirect solar UV irradiation. Figure 1.1 shows the direct solar spectral output in the UV and visible wavelength range (280-700 nm) measured in June 1999, noontime at Waterloo, Ontario, Canada (43 30N) at a sun elevation of 75-85 degree. The solar spectral irradiance is the distribution of the solar constant as a function of wavelength (Mecherikunnel et al., 1983). The measured solar spectral irradiance in Waterloo compares well with the data of Mecherikunnel et al., (1983). The literature

indicates that over 96% of the solar spectral irradiance on Earth is contained in the wavelength range beginning at about 270 nm and extending to 2600 nm while 49% lies in the visible spectrum in the 400 to 700 nm waveband. This means that half of the solar radiation is in the wavelength range that serves human vision (Pitts, 1988). Solar radiation on Earth called sunlight consists of approximately 13% UVR, 44% visible and 43% infrared (Pitts, 1988).

For the general population, the second largest potential source of UVR normally encountered, is from high-temperature lamps, which have become popular for workplace illumination, exhibition lighting systems, other indoor areas of activity, or for special occupation or health related-activities which may expose humans to near-UV (i.e., UVA: 320-400; UVB: 295-320 nm) energy (Zigman, 1985; Pitts, 1993). Pitts (1993) gave a list of occupations with light sources producing excess UVR that affects the eye. These light sources include welder's arc, light curing generators for dental procedures etc. Oriowo et al. (1997) have shown that the light sources used in glassblowing operations also produce some near-UVR. Baum and Pitts (1997) reported a case of 46-year old male caucasian with no other known risk factors, who developed bilateral posterior subcapsular cataracts 18 months after occupational repeated exposure to a non-filtered UVR device. All of these points emphasize the importance of further understanding the mechanisms of UV damage to the lens.

Figure 1.1. Solar spectral output as measured at Waterloo, Ontario, Canada on June 18, 1999 at noontime.

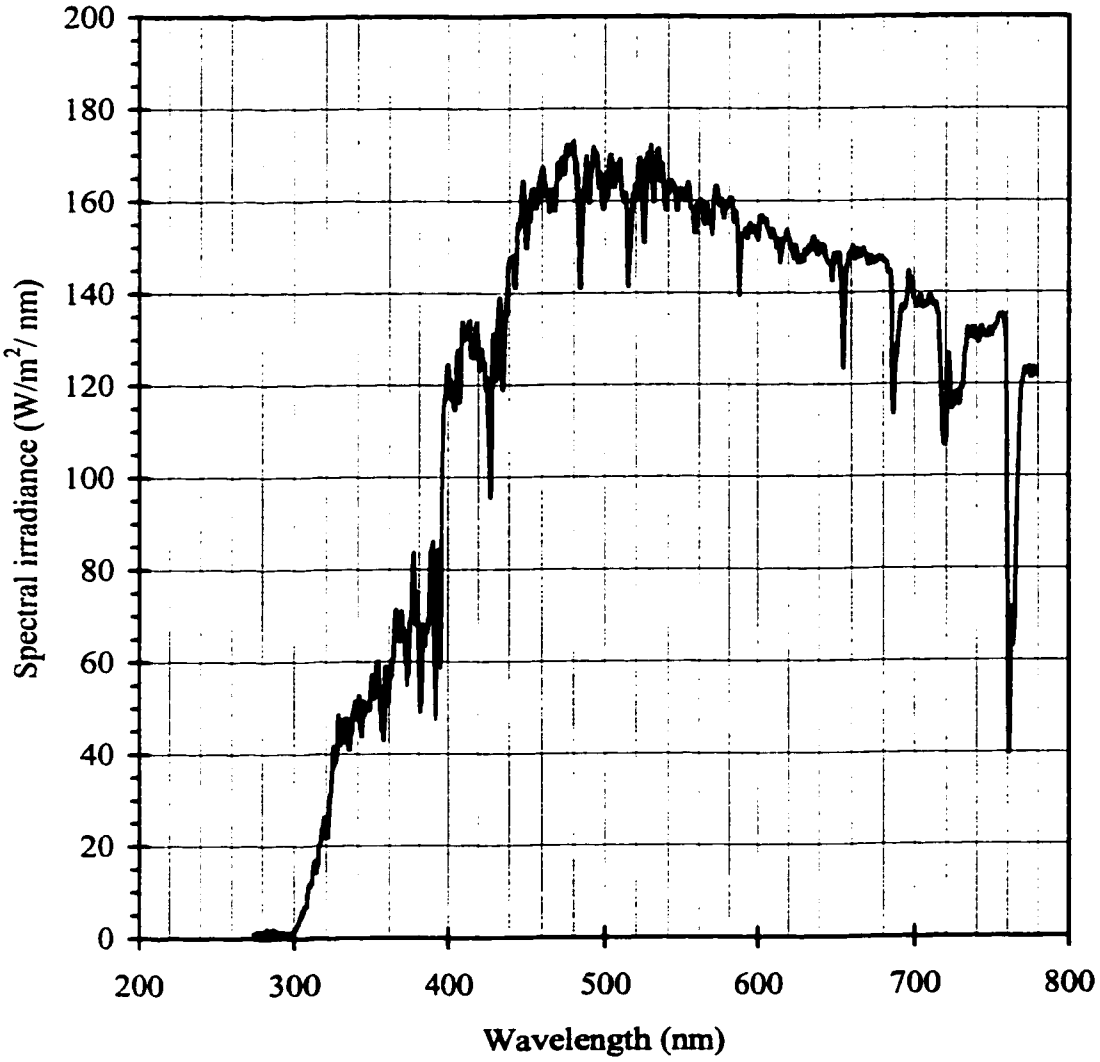

1.2.4 Ozone and Solar UV Radiation

It is known that the ozone layer helps protect all life forms from harmful UV radiation. Evidence in the literature shows that ozone depletion is actively ongoing. The importance of the ozone story to humans, animals and plants is that the lower wavelength and the intensity of the UVR falling on the Earth depends on the integrity of the ozone layer and the air mass of the atmosphere. Ozone (O_3) is formed through the action of short wavelength UV radiation on molecular oxygen by photolysis: $O + O_2 = O_3$; $O_2 + hv = 2O$, then $2O + O_2 = O_3$. It has been concluded that chlorofluorocarbons (CFCs) could harm the stratosphere by interacting with O_3 to produce O_2 and result in net increase in the UVR reaching the Earth. Prior to last 3 decades, CFCs were used as refrigerants in some industrial and household appliances. As well, the development and use of supersonic transport (SST) within the last 3 decades has created concern that the propulsion effluents from the SST aircraft engines could result in a degradation of the stratospheric ozone. Subsequently, studies were designed to analyze the impacts of the propulsion effluents of aircraft engines on the stratospheric ozone (Anon, 1979). These studies predicted an increase in solar UV radiation due to partial loss of ozone and changes in temperature and precipitation associated with the increase in pollutants such as aerosol sulphates and water vapour (Pitts, 1993).

Molina and Rowland (1974) first suggested that CFCs or chlorofluoromethanes (CFMs) could reduce the stratospheric ozone layer. Alyea et al., (1975), using the effluent production of the nitrogen oxides (Nox)s by the SST, predicted an annual depletion of 12% in the stratospheric ozone in the northern hemisphere and a depletion of 8% in the

southern hemisphere. By the late 1970s, different studies had established ozone depletion rates of 7.5%, 10.8% and 16.5% thus supporting Molina and Rowland (1974)'s hypothesis (Anon, 1979). In addition, Gille et al., (1984) reported a 12% reduction in stratospheric ozone over an 11 year solar cycle at a rate of 1.09% reduction per year in support of the ozone depletion hypothesis.

Clearly, the literature indicates that the plant and animal life, especially of the Antarctic is being affected by the increase in solar UV (Frederick and Lubin, 1988). The recognition by the United States, Canada, Europe, and other countries of the adverse impact of the increase in solar UV on humans, animals and plants led to an ozone treaty which was endorsed by more than 40 countries at a meeting in Montreal in September, 1987 (Montreal Ozone treaty, 1987). The purpose of the treaty was for countries to limit the production of CFCs, since it has been generally believed that a progressive decrease in atmospheric ozone globally would increase the amount of UVB reaching the Earth's surface (Bowman, 1988; Pitts, 1990; Blumthaler and Ambach, 1990). This belief was officially recognized in Europe in 1989, when the European Economic Community (EEC) banned all uses of CFCs by the end of the 20^{th} century (Dickson and Marshall, 1989). Data supporting the hypothesis that decrease in ozone will increase UVR intensity comes from Kerr and McElroy (1993) who monitored UVB (from 300 nm) levels as well as ozone thickness over Toronto (44°N), Canada between 1989 and 1993. They found that a downward trend in total ozone thickness (~4% per year in winter and ~2% in summer) was accompanied by increase in UVB intensity of 35% per year in winter and 7% per year in summer. Kerr and McElroy (1993) also found that total daily UVB ambient dose routinely reached levels of 0.01 J/cm^2 as measured on a flat surface. In 1988, Taylor and

associates, predicted a 1% increase in the prevalence of UVR-induced age related cortical cataracts with each year of exposure to sunlight.

Another factor that affects the solar UVR hypothesis is that in winter when temperatures in the stratosphere are very low (near –100 degree C), ice particles form in the stratosphere. These are called polar stratospheric clouds (PSCs). At low temperatures, PSCs become part of the process that destroys the ozone layer (Wardle et al., 1997). It has been mentioned that the buildup of carbon dioxide and other greenhouse gases contributes to cooling of the polar stratosphere which favours the formation of PSCs (Austin et al., 1992). The various reports of O_3 measurements show conclusively that the stratospheric ozone has decreased over the last 3 decades (Kerr, 1997).

1.2.5 The Crystalline Lens

The crystalline lens is one of the tissues in front of the retina which must be transparent to light for optimum vision to be maintained at the appropriate physiologic level (Harding, 1991). It is an avascular, cellular structure within an acellular capsule. The lens epithelium like other epithelia constantly produces new cells. However, since the basement membrane is located externally, new cell growth is directed inward. This makes the lens unique among the tissues of animals because all the fibres produced at all stages of life are retained within the adult lens (Hoyer, 1982). New cell growth is restricted to the peripheral equator so that older lens material is concentrated toward the centre as the number of lens cells increases through life (Duke-Elder, 1958). The lens, just as the corneal epithelium, is formed from the surface ectoderm, and yet lies deep within the eye (Pearson and Weleber, 1972). The lens has an onion-like layered structure (Wanko and

Gavin, 1958) and its refractive index is variable (higher at core). Figures 1.2A and B illustrate schematic diagrams of the crystalline lens regions and components.

Figure 1.2A. Diagramatic cross section of vertebrate lens with the various regions indicated as C, capsule; E, epithelium; GZ, germinative zone; PZ, preequatorial zone; CZ, centarl zone; MR, meridional rows; and DC, differentiating cells (Adapted from Harding et al., 1971).

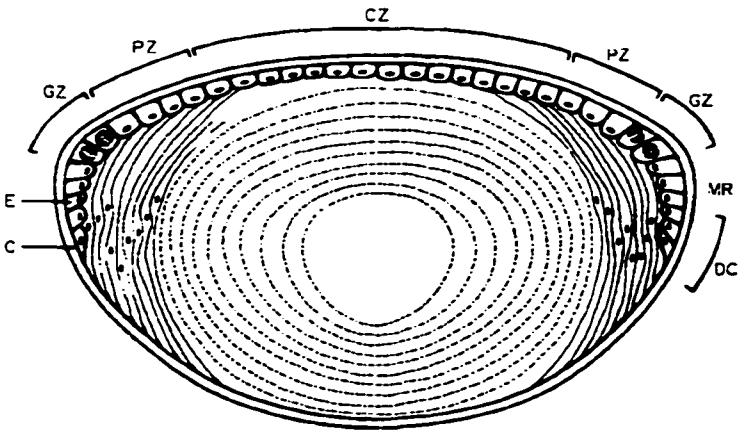

Figure 1.2B. Schematic representation of half of the crystalline lens showing the capsule, epithelium, cortex and nuclear zone. (Adapted from Hogan et al., 1971).

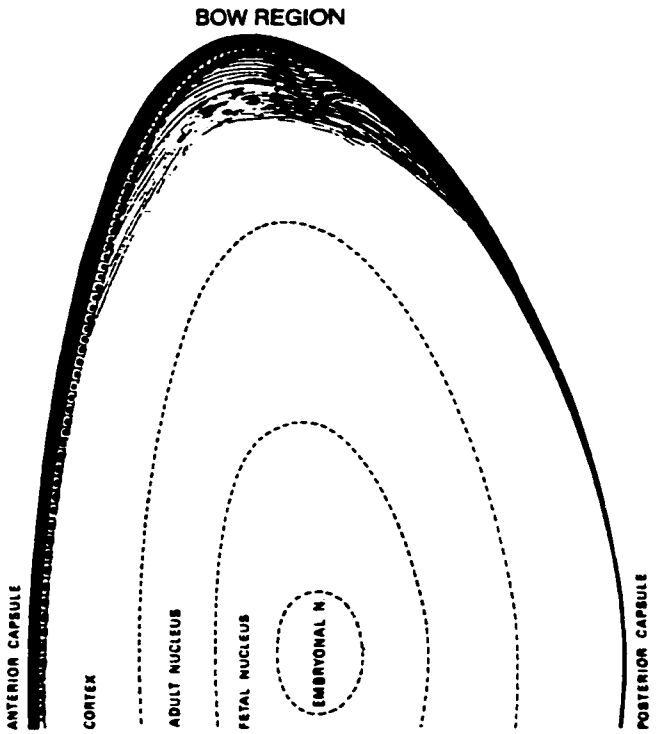

The crystalline lens provides 1/3 of the refractive power of the human eye. Although the cornea provides 2/3 of the refractive power in humans (Moses, 1981), it only provides a fixed refractive power. The human crystalline lens functions primarily to focus images onto the retina over a range of focal distances. The lens mainly consists of elongated cells within the cortex known as lens fibres. Anteriorly and laterally, a layer of cuboidal epithelial cells that secrete the basement membrane covers the cortex. This elastic basement membrane encapsulates the entire lens structure and is known as the lens capsule. The anterior capsule is over 5 times thicker than the posterior.

The metabolic systems in the lens are essentially the same as in other tissues (Harding, 1997). Cell nuclei, mitochondria and ribosomes are abundant mostly in the epithelium and outer fibres (Maisel, 1985; Harding, 1997). Mitochondria are the membranous cytoplasmic organelles capable of trapping chemical energy released by oxidation of compounds derived from nutrients (Weiss, 1988). Mitochondria then fix the trapped energy in form of adenosine triphosphate (ATP) that is readily utilizable by the cell. Maintenance of mitochondrial biogenesis is an important component of lens metabolism including normal differentiation of epithelial cells to lens fibres (fibrogenesis). It allows adaptive responses to biogenetic challenges such as ocular accommodation, exercise, and systemic influences like diabetes. The major source (80%) of energy for the lens is through anaerobic glycolysis of glucose, in the epithelial cells, with the end product, lactate, eliminated into the aqueous fluid (Maisel, 1985; Harding, 1997). Approximately 10-15% of the glucose is metabolised by the hexose monophosphate shunt (Maisel, 1985). The remaining 5% of the glucose is metabolised via the citric acid (Krebs) cycle pathway, through which an appreciable amount of ATP is

produced. For the performance of cellular function, oxidative metabolism through the Krebs cycle is of greatest importance due to its high caloric yields. Blocking oxidation through Krebs cycle would cause cell death (Weiss, 1988). The cell constantly fixes and stores ATP through the electron-transfer system of cytochromes, since the energy resulting from the oxidation of pyruvate to carbon dioxide and water would, by itself, yield only heat. Both the Krebs cycle enzymes and electron-transfer system of cytochromes are present in mitochondria (Weiss, 1988). The ATP is required for all pumping activities and for synthesis of macromolecules and glutathione. For instance, the amino acids required for protein synthesis are transported in from the aqueous humour (Harding, 1997).

A high level of glutathione (GSH), a thiol tripeptide is synthesized by the lens and is found almost entirely in the reduced form (Kinoshita and Masurat, 1957; Reddy, 1971; Reddy et al., 1980). GSH, present in high levels in the epithelium, is thought to protect lens proteins against oxidation and other forms of chemical attack (Harding, 1997; Stewart-DeHaan et al., 1999). It is known to help in maintaining tissue levels of ascorbate and tocopherol (Meister, 1992). Also, GSH protects NaK-ATPase and thus helps to maintain cation levels in the lens (Reddy and Giblin, 1984). The defense systems protecting the lens from oxidation are so efficient that essentially no protein or GSH disulfide is observed in the normal lens (Maisel, 1985). The synthesis of GSH requires two enzymatic (glutathione synthetase and γ-glutamyl-cysteine synthetase) reactions both using ATP (Harding, 1997). When GSH functions as an antioxidant it is converted to oxidized glutathione (GSSG). Restoration of the reduced form (GSH) is achieved by another enzyme, glutathione reductase using NADPH. By initiating repair whether by

reduction of GSSH or by *de novo* systhesis, the lens effectively maintains its GSH in a reduced state constantly (Reddy and Giblin, 1984). Other enzymes that detoxify deleterious oxidizing agents in the lens include GSH catalase, GSH peroxidase, and superoxide dismutase (Maisel, 1985).

1.2.6 Lens Epithelium and Cortical Fibres

The lens epithelium is the primary location of the pumping processes that preserves lens hydration (Jacob, 1999). Inside the lens anterior capsule is a single layer of epithelial nucleated cuboidal cells (Wheater et al., 1993). It is generally agreed that the main location of lens metabolism is in the epithelium. The elaborate system of gap junctions allows cells deep within the lens to communicate with the outer cell layers (Paterson and Delamere, 1992; Delamere and Dean, 1993). While the central epithelial cells are quiescent, the equatorial epithelial cells undergo mitosis and differentiate into fibre cells which in turn elongate throughout life to form the lens core (Harding et al., 1971; Harding, 1997). Thus damage to the epithelium from uncontrolled exposure to exogenous agents such as UVR can be expressed later in life in the cortical fibres (Worgul et al., 1989).

It has been shown that exposure of the anterior surface of the cultured rabbit lens to UVB radiation causes alterations in Na^+ and Ca^+ concentrations, a lowering of reduced glathatione, a reduction in NaK-ATP activity, and the induction of lens opacification (Hightower and McCready, 1992a). They showed that UV exposure of the posterior side of the lens, that lacks an epithelial layer, did not cause ionic imbalances or opacification. These findings suggest that the lens epithelium is of vital importance in the maintenance

of lens homeostasis. There is still the need for continued research efforts to determine the exact targets and the detailed mechanisms that are responsible for UV induced cataracts (Andley et al., 1994; Stuart and Doughty, 1996). Pharmacologic agents such as dexamethasone and prednisolone affect lens epithelial function and may cause cataract (Urban and Cotlier, 1986) by increasing cation permeability, inhibiting NaK-ATPases (Miller et al., 1979; Mayman et al., 1979), and disrupting the structure of the lens epithelium (Karim et al., 1989). The important functional role of the lens epithelium is reinforced by the loss of ion homeostasis and subsequent opacification when it is damaged by factors such as UV irradiation (Hightower et al., 1994a). It has been suggested that oxidation of membrane components (including pumps, channels and transporters) is the initiating event of cataract (Spector, 1984). Kise et al., (1994) showed that oxidative stress causes aerobically incubated rat lenses to swell, lose their electrolyte balance and opacify as a result of decreased epithelial NaK-ATPase activity. An hypothesis presented in this thesis is that UVR (UVB and/or UVA) would disrupt lens plasma membrane integrity and inhibit epithelial cell metabolism due to oxidative stress.

1.2.7 Pathophysiology of UVR-Induced Cataracts

There is currently general agreement that the photodamage mechanism of UVR-induced or enhanced cataracts is photochemical. Usually, exposure to UVR (especially UVB) exhibits a phototoxic effect on the lens by causing cellular proliferation in the subcapsular epithelium which may develop into swelling and partial (repairable) or complete destruction of the epithelium and the cortical fibres. Free radicals and unpaired electrons

are generated wherever some radiation energy process such as UVR (Pathak, 1986; Söderberg, 1990) breaks up molecules. Frequent exposure to low levels of UVR without adequate protection will damage ocular tissues photochemically by changing the chemical structure or composition of the intra- and extracellular biomolecules (Cullen, 1980; Bergmanson and Söderberg, 1995). In contrast, it has been suggested that exposure to higher levels of UVR, particularly the longer UVR wavelengths and shorter visible light wavelengths, will often initiate thermal damage (Sliney, 1986). However, it is not clear whether or not the mechanisms for acute and chronic UVR phototoxic effects are identical for the crystalline lens, making it difficult to correlate results from laboratory experiments on acute response with the chronic response in epidemiologic studies (Sliney, 1986; Pitts, 1993).

A predominant mechanism in the formation of cataracts involves a decrease in lenticular reduced glutathione (GSH), a component involved in the protection of lens proteins (Harding, 1991). In much phototoxic damage to the lens, the amount of GSH decreases, and as a result the amount of oxidised glutathione (GSSH) increases. The exact mechanism in this case involves the attachment of GSSH to the lens protein, the crystallins, and subsequent formation of mixed disulfides (Harding, 1991). These mixed disulfides, in turn are susceptible to photochemical insult and protein aggregation. This cycle might go on as long as exposure to the phototoxic agent continues, and subsequent partial or complete opacification of the crystalline lens results. Also, lipid peroxidation has been shown to be involved in the pathogenesis of some types of cataract (Bhuyan et al., 1983; Babizhayev et al., 1988). Cholesterol is an essential component of lens plasma membrane (Girao et al., 1999). During fibre cell differentiation there is 1000 fold

enhancement of lens plasma membrane (Piatigorsky, 1981), requiring an active *de novo* synthesis of cholesterol (El-Sayed and Cenedella, 1987). Changes in cholesterol homeostasis particularly during cell differentiation have been associated with some types of cataract (Cenedella, 1996). As other unsaturated lipids, lens membrane cholesterol is prone to oxidation by most reactive oxygen species (Zelenka, 1984).

1.3 THE PURPOSE AND RELEVANCE OF THIS THESIS

1.3.1 RATIONALE FOR STUDY

The mechanisms of the pathogenic effects of ultraviolet radiation (UVR) on human crystalline lens remain controversial (Stuart and Doughty, 1996; Baum and Pitts, 1997; Dillon et al., 1999b). Most laboratory and epidemiological data have supported the concept of association between solar UVR exposure and cataract formation (Hiller et al., 1983; Taylor et al., 1988; Dolin, 1994; West et al., 1998). Recently, opposing views have been expressed about the concept of association between sunlight and cataract. Young (1991, 1993) suggests that sunlight is the primary causal factor in cataractogenesis, and strongly advocates protection by the use of sunglasses to prevent cataract. However, Harding (1992) had an opposing stance that sunlight is not a major factor in human cataractogenesis. Dillon (1999) argued that even UVA cannot be excluded from UV enhanced cataracts. Though limited, evidence existing in the literature still points to the fact that exposure to solar UVB causes cortical opacities in the human lens (Taylor et al., 1988; Schein et al., 1994; West et al., 1998).

Several authors have proposed that the increased pigmentation may have resulted from the generation of free radicals after exposure to near-UVR (Lerman and Borkman, 1978). This free radical hypothesis postulates that tryptophan exposed to near-UVR is involved in the increased pigmentation in a nondestructive fashion by generating free radicals and other oxidants. It may be argued that *in vitro* investigation cannot be assumed to mimic *in vivo* condition, but results from *in vitro* studies can be at least suggestive (Rafferty et al., 1997). It was the goal in this thesis to develop a new *in vitro* assay technique for UV-lens study.

1.3.2 DEVELOPING A NEW BIOASSAY TECHNIQUE

One aim of this thesis is to explore the applicability of two fluorescent indicator dyes; 5-carboxyfluorescein diacetate-acetoxymethyl ester (CFDA-AM), and alamarBlue™ to UV cataractogenesis studies in order to be able to study the cellular and biophysical aspects of a whole organ cultured crystalline lens without having to separate the component layers, or using lens homogenates. These two fluorescent dyes target different cellular activities in the lens. They have different and non-interfering excitation and emission wavelengths; thus the dyes can be assayed together. The CFDA-AM measures the integrity of plasma membranes, while the alamarBlue™ measures cellular metabolic activity, respectively (Schirmer et al., 1997). Bearing in mind that assay dyes used for a non-terminal and long term *in vitro* study must be non-toxic to the cells, the author carried out pilot study with non-irradiated lenses to investigate if assaying cultured lenses with the dyes would not demonstrate any toxic trend. In order to verify the data collected from the assay method, the optical quality of the same lenses was assessed with a laser scanning system (Sivak et al., 1986; Weerheim and Sivak, 1991). The findings from the pilot study and other subsequent experiments with the assay system will be discussed in the following chapters.

In order that extrapolation of animal cataract data to the human may be repeatable among investigators, further development of a viable, practical and repeatable experimental model is necessary. Most previous UVR cataract studies have used rabbit, monkey, cow, fish and mouse eyes as *in vivo* and *in vitro* experimental models. Coupled with earlier mentioned limitations, it is becoming increasingly expensive to use live animals for laboratory research. Therefore, the organ cultured porcine crystalline lens was

examined as a viable *in vitro* biochemical model for UV cataract study. The pig eye was chosen because of its close similarity to the humans (Duke-Elder, 1958; Zubay, 1985), and similar lenticular dimensions (Elliott, 1993). As well, Beauchemin (1974) found that the ultrastucture of porcine retina resembles that of humans, although it is afoveate and there is no true macula (Vestre, 1984). Biochemical studies have demonstrated that leucine aminopeptidase (LAP) is present in the epithelium and outer cortex of porcine lenses just as it is in bovine lenses and human (Taylor et al., 1983; Stuart and Doughty, 1996). It may be argued that inter-species differences in ocular anatomy and physiology can greatly affect the applicability of animal data to human. However, Geeraets et al. (1963), Cavonius et al. (1974), and Pitts (1978) have suggested that if experimental animal data were scaled by the appropriate weighting factors they can be applicable to human situations.

Most laboratory UV cataract studies have concentrated on bovine, rabbit, squirrel, rat and fish lenses. Apart from the fact that the traditional use of rabbits for *in vivo* UVR studies, requiring a large number of subjects for acute and chronic UV radiation studies has become difficult, the rabbit eye is nocturnal with a retinal photoreceptor population very different from humans. The lens of a diurnal animal tends to be relatively flatter than that of a nocturnal animal, and has some degree of yellow colouration (Chou, 1982). Furthermore, the retinal circulation of rabbit is superficial, penetrating only to the nerve fibre layer, while that of human eye penetrates to the outer plexiform layer (Duke-Elder, 1958; Newell, 1992). As mentioned earlier, Beauchemin (1974) has shown the porcine and human retinal vasculature to be closely similar. The retinal vascular system in pig is trilaminar with the capillary network extending externally to the outer part of the inner

nuclear layer, and internally to the ganglion layer, except in the peripapillary area where capillaries are also found in the nerve fibre layer. The presence of capillaries in porcine nerve fibre layer in the peripapillary region explains why the nerve fiber layer was found to be thicker than in humans (Hogan et al., 1971). Beauchemin (1974) also noted the abundance of cones distributed among the rods in porcine eye, however the implication of this on whether the pig is predominantly diurnal has not been fully studied. Evidence in the literature shows that porcine lenses have not been fully explored as a possible viable and comparable *in vitro* animal model for cataract and lens research. To date just a few *in vivo* studies using pig's eye as a model (Boisvenue et al., 1978; Begue and Moran, 1979; Sanford and Dukes, 1979; Sanford et al., 1981; Creighton et al., 1982) have been done. Thus, it was deemed necessary to revisit the use of pig eyes as experimental model, and based on the results, to possibly propose the porcine crystalline lens as a model for future *in vitro* UV-lens investigations.

In summary the objectives of this thesis were to:

1. Determine the suitability of porcine lens as a model for long-term organ culture study.
2. Determine the *in vitro* action spectrum for UVB and UVA radiation phototoxicity using organ cultured porcine lenses.
3. Determine the UVB threshold for damage using a fluorometric bioassay technique.
4. Determine the UVA threshold for damage using the same method as in the UVB study.
5. Investigate the synergistic effects of UVB and UVA together on lens epithelial cell mitochondrial integrity (hypothesis - synergism will lower UVB and UVA radiant energy level required to induce phototoxicity in the crystalline lens *in vitro*).

Chapter 2

Organ Cultured Porcine Lens as an *In vitro* Experimental Model for Ultraviolet Induced Cataract Studies

2.1 Abstract

The purpose of this section of my thesis was to investigate the suitability of using cultured porcine lens to study lens damage by UV radiation, and to determine how long the porcine lenses could be cultured without deterioration. Intact porcine crystalline lenses aseptically dissected from pig eyes obtained from a local abattoir were immersed in a culture medium in two-chambered containers. The culture medium was comprised of modified medium M199 supplemented with 1% penicillin/streptomycin and 4% sterile-filtered porcine serum. Lenses were incubated at 37°C with 4% CO_2 and 96% air. Lenses were assessed in terms of cell biology and optical function. The cell biology technique involved the use of two fluorescent indicator dyes, alamarBlue™ and CFDA-AM which have been reported to be non-radioactive and non-toxic for cell culturing. The two dyes were assayed together and used to monitor lens metabolism and membrane physiology at one week intervals, for up to 8 weeks. For the assay measurements lenses were transferred into a 24-well culture plate with one lens per well. The assay solution was added to each well containing a lens, and the lenses were incubated for 50 minutes. After the 50 minute incubation with the assay, fluorescence values were measured with a computer controlled CytoFluor™ II fluorescence multi-well plate reader. The optical quality of the same lenses was monitored as a measure of focal length variability

(sharpness of focus) with an automated laser scanning system (Sivak et al., 1986) at approximately the same interval as the assay measurements. The first sets of readings, taken at week one of culture, were compared to subsequent readings using a paired *t* test with *P* values set at 0.05 level. Beginning from week seven there was a significant decrease in lens cellular metabolism ($P = 0.005$) and membrane integrity ($P = 0.0006$) as indicated by alamarBlue™ and CFDA-AM measurements, respectively. Also, the optical quality of the lenses showed some deterioration ($P = 0.02$ for both mean focal length and focal length variability) at week seven of culture. These findings show that in an appropriate physiological medium, the intact porcine lenses could be cultured for at least six weeks with no significant compromise of integrity. This confirms that porcine lens is a viable experimental model for *in vitro* cataract studies.

2.2 Introduction

Acute and chronic exposures to solar ultraviolet radiation (UVR) have been implicated in a wide range of dermal and ocular pathologies including UV induced cataract. Cataract (opacification or compromised clarity of the crystalline lens) is the leading cause of blindness in the world (Harding, 1999). The mechanisms underlying UV cataract formation are still not fully understood. An *in vitro* optical method using a laser scanning approach for long-term study of the intact cultured crystalline lens was developed by Sivak et al., (1986). The present study was designed to develop an *in vitro* cell biology approach that can be used to study UV toxicity in organ cultured whole lens on a long-term basis.

Various *in vitro* approaches have been used to assess UV effects on the crystalline lens. Morphologic methods, including ultrastructural studies, do not easily yield quantifiable results. Moreover, these methods involve the destruction of the sample (Van Horn et al., 1970). There are limitations to methods that monitor cellular morphology and function of an intact "living" lens over a long period of time. For instance, assaying RNA synthesis with [^{3}H]-uridine, and assessment of protein synthesis in lens membranes by measuring the rate of [^{14}C]-histidine incorporation (Hightower et al., 1994b), both of which involve the use of radioactive isotopes to study normal epithelial cell metabolism, are toxic approaches. The use of radioisotopes is a terminal, labour-intensive procedure with handling and disposal problems. Therefore, repeated measurements at different time intervals cannot be made on the same tissue sample for a long period. Most previous studies using the porcine lens have used lens homogenates (Sen and Pfeiffer, 1982; Wang et al., 1997).

The present study investigated the possible use of the cultured intact porcine lens for UV cataract study on a long-term basis, under conditions similar to those *in situ*, and addressed a concern in the literature as to whether or not porcine lenses from abattoir-supplied pig eyes are suitable for organ culture. The present study used a fluorometric bioassay (FB) and an optical laser scanning lens monitor (SLM) as approaches to assess the viability of the porcine lenses *in vitro*. The SLM system, an objective *in vitro* device, developed by Sivak et al. (1986), has been used in several studies for quantitative assessment of the optical characteristics of the crystalline lens from different animal species. The SLM method incorporates a relatively simple computer-operated device that objectively measures focal length characteristics of the intact lens (Sivak et al., 1994).

Change in lens focal characteristics is a sensitive measure of change in lens biology (Saar et al., 1989). The fact that the lens maintains its refractive function in culture makes it easy to quantify and evaluate repeatedly (Sivak et al., 1994). Increase in the focal length variability has been shown to be associated with lens opacification (Sivak et al., 1990)

A novel fluorometric bioassay approach involving the use of a fluorescent indicator dye, the alamarBlue™ assay (MEDICORP Inc., Montreal, Quebec, Canada; US Patent No. 5,501,959), to quantify reduced enzyme activity at the cellular metabolic level in the intact crystalline lens was explored. The alamarBlue™ assay is water soluble, stable in solution, non-toxic, and produces easily quantifiable changes. The use of this non-toxic dye to study UV effects on cultured intact crystalline lens has not been previously reported. The possible use of 5-carboxyfluorescein diacetate-acetoxymethyl ester (CFDA-AM) (Molecular Probes Inc., Eugene, Oregon, USA; cat. no. C-1354). another fluorescent indicator dye was explored as well. The CFDA-AM fluorescent indicator dye is an esterase substrate that can penetrate living cells.

The goals of this research are:

◆ To develop a valid and inexpensive *in vitro* assay procedure that can be used to monitor the cellular function of the cultured porcine lens.

◆ To determine how long intact porcine lenses can be cultured.

◆ To correlate findings from the assay procedure with findings from the automated optical laser scanning lens system.

2.3 Materials and Methods

Experimental procedures conformed to the Association for Research in Vision and Ophthalmology (ARVO) statement for the Use of Animals in Ophthalmic and Vision Research.

2.3.1 Porcine Lenses and Culture Medium

Whole eyes, from 6-8 month old pigs (weight ~90kg) were obtained from a local abattoir, usually within ½ to 2 hours post-mortem, and held at room temperature until the dissection of the lenses, 2 to 4 hr post-mortem. To isolate the lens, the posterior of the eye was aseptically dissected, the suspensory ligaments of the lens were cut, and the adhering vitreous removed. The lens was placed in a custom designed two-compartment borosilicate glass chamber containing culture medium, with the anterior surface facing up throughout the incubation and during experimental procedures. Both lens surfaces were bathed in approximately 25 mL of sterile medium. The culture medium comprised of modified medium M199 (9.8 g/L) with Earl's salts, without phenol red (Sigma Chemical Co., St. Louis, MO, USA, Catalogue. No. M-3769), supplemented with 1% antibiotics (100 units/mL penicillin and 100 μg/mL streptomycin: Sigma Chemical Co., cat. no. P-0781) and 4% sterile-filtered porcine serum (Sigma Chemical Co., cat. no. P-9783), 2.2 g/L sodium bicarbonate and 5.96 g/L HEPES (N-2-hydroxyethylpiperazine-N'-2-ethanesulfonic acid) as buffers, and 0.1 g/L L-glutamine. The culture medium was replaced with sterile medium every 48 hours. Cultured lenses were maintained in a water-jacketed incubator at 37°C and in a 4% CO_2 - 96% air atmosphere for the duration of experiments. The culture medium was kept at a pH of 7.6±0.2.

2.3.2 Bioassay and Fluorometry

The alamarBlue™ assay is a proprietary assay designed to quantify cell proliferation, cytotoxicity, and viability by incorporating resazurin and resorufin as a fluorometric-colorimetic oxidation-reduction (Redox) indicator that fluoresces and changes colour in response to reduction resulting from cell metabolism (Pagé et al., 1993; Larson et al., 1997). Experimentally, alamarBlue™ assay reduced fluorescence equals reduced metabolic activity. AlamarBlue™ acts as an intermediate electron acceptor in the electron transport chain between the final reduction of O_2 and cytochrome c oxidase by substituting for molecular oxygen as an electron acceptor (Pagé et al., 1993). Since the proximity of its excitation (530 nm) and emission (590 nm) wavelengths, is not close, distortion of fluorescence would be minimal. Following the protocol of Schirmer et al., (1997), 5-carboxyfluorescein diacetate-acetoxymethyl ester (CFDA-AM), another fluorescent indicator dye that quantifies change in lens membrane integrity, was assayed together with the alamarBlue™ dye. Cells with intact plasma membrane maintain a cytoplasmic milieu that supports esterase activity and the production of the fluorescent probe. Increase or decrease in CFDA-AM assay fluorescence would suggest disrupted membrane. CFDA can moderately permeate most cell membranes, with uptake greater at pH 6.2 than at pH 7.4 (Haugland, 1996). The pH of culture medium in this study was kept constant at 7.6±0.2. The esterases in the cytoplasm cleave CFDA-AM, releasing carboxyfluorescein (CF), which is fluorescent in contrast to the nonfluorescent CFDA-AM. The excitation and emission wavelengths for the CFDA-AM dye are 485 nm and 530 nm, respectively.

At one week after preincubation, the experimentally enhanced fluorescence levels of the lenses were measured with a prepared bioassay containing the two fluorescence indicator dyes. The readings obtained at week one were taken to be a baseline, and compared to subsequent readings taken at one-week intervals. Figure 2.1A illustrates a flow chart for the assay protocol. The alamarBlue™ was diluted into the culture medium (modified M199 and other culture media ingredients mentioned above) without serum, to 5% (v/v). Serum has been reported to interfere with alamarBlue™ readings (Goegan et al., 1995). Each micro-culture well containing a lens received 1.5-mL of the assay solution using a sterile 250-µL adjustable pipette tip and Eppendorf Repeater™ pipette (VWR Canlab, Mississauga, Canada).

Because of CFDA-AM's low water solubility, high quality, anhydrous dimethylsufoxide (DMSO) was used to dissolve it as recommended by the manufacturer (Molecular Probes Inc.). A previous study in our laboratory (Motluk and Cullen, 1994 unpublished data) found DMSO (1.8%) to be minimally toxic to organ cultured bovine crystalline lenses. With the above information and based on the report of Schirmer et al., (1997) DMSO was used as the organic solvent to dissolve the CFDA-AM to 4 mM stock solution, which was kept in a well sealed bottle and stored at –20°C in a container with desiccant beads. The manufacturer recommends a final working concentration of between 1 and 10 µM. A low concentration is needed to reduce potential artifacts from overloading of the cells, including incomplete hydrolysis, compartmentalisation and possible toxic effects of hydrolysis by-products such as formaldehyde or acetic acid. In this study, the stock solution was diluted in the culture medium without serum to give a

4-μM CFDA-AM concentration. CFDA-AM assay loading time of 15 to 60 minutes is recommended by the manufacturer. A fifty minutes loading time was used in this study.

For fluorometry, the alamarBlue™ (5% v/v) and CFDA-AM (4 μM) were assayed together using a 100 μL capacity pipette tip and Eppendorf® "Tip-Ejector" microlitre pipette. The lenses were transferred into a sterile flat bottom 24-well culture plate (Falcon® tissue culture plate, Becton Dickinson Labware, Franklin Lakes, NJ, USA) with one lens per well. The culture medium containing serum was carefully aspirated, and the lenses rinsed with 2 mL of experimental medium with no serum. Then 1.5 mL of the dual assay solution was added to each well containing a lens. The lenses were then incubated for 50 minutes. To prevent possible precipitation, the assay solution was prepared immediately before each use. At the end of 50-minute incubation, the fluorescence measurements were then taken with a CytoFluor™ II fluorescence multi-well plate reader (PerSeptive Biosystems Inc., Framingham, MA, USA) shown in Figure 2.1B.

Measurements were carried out as 2 scans per one cycle of reading. Prior to measurements, the excitation / emission wavelengths settings on the cytoFluor™ plate reader were adjusted to 530/590 nm and 485/530 nm for alamarBlue™ as scan 1 and for CFDA-AM as scan 2, respectively, with the sensitivity gain set at 50, and temperature at 37°C. The plate reader probe scans through 10 different positions in each lens. Thus, an average of 10 readings was obtained for every lens with both the alamarBlue™ and CFDA-AM dyes. Each scan by the plate reader probe was programmed to take 10 readings each time to obtain the lens fluorescence values, and each lens was measured on at least 8 different weekly sessions. An additional protocol in each measurement session involved replacing the assay medium in each well with serum-free culture medium after

each cycle, and then taking a second set of readings. The results reported here are based on the first set of minimum of 2400 quantitative fluorescence readings of the lenses. All procedures were carried out under sterile conditions.

Figure 2.1A. Flow chart illustrating the assay protocols for 8 weeks.

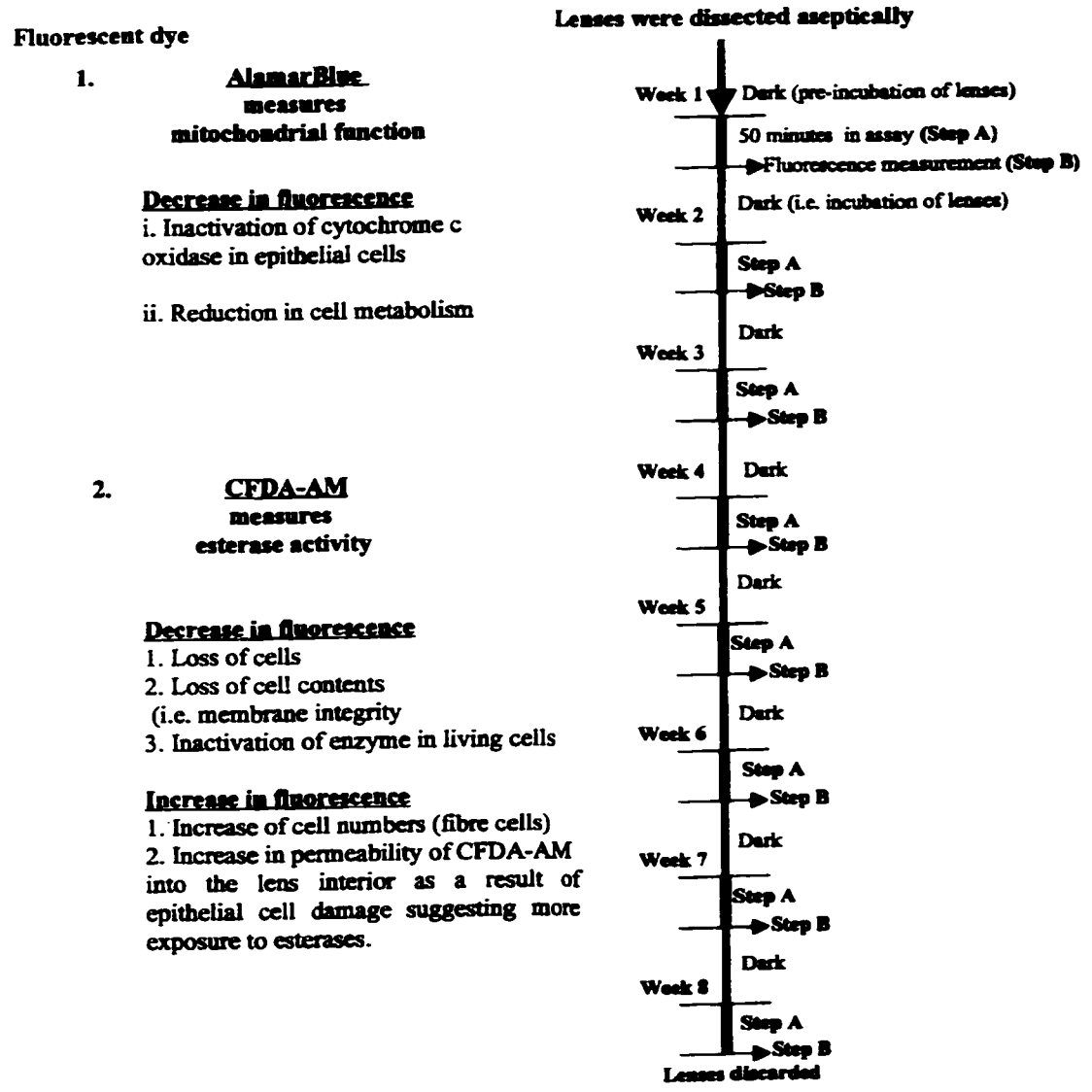

Figure 2.1B. The automated fluorescence plate reader system. (A) the cytoFluor™ II fluorescence plate reader; (B) a 24-multiwell plate which holds the lenses at one lens per well. (C) the computer unit which controls the operation of the plate reader.

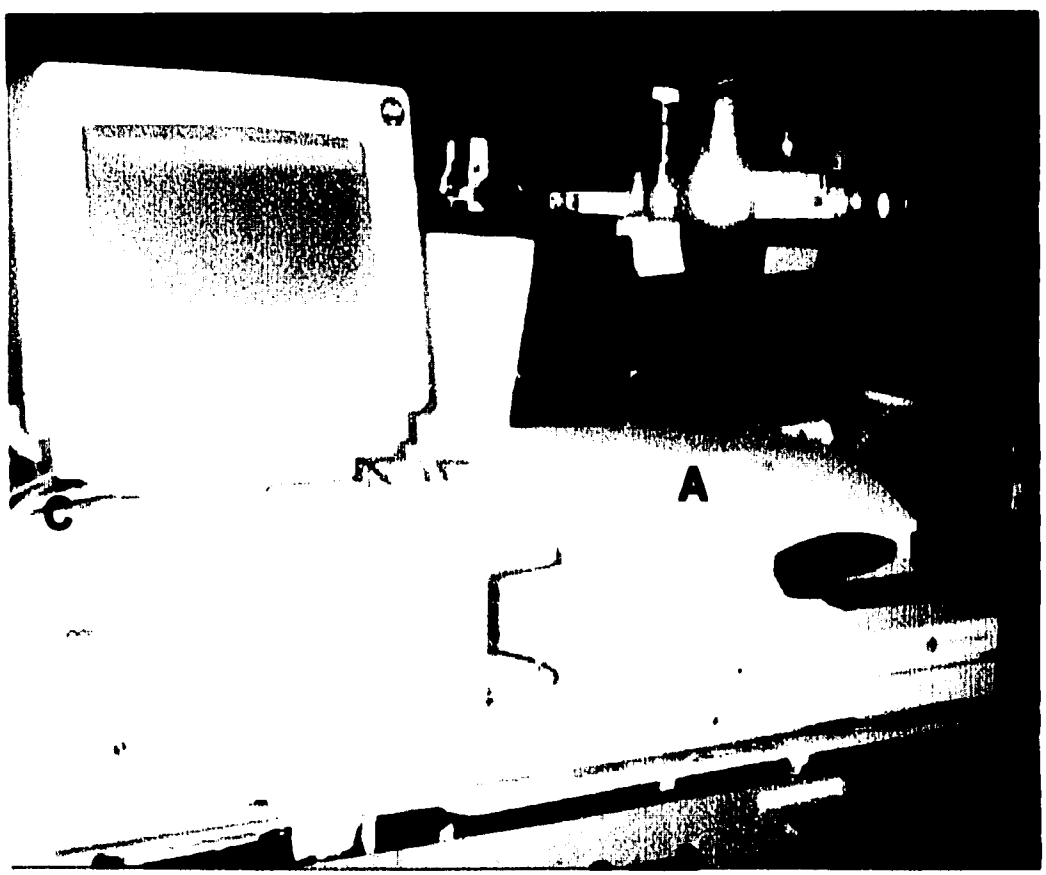

Figure 2.2. A schematic diagram of the scanning laser monitor system (modified from Dorfman-Hecht, 1993 and Elliott, 1993).

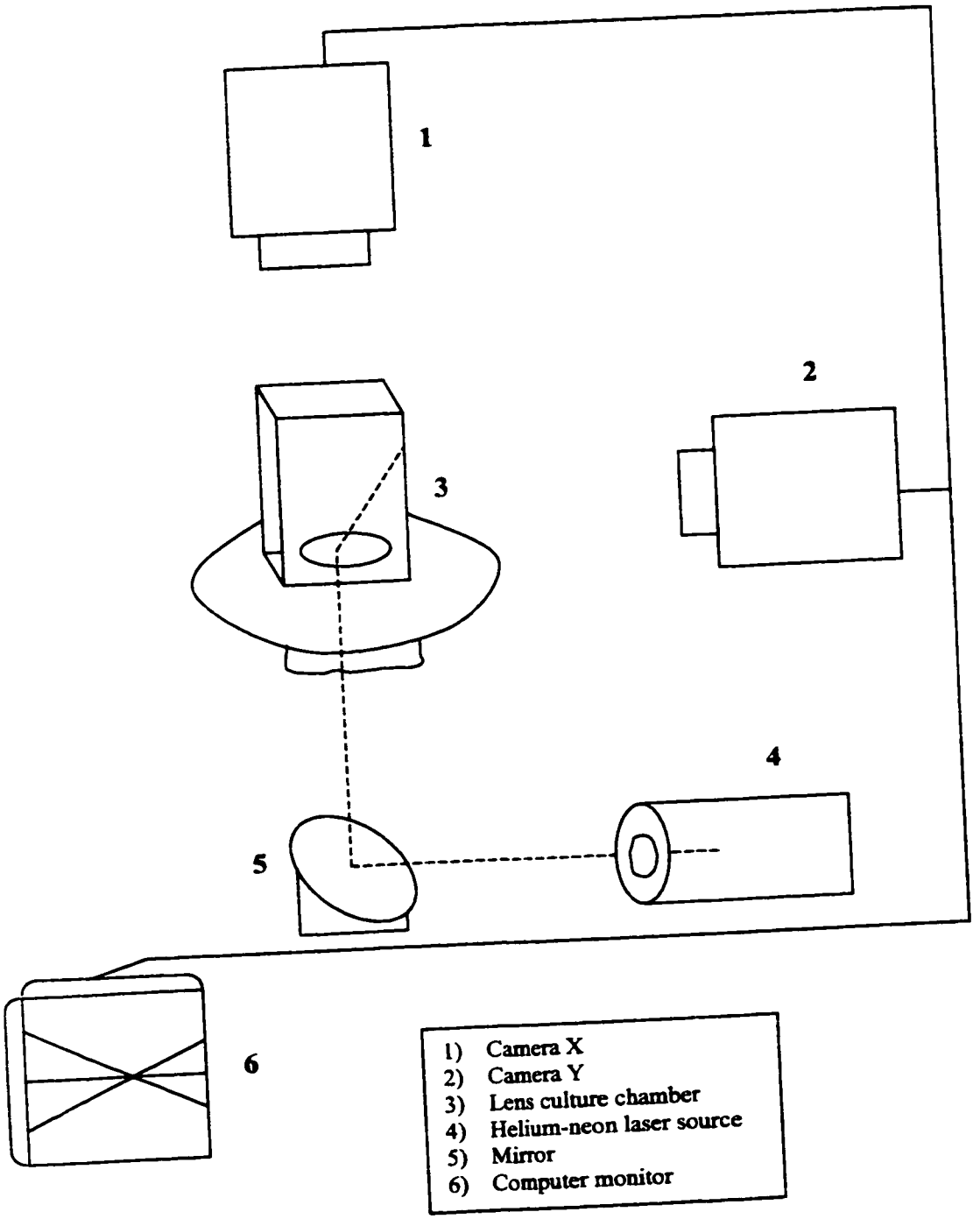

2.3.3 Automated Scanning Laser Monitoring

The automated scanning laser "lens" monitor (SLM) as previously described by Sivak et al., (1986 and 1994) was used to objectively assess the optical integrity of the lenses for the duration of the culture. Preincubation of lenses for one week before optical measurements were taken, was necessary because pilot experiments showed that it takes approximately a week for porcine lenses to become homeostatically stable and visually clear in culture media. Each lens was cultured in a specially designed two-chamber container filled with the porcine lens culture medium. The lens container was then placed in the automated scanning laser monitor (Figure 2.2), to obtain a quantitative analysis of the optical characteristics of the lens. The initial measurements taken after incubating the lenses for one week were used as a baseline. These baseline measurements were compared to subsequent ones at one-week intervals through the eight-week study duration.

The laser scanner consists of a low power (2.0 mW) helium-neon laser (λ 632.8 nm), mounted on a computer directed X-Y table using stepping motors, two television cameras and a video frame digitizer (Sivak et al., 1986). The two cameras, 90 degrees from each other, capture the laser beam image and transfer it to a computer where the beam's initial position and the slope of the refracted beam are recorded. The SLM was programmed to scan across the lens in the axial direction, at 23 positions in 0.3-mm steps for a total range of 6.9 mm, while the digitizer determined the exit direction of each beam after it was refracted by the lens. The threshold of the image analyzer was constant for all the measurements. The laser scanner first locates the optical centre of the lens being

measured by finding the point where the slope of the laser beam approaches infinity. After finding the optical centre, the program determines the focal length at each of the 23 beam positions across the lens. Equivalent focal lengths were measured from the principal plane (intercept of the incident beam with exiting beam) to the intercept of the beam with the optical axis. Figures 2.3A – C show representative focal length profiles of a porcine lens at three different times during culture. Data collected for all lenses are expressed graphically either as mean focal length (for all 23 beam positions) or as focal length variability (i.e., sharpness of focus) (SEM of the average focal length). Thus, change in mean focal or focal length variability could be used to monitor lens focal characteristics over time. Twenty-three lenses were used in this section of the study. Eight lenses were discarded during the study because of culture contamination or handling mishaps. Since each scan by the laser produces 23 measurements of focal length, and each lens was scanned at least 8 times, the results reported here are based on minimum of 2,760 objective measures of the optical function of the lenses. Both focal lengths and focal length variability were calculated and used as indicators of change in lens optical function over time in culture.

A paired Student *t* statistical test ($p < 0.05$) was used to compare the baseline measurements with subsequent ones. Repeated measures analysis of variance (using the Greenhouse-Geisser test) was applied to verify the assumptions or hypotheses that: 1) variance within the samples is homogeneous, 2) the samples are random and normally distributed. The relationship between SLM and Fluorometric bioassay (FB) measurement variables in the same set of lens was considered using correlation analysis (e.g. $y = \alpha + \beta x$ [regression line]; where α is the intercept and β is the slope of the regression line).

In the course of this investigation, samples of porcine lenses totaling 445 were randomly used to obtain the wet weight±SEM (g), equatorial diameter±SEM (mm) and axial thickness±SEM (mm). The lens dimensions were measured using a digital balance and a vernier caliper.

Figure 2.3. Representative focal length profiles for a single porcine lens over a period of six weeks in culture. Equivalent focal length (mm) is shown on the horizontal axis. Eccentricity (mm) of laser beam position from optic axis (0.0) is shown on the vertical axis. The plus signs indicate where the beam crossed the axis at each eccentric position. (A) week 1 scanning; (B) week 3; (C) week 6 scanning.

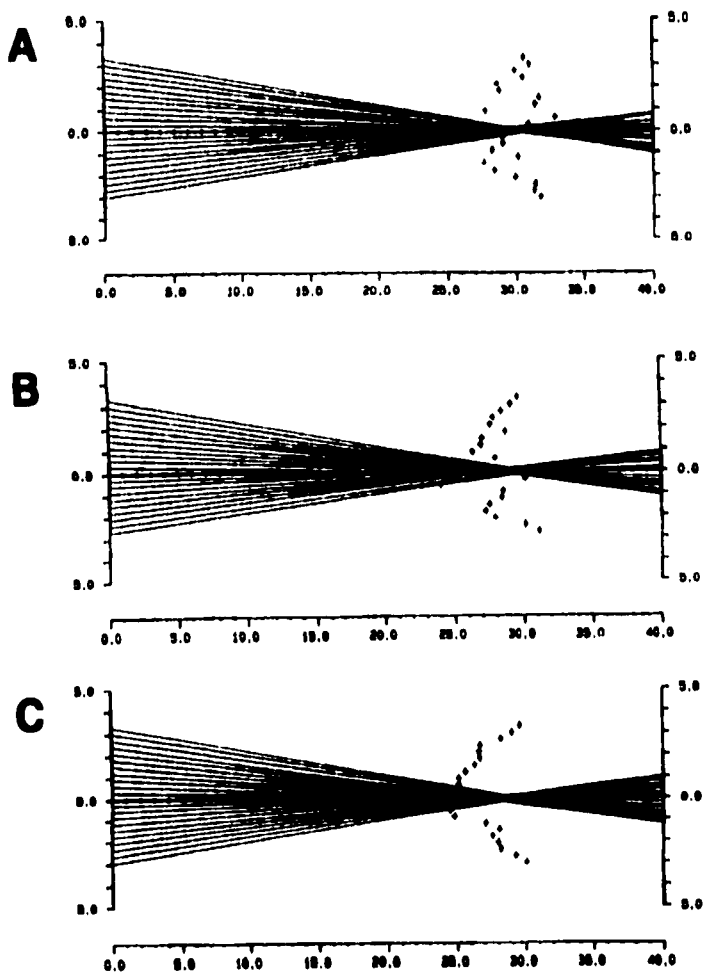

2.4 Results

Twenty-three porcine lenses were used for the assay and optical scanning laser measurements. Only data for 15 out of the 23 lenses are reported due to discontinuation of 8 lenses as a result of contamination or damage. The 15 lenses which lasted the 8 week duration stayed transparent throughout this time period. The Greenhouse-Geisser test of the assay and SLM measurements of the 15 lenses gave a P-value of 0.6937, indicating that the variance within the samples is homogeneous, and that samples are random and normally distributed. The original size and shape of the lenses seemed unaffected by the experimental procedures throughout the duration of study. For instance, P values for week 6 versus week 1 lenticular dimensions did not indicate any significant difference between week 1 and week 6 measurements (Table 2.3). The assay readings are presented in arbitrary units. The results show that the porcine lenses used in this study have an average lenticular fluorescence ranging from ~7887 to ~11445 arbitrary fluorescent units (AFU) with alamarBlue™ assay, and ~31263 to 43328 AFU with CFDA-AM assay. Table 2.1 shows the mean (±STD) fluorescence readings for both alamarBlue™ and CFDA-AM. From week 7, there is a significant reduction in cellular metabolic activity and plasma membrane integrity (esterase activity).

Optical analysis shows that average focal lengths of porcine lenses range from 27 to 32 mm, while focal length variability ranges from 0.2 to 1.1 mm (Table 2.2). The SLM data show that there is a significant perturbation in average focal length of the lenses at week 7 (P = 0.019), and focal length variability at week 6 (P = 0.016). Focal length variability appears to be nonmonotonic for all lenses, however, in general, the focal lengths for beams further from the optical axis are longer (see figure 2.3A – C) than focal

lengths for beams located close to the centre (negative spherical aberration). Some lenses exhibit both negative and positive spherical aberration, i.e. non-monotonic, thus suggesting that focal length variability should be used along with average focal length as indicators of change in lens optical quality over time. Some extraneous values were noted near the optical centre. It is likely that the paraxial rays hit the lens sutures, which may often produce an erratic scatter and change in equivalent focal length (Kuszak et al., 1991). Therefore, focal length values more than 2½ times the general average focal lengths (~28 mm) were arbitrarily removed from the calculations.

Concerning the correlation analysis, the relationship $y = \alpha + \beta x$ is not expected to hold for every lens in each sample (Rosner, 1990). Thus, an error term e, which represents the variance among all lenses needs to be introduced into the equation, i.e., $y = \alpha + \beta x + e$. However, it can be assumed that the term e follows a normal distribution with mean "0"; thus, the linear regression equation is $y = \alpha + \beta x + e \equiv y = \alpha + \beta x$. For the purpose of relating SLM and FB variables, "y" is referred to as the dependent variable and "x" as the independent variable in the equation and plots. In Figures 2.5 – 2.8, the slope is almost equal to zero (weak correlation). This may indicate that the SLM and FB measurements are independent of one another. However, except for Figure 2.5 showing slight (close to zero) positive trend, the slope trends in Figures 2.5 – 2.8 show a fair negative relationship.

In terms of lens dimensions, there was no difference between measurements taken at 48hr (97 lenses) and 168hr (1 week) (340 lenses) of lens culture (Table 2.3).

Table 2.1. The mean (±STD) fluorescence with alamarBlue™ and CFDA-AM dyes over 8-week period.

(n=15)	AlamarBlue™ mean±STD	*P* value Contrast to week 1	CFDA-AM mean±STD	*P* value Contrast to week 1
Week1	9609.4±1004.6		35573.1±4040.2	
Week2	9257.2±1090.5	0.303	37478.8±7311.6	0.168
Week3	9442.4±930.3	0.494	38320.5±5960.1	0.105
Week4	9107.3±1301.8	0.085	39432.3±6908.7	0.096
Week5	9068.6±1056.1	0.157	38063.7±5319.2	0.151
Week6	9836.9±1028.5	0.487	37260.1±5190.2	0.333
Week7	8585.9±742.80	0.005*	43103.7±5686.2	0.001*
Week8	8083.3±674.90	0.0001*	39506.1±4270.2	0.038*

Note: *P* values with asterisk (*) indicate that the fluorescence readings were significantly different from baseline.

Table 2.2. The mean (±STD) focal lengths (AFL) and the mean (±STD) focal length variability (FLV) of all lenses over 8-week culture period.

(n=15)	AFL mean±STD	*P* value Contrast to week1	Mean FLV mean±STD	*P* value Contrast to week1
Week1	29.695±1.35		0.535±.28	
Week2	28.691±1.12	0.001	0.533±0.23	0.982
Week3	29.015±1.23	0.081	0.821±0.45	0.084
Week4	29.467±1.25	0.551	0.746±0.35	0.073
Week5	29.179±1.19	0.184	0.712±0.41	0.055
Week6	29.082±1.21	0.141	0.784±0.25	0.016
Week7	28.659±1.79	0.019	0.745±0.34	0.019
Week8	29.886±2.67	0.737	1.088±0.63	0.005

Table 2.3. Mean (±SEM) dimensions and *P* values as a function of culture time for samples of porcine crystalline lenses.

Dimension Mean ±SEM	Time in organ culture		*P* value 2-tail	
	48hr (n = 97)	168hr (n = 340)	48hr Vs 168hr	1008hr Vs 168hr
Wet Weight (g)	0.406 ± 0.008	0.402 ± 0.003	0.63	0.33
Axial thickness (mm)	7.496 ± 0.044	7.585 ± 0.020	0.07	0.64
Equatorial Diameter (mm)	9.369 ± 0.062	9.450 ± 0.027	0.24	0.12

Note: 168 hours equal 1 week in culture, and 1008 hours equal 6weeks in culture. The number of lenses used for week 6 measurements was 32.

Figure 2.4. Correlation between mean focal length and focal length variability at week 1.

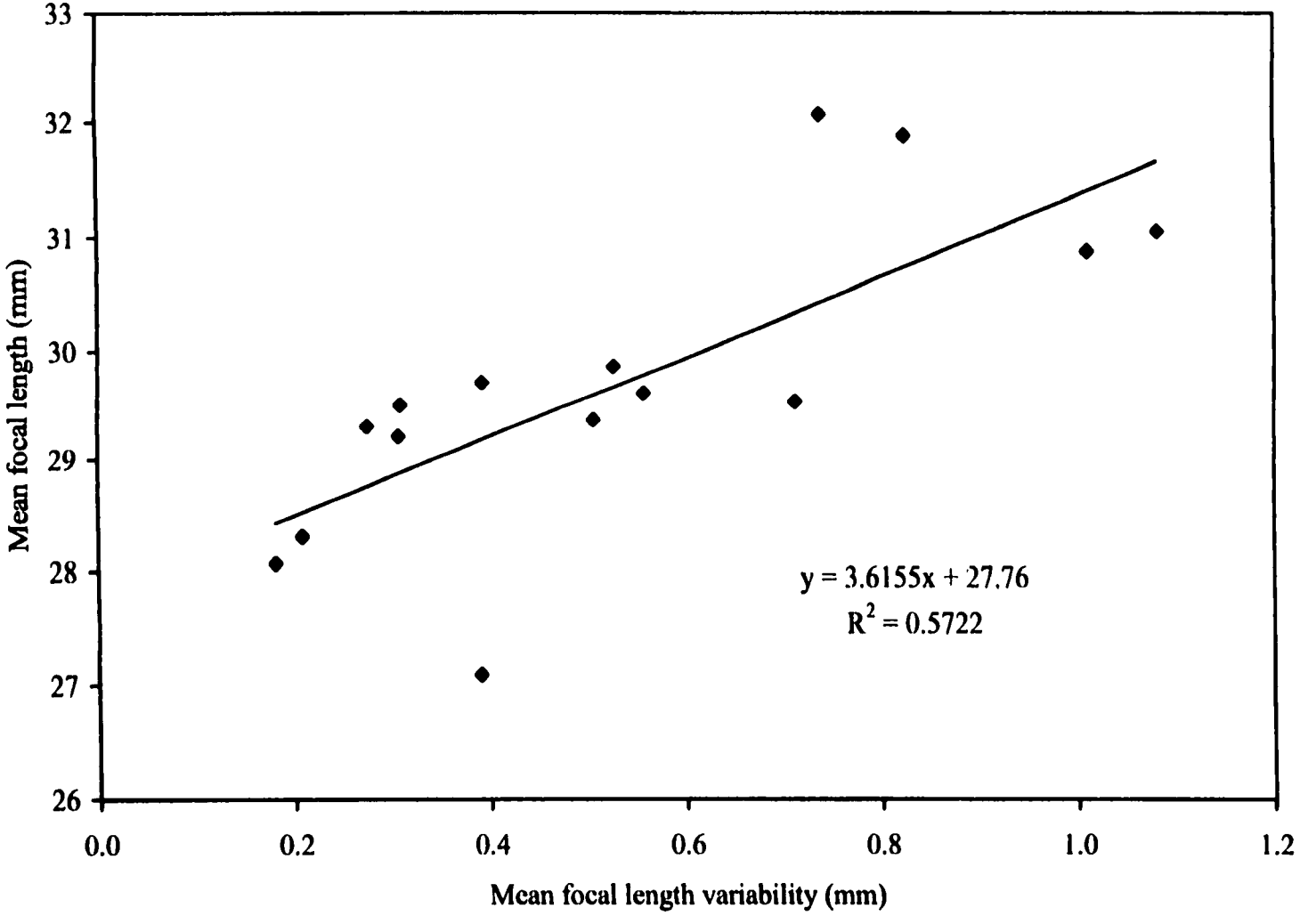

Figure 2.5. Correlation between mean fluorescence with CFDA-AM assay and mean focal length at week 1.

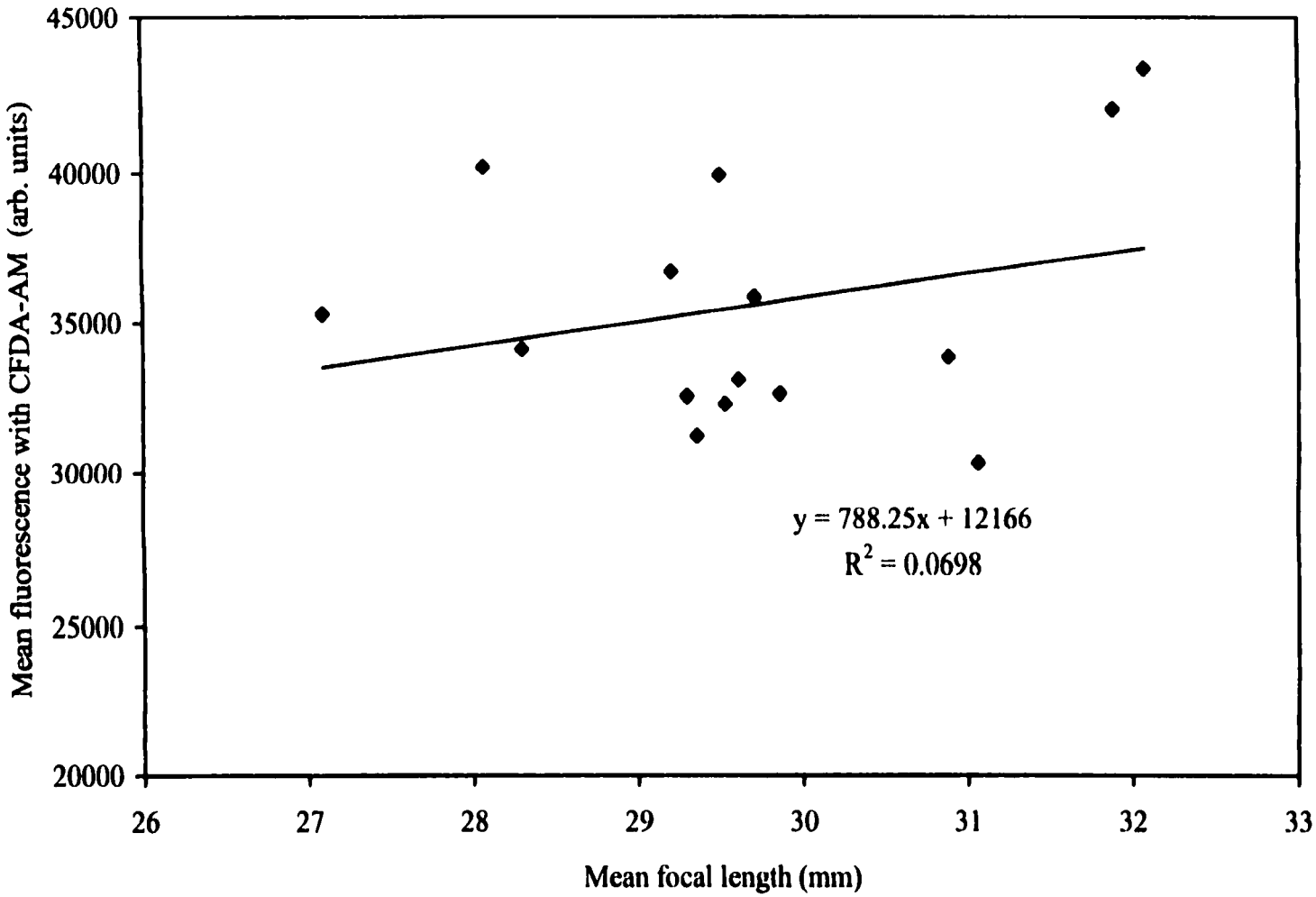

Figure 2.6. Correlation between mean fluorescence with alamarBlue assay and mean focal length at week 1.

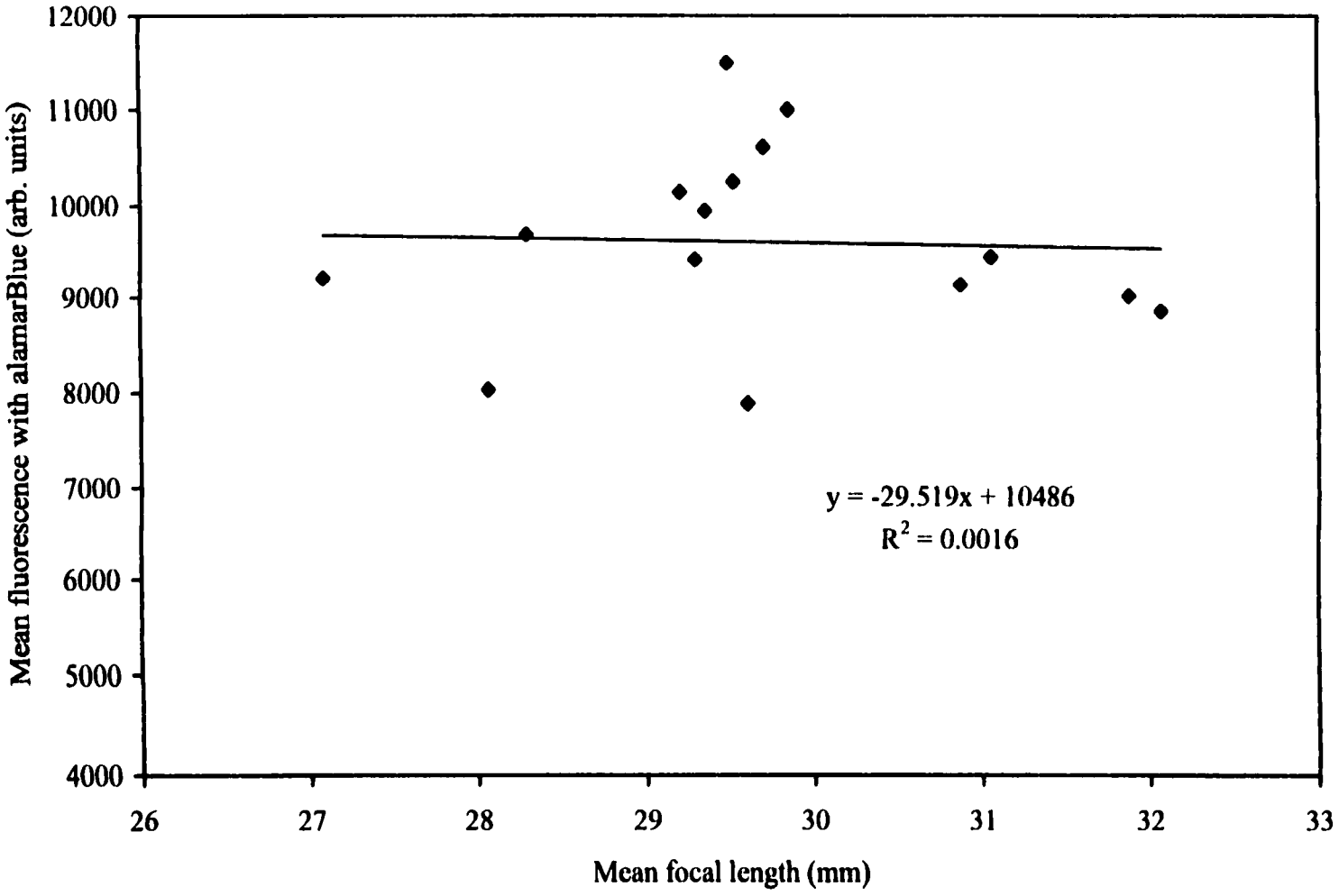

Figure 2.7. Correlation between mean fluorescence with alamarBlue assay and mean focal length variability at week 1.

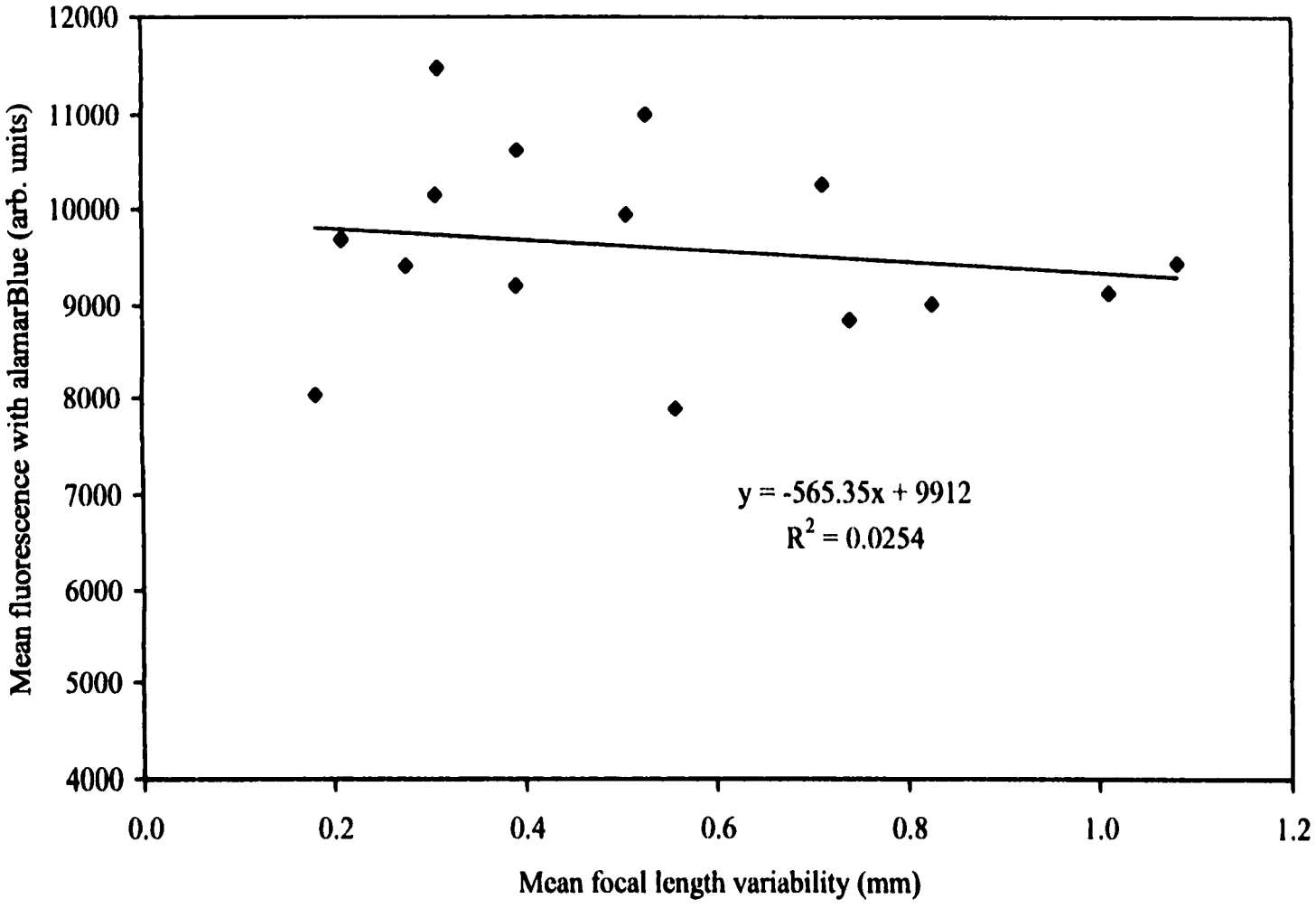

Figure 2.8. Correlation between mean fluorescence with CFDA-AM assay and mean focal length variability at week 1.

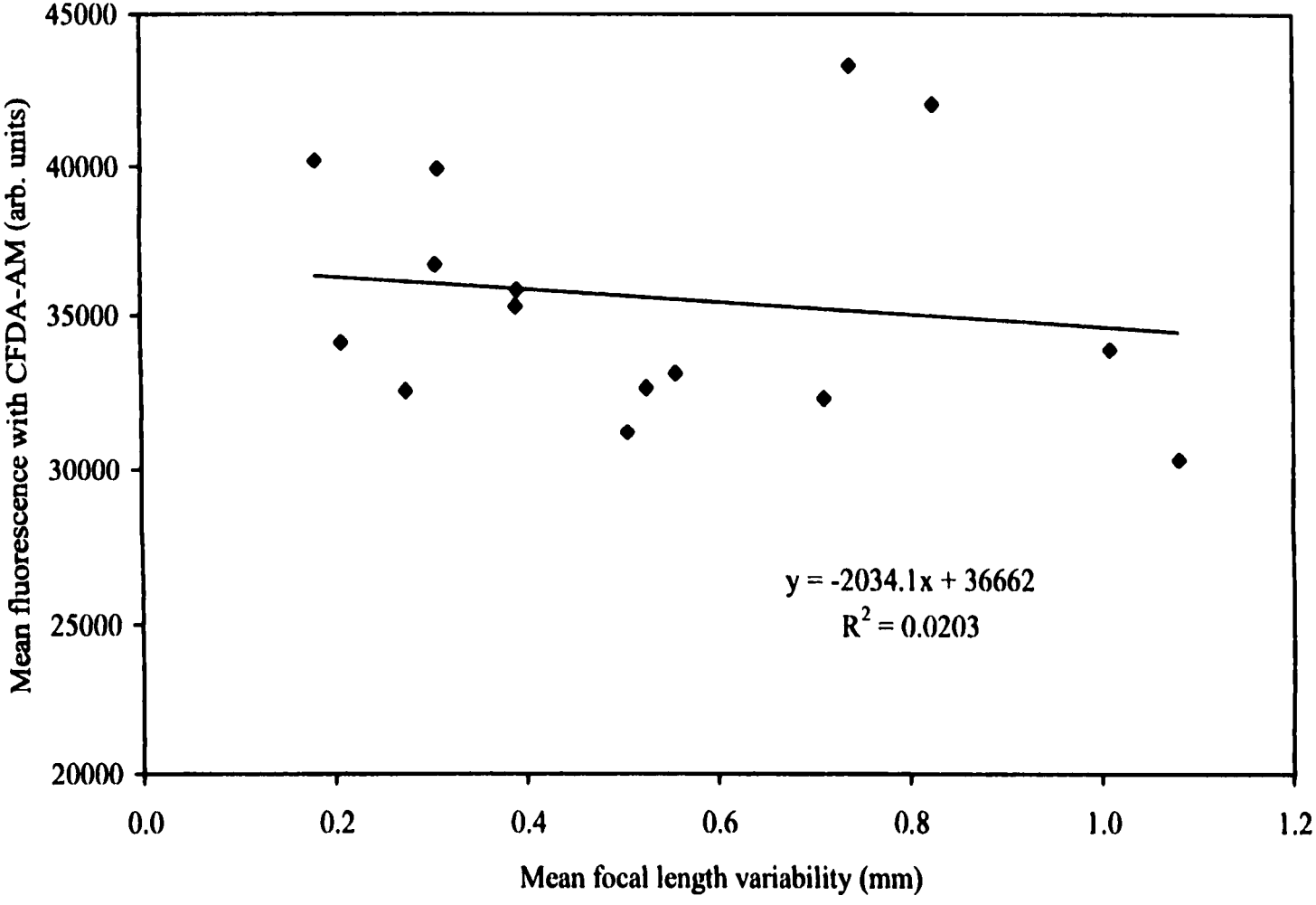

2.5 Discussion

The need to develop more *in vitro* experimental models for UV cataract studies arises from the increasing concerns for animal welfare, which have become central features of society (Sivak et al., 1994; Malakoff, 1999). These concerns have led to a decrease in or elimination of *in vivo* animal studies. The data in the present study indicate that the cultured porcine lens is a good model for organ culture studies relating to lens biology. The assay methodology developed in this study offers a new valid and reproducible *in vitro* cell biology approach to UV cataract and other crystalline lens investigations. Sivak et al., (1994) noted that lens refractive effects are a result of more than one variable, curvature and refractive index distribution, with the effect of change in one variable being neutralized by the other, and suggested that both the average focal length and focal length variability (sharpness of lens focus) could be used as indicators of change in optical function. The data in this study show that both the average focal length (AFL) and focal length variability (FLV) are good indicators of lens change at between weeks 6 and 7, with FLV showing a significant increase ($P = 0.016$) at week 6, and AFL a significant decrease ($P = 0.019$) at week 7 (Table 2.2). Evaluating the correlation between the two optical variables, AFL and FLV, Figure 2.4 shows that lenses with higher AFL tend to have higher FLV ($r = 0.76$). In terms of correlation between SLM and the bioassay measurements, it cannot be readily predicted that a lens with a large average focal length or increased focal length variability will give high fluorescence values with alamarBlue™ or CFDA-AM or vice versa because of the relatively weak correlation between the cellular and optical variables (Figure 2.5 – 2.8). However, interestingly the alamarBlue™

and CFDA-AM readings (Tables 2.1) also begin to show significant alteration at the cellular level at week 7, the same as AFL and FLV (see Tables 2.1 and 2.2), which suggests that the time limit to culture porcine lenses with the culture medium used in this study would be 6 to 7 weeks.

Table 2.3 shows that the wet weight of porcine lenses (age 6-8 month) is 0.406 g, while the *ex-vivo* axial thickness and equatorial diameter are 7.496 mm and 9.369 mm, respectively. Some lenses exhibit little spherical aberration in agreement with Sivak and Kreuzer (1983), however the majority of the lenses in the present study exhibit negative spherical aberration (see Figure 2.3A-C), which is in agreement with Elliott (1993) and Roorda and Glasser (1999). The average focal length was found to be ~28 mm in the present study while Elliott (1993) reported 24 mm for porcine lenses. This could be due to difference in age of animals or to differences in the culture medium. The latter study used 0.9% NaCl within three hours of dissection, while the present study used M199 supplemented with other ingredients. The measurements in Elliott's (1993) study were taken 3-8 hrs after dissection, whereas, measurements in the present study were done at 48 hr and 168 hr (1 week). The above reasons may also explain why an average equatorial diameter of 9.3 mm was obtained in the present study as opposed to 8.5 mm for porcine average lens diameter reported by Elliott (1993). However, the focal length profiles appear the same in both studies. Because majority of the lenses appeared hazy until approximately one week, a 1-week preincubation was chosen for this study. There appears to be no difference in the lens physical dimensions between 48 hour and 168 hour (1 week).

The first study to report the successful use of the porcine lens for organ culture was by Wang et al., (1997). This study compared pig lenses obtained from commercial and non-commercial sources, and concluded that porcine lenses from local commercial sources are not suitable for organ culture since abattoirs routinely use boiling water or hot steam to remove pig hair. They found that 6-8 months old pig lenses kept in TC-199 media supplemented with 1% porcine serum could maintain viability and transparency for up to six days (Wang et al., 1997).

In another study, Wu et al., (1998) used organ cultured porcine lenses to test the effect of commercial balanced salt solution which is used as an irrigating solution during intraocular surgery on crystalline lens. They found that commercial balanced salt solution might increase the risk for lens opacity because of the calcium contained in the solution. The culture duration of Wu et al.'s (1998) study was 7 days, which was approximately the same duration as the study of Wang et al., (1997). Thus, it is evident that there is no previous report in the literature where porcine lens has been cultured longer than 7 days. However, the present study shows that, in an appropriate physiological medium, porcine lenses from abattoir-supplied eyes can be cultured for at least 6 weeks. The lenses used in this study maintained their viability and transparency for up to 6 weeks, as shown by the quantitative measurements obtained from both the fluorometric bioassay and SLM procedures. The fluorometric bioassay approach described in this study appears to be a potential useful methodology for crystalline lens studies. In conclusion, there appears to be agreement in findings from the assay methodology and optical scanning laser system (Tables 2.1 and 2.2) in that both indicate that the porcine lens can be successfully cultured for a minimum of about 6 to 7 weeks.

Chapter 3

Determination of *in vitro* action spectrum and recovery for UV induced photodamage using organ cultured porcine crystalline lens

3.1 Abstract

To determine the median effective dose (ED_{50}) of UVB and UVA required for induction of UV cataract formation and the action spectrum for acute *in vitro* UV cataractogenesis, the organ cultured intact whole porcine lenses were used as a model. The recovery pattern was also investigated. Aseptically dissected lenses were preincubated in culture medium maintained at 37°C and 4% CO_2 and 96% air for one week. At one week, lenses were exposed to a predetermined UV radiant exposure (J/cm^2) at specific waveband ranging from 270 nm to 370 nm. The UV energy was generated from a PRA integrated arc lamp system using a water cooled 1000 W high pressure xenon lamp. The output was limited with a water filter, a monochromator, and secondary optics. The monochromator was used to select a specific wavelength. The exposure time was controlled using a preset electronic shutter. The ED_{50} was determined by using probit analysis of responses versus number of lenses exposed at defined energy levels by up-and-down (staircase) method. Irradiated spots (3.06 mm^2) on the lenses were monitored every 6-12 hrs up to 48 hr post irradiation for any morphologic changes (i.e. UV photodamage) with photomicrography. Mean (±STD) induction time was 44±4.7 hr. Permanent UV induced cataract was obtained at twice the threshold values for UVB and UVA. An action spectrum for *in vitro* UV induced cataract using whole organ cultured lens is established. The recovery pattern

appears to be similar to the *in vivo* situation. The relationship between these *in vitro* data and the data from previous studies is discussed.

3.2 Introduction

It is a generally agreed that high solar UVB irradiance levels in the environment would increase the risk of cataract, skin cancer, and perhaps immune problems in humans, terrestrial and aquatic animals (Brown, 1999). Moreover, elevated UVB levels may perturb marine ecology, killing important algae and bacteria. Atmospheric scientists first detected the ozone hole over the South Pole in 1985, the apparent result of chemical reactions caused by chlorofluorocarbons (CFCs) and other pollutants in the stratosphere. Ever since, their calculations have predicted that loss of stratospheric ozone (which absorbs much of the harmful UVB radiation (290-315 nm) would allow more abiotic UVR to reach the surface of the Earth. Recently scientists at the National Institute of Water and Atmospheric Research in Lauder, New Zealand reported that over the past 10 years, peak levels of dermatogenic and DNA-damaging UV rays have gradually been increasing in New Zealand, just as the concentrations of stratospheric ozone have decreased (McKenzie et al., 1999). According to their report, by the summer of 1998-99, peak sunburning UV levels were about 12% higher than they were during similar periods earlier in the decade. Their report provides the strongest evidence yet that degradation of the stratospheric ozone layer is ongoing, and causes more hazardous UV exposure conditions for life on the Earth's surface (Brown, 1999). It is evident that stratospheric ozone thinning is occurring not just in the sparsely populated polar regions, but also above populous mid-latitude regions such as northern Europe, Canada, New Zealand, and

Australia (Brown, 1999). This underscores the need for further UV induced cataract and lens research.

In the eye, it is believed that UV photochemical damage occurring in the crystalline lens can persist for a long time, causing temporary or permanent impairment of vision. The exact targets and the detailed mechanisms that are responsible for UV-induced cataracts remain to be determined. An important aspect of solar UVR investigation is the UV cataractogenic action spectrum in the waveband to which humans are exposed. In terms of UV-lens research, the *in vivo* UV action spectrum by Pitts et al., (1977a and 1977b), and the *in vitro* UV action spectrum for lens epithelial cells by Andley et al., (1994; 1995), are available in the literature. However, *in vitro* UV action spectrum data for the cultured intact whole lens are lacking. Since many experimental models now focus on the intact cultured whole lens, and because the cellular targets and mechanisms of action of UVR vary as a function of wavelength, it is necessary to establish an *in vitro* UV action spectrum for the cultured crystalline lens. From the action spectrum, the mechanisms of UV effects within the wavelength range can be effectively studied.

The action spectrum of a biological response is the variation in magnitude of the response with wavelength. The shape of the resulting curve is related to the absorption of the radiation-absorbing molecule initiating the response. This section of my thesis determined the action spectrum for *in vitro* UVR cataract formation (gross superficial opacities) using organ cultured whole porcine crystalline lens. Pitts et al., (1977a and 1977b), developed the current data on the crystalline lens in vivo UV action spectrum for wavelengths from 295 nm to 365 nm. These data are the best existing data on *in vivo* UV

action spectrum for cataractogenesis (Soderberg, 1990). The effort to reduce or eliminate the use of live animals in biomedical research is now shifting experimental approaches from *in vivo* to *in vitro*. The data of Pitts et al., (1977a and 1977b) have been used for some time for most *in vivo* UV experimental applications. More recently, a series of experiments on *in vitro* UV action spectra for isolated lens epithelial cells has been reported by Andley et al., (1994). Their data may not be directly applicable to studies involving the whole intact lens. Thus, the purpose of this study was to determine the *in vitro* action spectrum for UV lenticular damage in porcine lens and to study the recovery pattern. The cultured porcine lens was used. Since its embryological growth and development is typical of mammals, and its shape and size are similar to the human lens, some inferences may be made to the human lens.

3.3 Methods and Materials

3.3.1 Tissue Preparation and UV Exposure

Porcine eyes were collected from a local abattoir. The lenses were aseptically dissected 1-3 hr post-mortem and placed in a two-compartment chamber for preincubation for one week in culture medium maintained at 37°C and 4% CO_2 and 96% air. The composition of the culture medium is the same as reported in chapter 3. At one week, the anterior surface of the lens was exposed to a predetermined UV radiant exposure (J/cm^2) at a specific waveband with the bandwidth centred on 270, 275, 280, 285, 290, 295, 300, 305, 310, 315, 320, 330, 340, 350, 360, 365 and 370 nm wavelengths. During exposure, the medium was reduced so that approximately 1 mm remained on top of the anterior surface

of the lens. The lens exposures to different UV radiant energy levels at the defined wavelengths were done at room temperature.

3.3.2 UVR Exposure System

UV energy was generated from a Photochemical Research Associates (PRA) integrated arc lamp system using a water cooled 1000 W high pressure xenon arc (Photochemical Research Associates Inc., London, Ontario, Canada), (see Figure 3.1). The source for UVB and UVA radiation was controlled by a PRA lamp power supply (model 301), which is water-cooled for optimal stability. In the power supply, provision is made for automatic shutdown if the supply temperature exceeds preset limits in case of coolant failure. An automatic reset resumes power supply operation when safe temperature limits are re-established. Figure 3.2 shows a schematic diagram of the UV irradiation apparatus. The infrared (IR) output was absorbed by a 9 cm long quartz-enclosed de-ionised distilled water chamber placed between the arc source exit and a quartz condensing lens. The quartz condensing lens (~5 cm diameter) placed between the water chamber and monochromator focused the UV radiation to the entrance slit of the monochromator.

Monochromatic radiation at desired wavelengths was obtained using an Oriel monochromator (Oriel Corporation, Stamford, Connecticut, USA; model 7240) with a 2400 lines / mm holographic grating blazed at 200-400 nm and secondary optics including transmittance and reflectance filters. The monochromator wavelength reading was multiplied by the wavelength dial and bandwidth factor of 0.5, for each wavelength setting by the investigator. A front surface mirror was used to deflect the beam by 90° to impinge on the lens anterior surface at a distance of 8 cm. A 50.8 mm diameter quartz-

condensing lens (Edmund Scientific Co., Barrington, New Jersey, USA) was placed at the entrance, and another 25.4 mm diameter quartz-condensing lens at the exit aperture of the mirror housing, respectively. The UV beam area on the lens was 3.06 mm^2. A black bellows was used to join the monochromator exit slit and the front surface mirror housing to reduce any room light effect, and also to eliminate radiation leakage. The shortest and the longest wavelengths for this study were 270 nm and 370 nm, respectively. The wavelengths and corresponding average irradiance levels used for the action spectrum determination are given in Table 3.1. The average bandwidth at half peak ranged from 12 to16 nm for the wavebands. As examples, Figures 3.3A and B show the spectral outputs of 305 nm and 365 nm wavebands. The arc lamp and optical system were enclosed, and before each use purged with nitrogen to prevent ozone formation. Before each irradiation of a lens, the UV output in μW was measured with an 88XL Photodyne radiometer together with a model 450 UV sensor head (serial no. 10205A; Optikon Corp., Kitchener, Ontario, Canada) which was cross calibrated against a standard source traceable to US National Institute of Science and Technology (NIST). The 88XL radiometer is a current measuring meter with a digital display. The conversion from irradiant power to electrical current takes place in the plug in sensor head. The UV sensor head connected to the radiometer with a Photodyne extension cable model #3001 was placed in the position to be occupied by the anterior surface of the cultured lens. During the exposure, the lens was centred normally to the UV beam. The lens in its culture chamber was placed on a container holder (from an Olympus light microscope) for accurate alignment and distance (Figures 3.1 and 3.2). Stray UV energy was measured to be less than 0.1%; and since this amount is negligible, it was ignored in the evaluation of the radiant exposures.

Figure 3.1. Photograph of UV irradiation and dosimetry instrumentation.

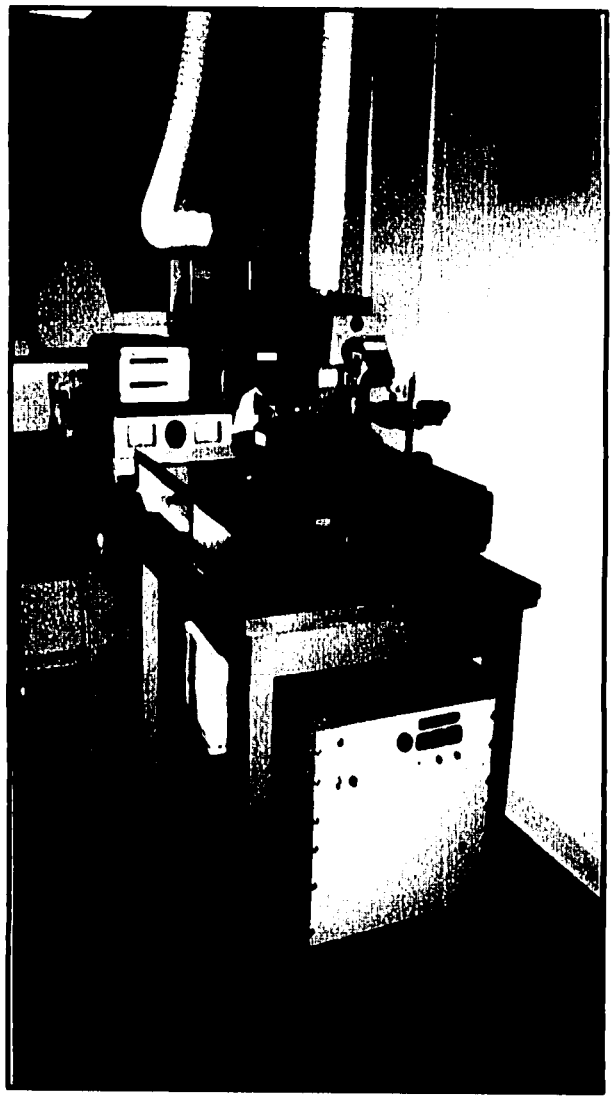

Figure 3.2. A schematic diagram of the UV narrow band irradiation system.

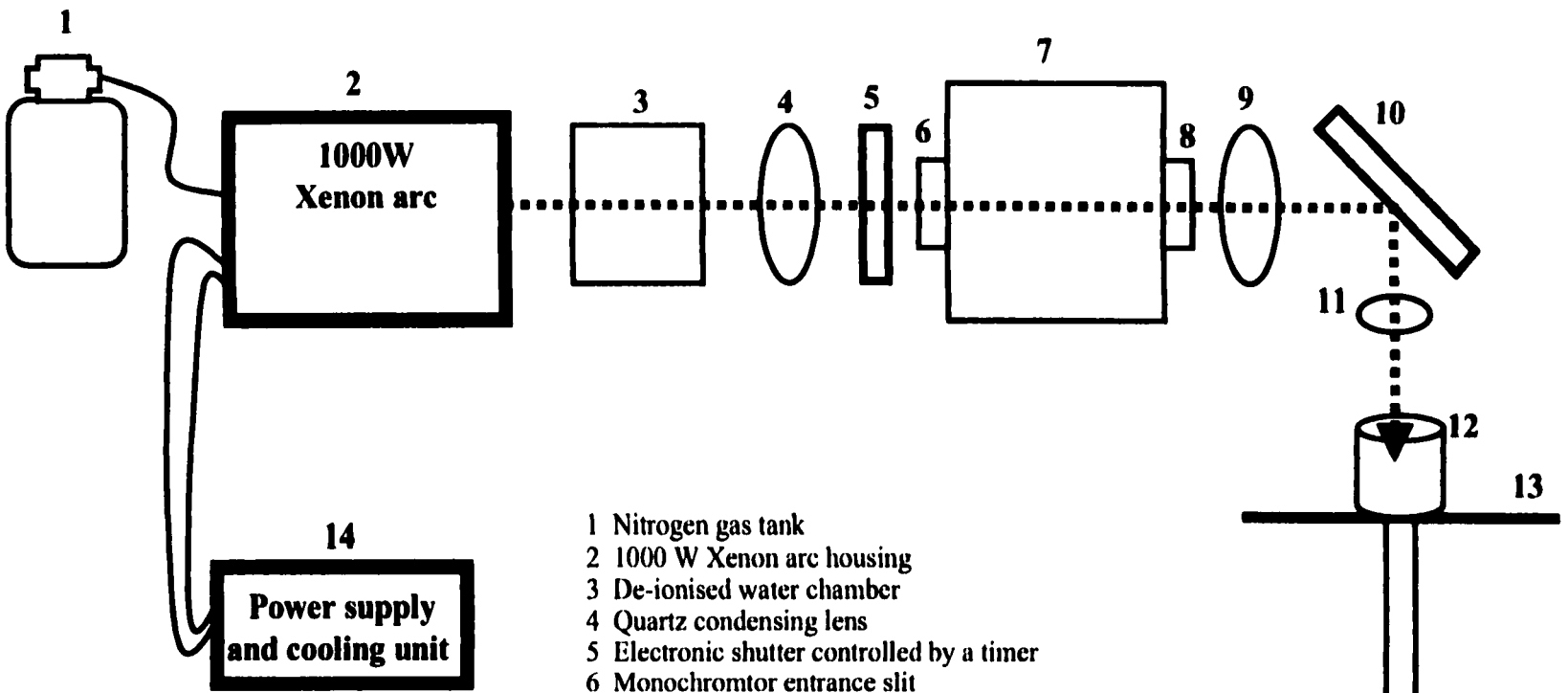

1 Nitrogen gas tank
2 1000 W Xenon arc housing
3 De-ionised water chamber
4 Quartz condensing lens
5 Electronic shutter controlled by a timer
6 Monochromtor entrance slit
7 Grating monochromator
8 Monochromator exit slit
9 Quartz condensing lens
10 Front surface mirror
11 Quartz condensing lens
12 Crystalline lens holder
13 Base for lens container and aligning lens
14 Regulated power supply and cooling system

Figure 3.3 (A and B). Spectral outputs of 305 nm and 365 nm wavebands.

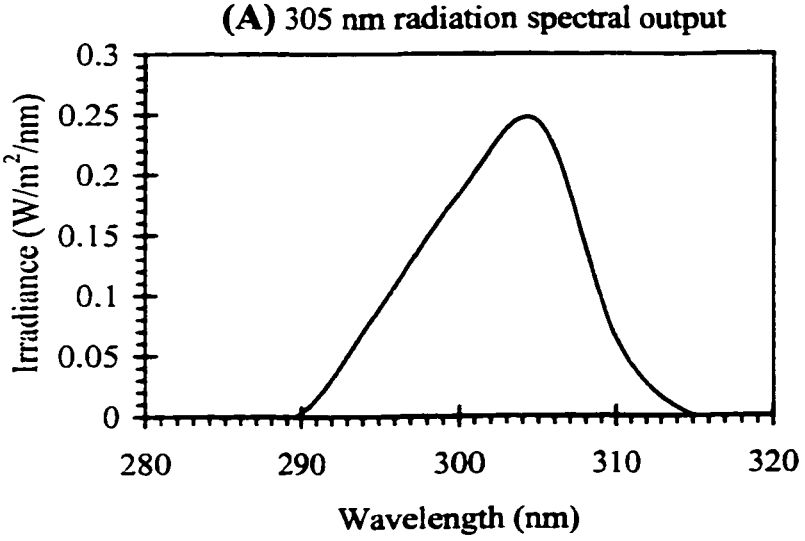

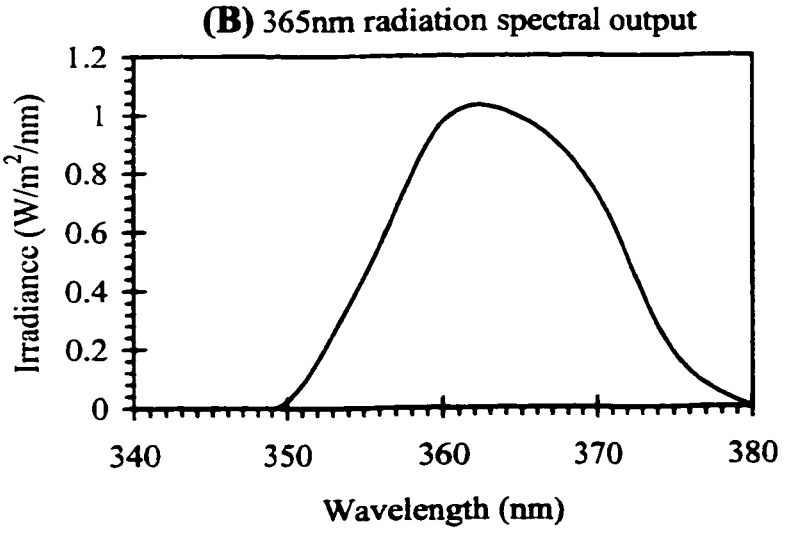

To convert the radiometer measurement to irradiance, the measured value was multiplied by area irradiated on the lens and the linear multiplication factor from the calibration curve. The irradiated area at the lens surface was 3.06 mm^2 (0.0306 cm^2). The reciprocal of 0.0306 equals 32.68; thus, the unit area multiplication factor for conversion to irradiance was 32.68 throughout this experiment. For example, the linear multiplication factor for 300 nm was 1.08; therefore, a reading of 48μW would be equal to 1694 (i.e. 48x1.08x32.68) $\mu W/cm^2$ as irradiance. Radiant exposure time was determined using the following radiometric equation:

$$t = H/E_\lambda,$$

where t = exposure duration (seconds), H = radiant exposure (J/cm^2), and E_λ = measured irradiance (W/cm^2). The duration of exposure was controlled by a preset electronic counter, which automatically closed the shutter after each predetermined exposure. The shutter system allowed the control of exposure duration to any length. In this study exposure time ranged from 49 seconds to ~22 hours.

3.3.3 Exposure Sequence and Assessment

A modified staircase (up-and-down) method (Finney, 1971), with doubling, 50%, 25% and 10% decrement / increment steps, was used to obtain threshold values for each waveband from 270 to 370 nm. Five lenses were irradiated for each energy level at each waveband. If none of the 5 lenses at a given exposure level showed damage, then the dose was doubled. If all 5 lenses showed damage, the dose was reduced by 50%. If 3 out of 5

lenses did not show damage, the energy level was arbitrarily increased by 25% or 10% of the immediate previous dose. This was continued until at least 3 out of 5 lenses were observed to show damage before proceeding to the next energy level or waveband.

For the purpose of deciding on the starting point, the threshold data of Pitts, Cullen and Hacker (1977a and b) were used. They found that the most efficient waveband for lenticular damage was 300 nm, which had a radiant exposure threshold of 0.15 J/cm^2. An approximate UV energy level of 0.2 J/cm^2 at 300 nm was chosen as the starting point in the present study. Therefore, the first exposure was made at 300 nm, with 0.2 J/cm^2 delivered to the anterior lens surface. The sequence involved irradiation for wavelengths from 300 to 270 nm in 5 nm intervals, and then 305 to 370 nm, in 5 nm or 10 nm intervals. Observation time was limited to a maximum of 36 to 48 hr after irradiation. Irradiated spots on the lenses were monitored every 6-12 hrs for any morphologic lesions (i.e. superficial or subcapsular opacities), induction time and lesion pattern with photomicrography (NIKON dissecting microscope, Japan). During photomicrography, the eyepiece magnification was set at 10X and microscope magnification at 2.5X.

Photographs of the lesions patterns (square-shaped area of 3.06mm^2) were randomly taken at appearance or during recovery. UV irradiated lenses were visually compared to untreated controls. Again, if no lesion was found at 36-48 hr, the dose was doubled or increased by 50%, 25% or 10% for the next exposure. If there was a lesion with the increase, the dose was arbitrarily decreased by 25% or 10% until there was no lesion. For each subsequent set of lenses, the dose was decreased or increased on the basis of the response of the previous set of lenses lens to a lower radiant exposure, until moderate or severe lesions were observed in at least 3 lenses out of 5. The ED_{50} (i.e. 50%

probability of damage, with 95% confidence interval) was then calculated by using probit analysis (Finney, 1971) (Appendix 7.1B – 7.17B). Induction time, how many lenses were used per dose and other observations were recorded. Table 3.3 shows how the data were arranged for probit analysis. With probit analysis ED_{50} was determined for wavelengths 270, 275, 280, 285, 290, 295, 300, 305, 310, 315, 320, 330, 340, 350, 360, 365 and 370 nm. The 365 nm waveband was included because most studies on UVA effects centre on this wavelength. The ED_{50} values were plotted as a function of wavelength to determine the action spectrum curve.

The second part of this section of the study was to investigate the time course for recovery of *in vitro* UV induced cataract at 300 nm and 350 nm, for UVB and UVA, respectively. The threshold values obtained in the first part were used as reference radiant energy levels. Organ cultured porcine lenses (group 1) were irradiated with 300 nm UVB at threshold level (0.07 J/cm^2), two times threshold (group 2), and five times threshold (group 3). Group 4 lenses were exposed to 222.6 J/cm^2 of 350 nm UVA, which was two times threshold. Each irradiated spot on the anterior lens surface (3.06 mm^2) was monitored by photomicrography for 4 weeks post-irradiation. The lenses were examined every 12-24 hrs in the first 2 weeks and then once each week post-exposure. UVR experimental cataract was defined as a cluster of discrete dots in the lens anterior subcapsular layer. The criterion for recovery was the complete disappearance of the lesions.

3.3.4 Damage Grading

The severity of the lesions in the lenses was graded as follows:

1) (–) no damage

2) (+) moderate or threshold damage, lesions ≤ half of square pattern

3) (+ +) severe damage, lesions fill more than half of square pattern

4) (+ –) lesions disappearing (sign of recovery)

5) (– –) lesions completely disappeared (full recovery)

Any lens having a (+) sign means that the lens showed damage at that particular energy level (dose). For analysis, a lens with (+) or (+ +) grade is counted with the number of lenses damaged. Any lens with a lesion showing recovery was graded (+ –), and the time that the repair trend was observed was recorded. If a lens lesion showed complete recovery, it was graded (– –), and the time of the observation noted. Any lens with a damaged capsule was discarded. The control lenses were also observed for any morphological changes.

3.4 Results

Part I: Approximately six hundred and forty-eight lenses were used in this study. The irradiated spots on the lenses showed anterior subcapsular discrete dot opacities, which appeared initially as small white dots and slowly coalesced into a white patch within the irradiated spot. The pattern of the discrete dot opacities (lesion) was graded using the scheme explained in section 3.3.4. Using the 300 nm waveband data as an example, an ED_{50} value of 0.06952 (95% confidence interval, 0.05746 – 0.08781) was obtained for 300 nm using probit analysis. Table 3.2 shows the ED_{50} (with 95% confidence interval) for all wavebands. Figure 3.4 is a representative plot of the 50% probability of damage for defined radiant exposures at the 300 nm waveband. The 50% probability radiant exposures (i.e., ED_{50} values) were significantly dependent on wavelength (Figure 3.5). The data indicate shorter damage latency and slower recovery for higher UV energy levels, while the reverse is the case for lower energy levels.

Data arrangements for all wavebands are shown in Appendices 7.1A to 7.17A. The summary of the probit analysis for other wavebands are shown in Appendix 7.1B – 7.17B. Graphically, a threshold can be obtained by connecting the 50% probability on the Y axis to the corresponding radiant exposure value on the X axis through the regression line intercept. The different ED_{50} values of all the wavebands were collated and plotted to obtain the action spectrum (see Figure 3.5). It should be noted that at 370 nm, the highest dose that could practically be given produced no visually observable lesion. At some high dose levels, e.g. for a 47.45 J/cm^2 dose at 330 nm waveband, a lesion was observed earlier at about 18-24 hr post irradiation (see Appendix 7.1A – 7.17A). For example, a 0.065 J/cm^2 dose at 275 nm waveband gave an earlier lesion at 24 hr post-irradiation (see

Appendix 7.2A). The contribution of the adjacent wavelengths was considered to be relatively negligible.

Part 2: With respect to damage reversibility, group 1 lenses showed lesions at 36 to 48 hr post exposure, and complete recovery after 10 days (Figure 3.6). In group 2 lenses, lesions were visible at 24 hr, with no complete recovery occurring at week 4 after exposure (Figure 3.7). The lesions in group 3 lenses appeared at 12 to 24 hr, and 40% or more of the lesions persisted with suture prominence in all lenses at least 4 weeks post-exposure (Figure 3.8). Among group 4 lenses, lesions were visible at 24 hr post irradiation, with approximately 50% of the lesions persisting in all the lenses up to the 4 week duration of study (Figure 3.9).

Table 3.1. Wavelengths and average irradiances used for the action spectrum determination.

Wavelength (nm)	Irradiance ($\mu W/cm^2$)
270	499
275	695
280	1408
285	1553
290	1553
295	1447
300	1768
305	2365
310	2753
315	2753
320	2682
325	2549
330	2576
340	4589
350	5336
360	5529
365	5591
370	5794

Table 3.2. Summary of probit analysis (ED_{50}: 50% probability and 95% confidence limits) for effective dose for respective wavebands.

Wavelength (nm)	ED_{50} Radiant exposure (J/cm^2)	95% confidence limits	
		Lower	Upper
270	0.05718	N/A	0.06754
275	0.04215	0.03060	0.05007
280	0.02776	0.02014	0.03113
285	0.02193	0.01977	0.02455
290	0.02720	0.24690	0.03017
295	0.02949	0.01396	0.03154
300	0.06952	0.05746	0.08781
305	0.09576	0.07406	0.11240
310	0.23400	0.19787	0.28886
315	0.74254	0.54887	0.89013
320	3.13211	2.47667	4.14227
325	18.7036	15.55044	23.47022
330	28.0106	24.94882	32.33166
340	48.2662	34.96831	55.54889
350	111.269	N/A	N/A
360	164.030	N/A	N/A
365	137.193	N/A	N/A
370*	N/A (*445.92)	N/A	N/A

Note: *No damage was obtained with ~7 trial exposures for 370nm at 445.92J/cm^2 which was greater than 3X ED_{50} for 365nm. N/A indicates not available, could not be determined, or negative values.

Table 3.3. An example of data arrangement for probit analysis at the 300 nm waveband.

Set of lenses	Radiant exposure (J/cm^2)	# of +ve responses	# observed
1	0.0500	0	5
2	0.0625	2	5
3	0.0780	4	5
4	0.1000	5	5
5	0.2000	5	5

Note: Using the SPSS for Windows involved the following steps:

1) Go to SPSS for Windows under program,

2) click on SPSS 10.0 for Windows, enter data using data editor [with columns as I) set of lenses; II) radiant exposure; III) # of positive response (i.e. damage); and IV) number of lenses observed for the particular radiant exposure],

3) go to "analyse" and click on "probit" under "regression,

4) in the probit interface put: a) response under the Response frequency, b) number under the Total observed, c) exposure under Covariate, and

5) ensure to check probit under Model, then click OK.

Table 3.4. Relative effectiveness of the *in vitro* UV action spectrum to induce cataracts.

Wavelength (nm)	Threshold Radiant exposure (J/cm^2)	Relative efficiency
270	0.05718	0.5
275	0.04215	0.7
280	0.02776	1.1
285	0.02193	1.3
290	0.02720	1.1
295	0.02949	1.0
300	0.06952	0.4
305	0.09576	0.3
310	0.23400	0.1
315	0.74254	0.04
320	3.13211	0.009
325	18.7036	0.002
330	28.0106	0.001
340	48.2662	0.001
350	111.269	0.0
360	164.030	0.0
365	137.193	0.0

Note: The relative efficiency is with respect to the 295nm waveband.

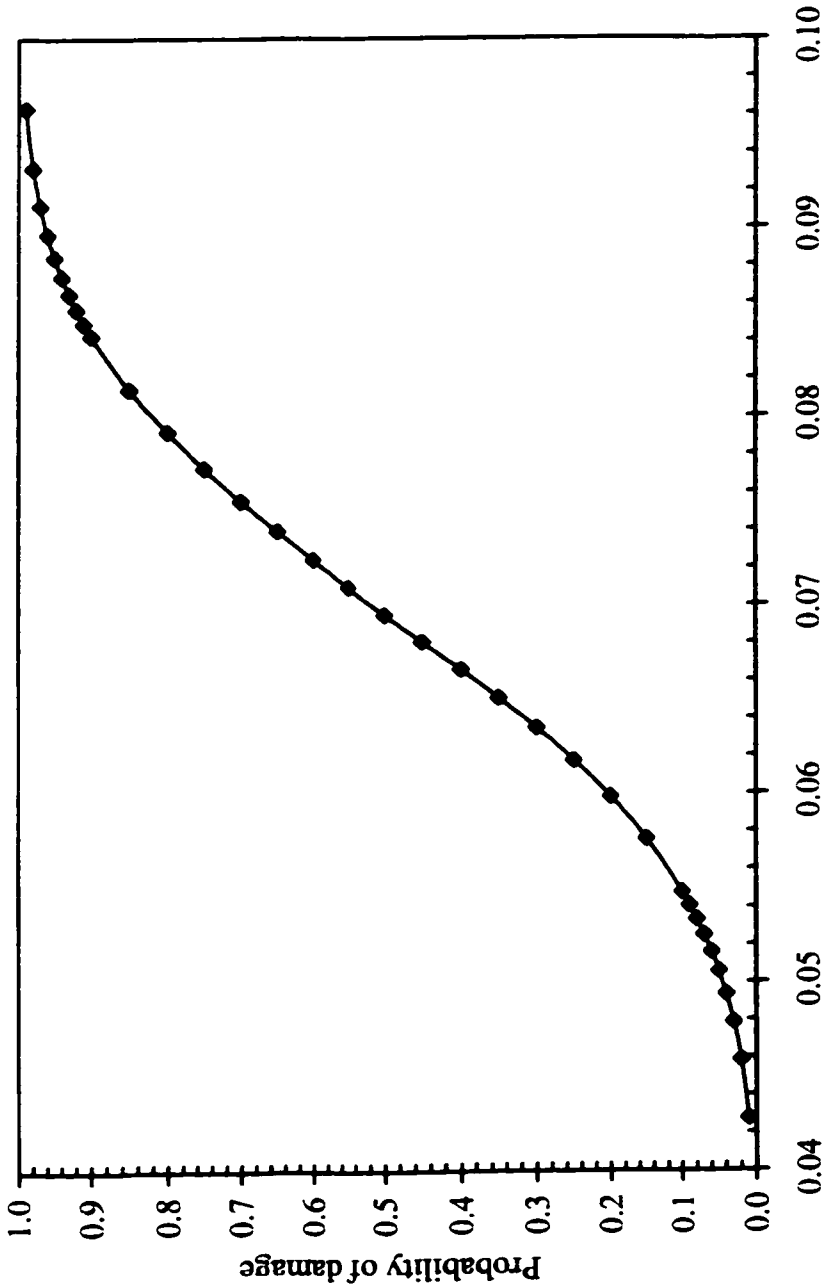

Figure 3.4. Plot of damage probability versus radiant exposures for the waveband centred on 300 nm.

Figure 3.5. Plot of radiant exposure (ED_{50}) versus wavelengths showing the action spectrum for *in vitro* UV cataract formation using organ cultured porcine lenses.

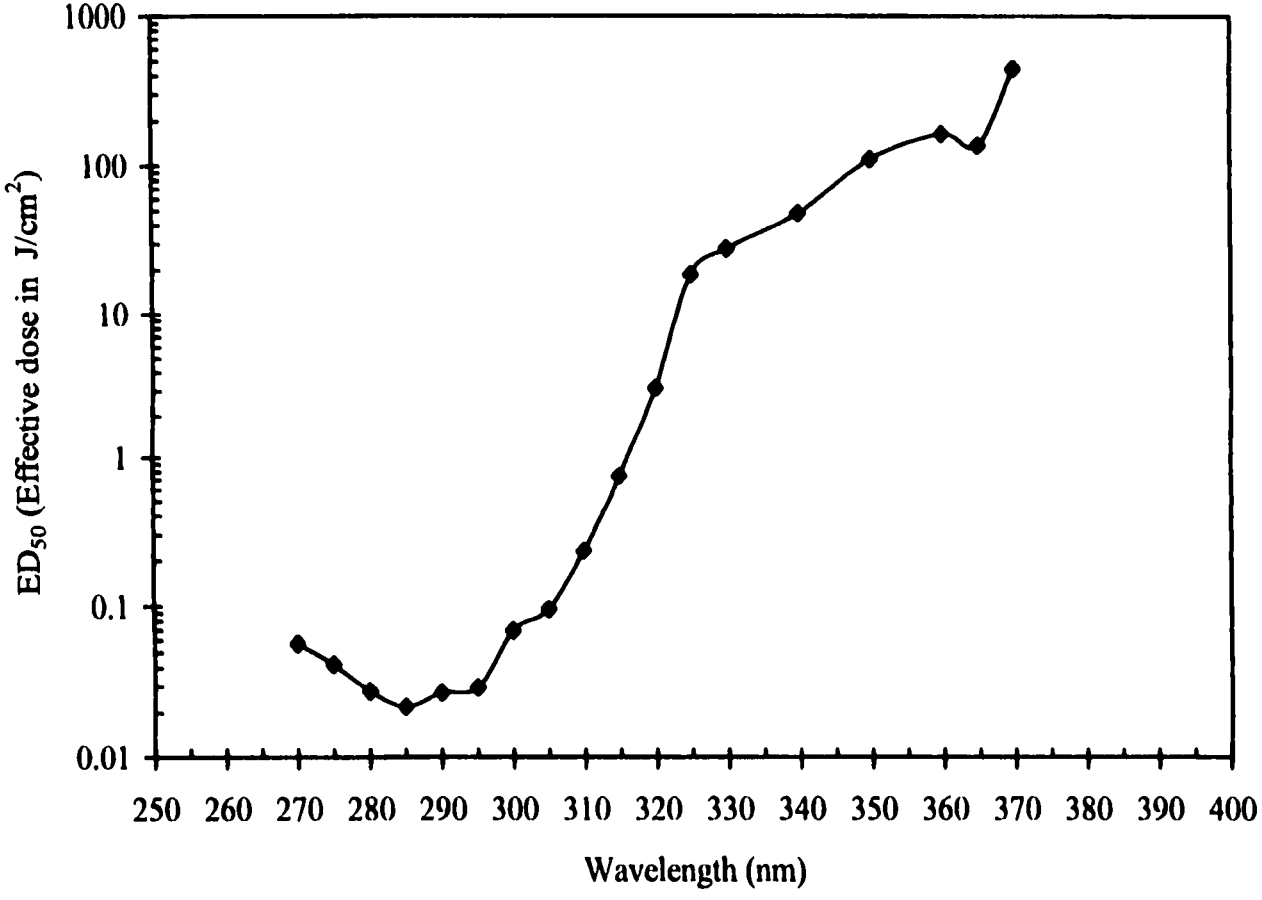

Figure 3.6. A representative illustration of morphological changes in exposed group 1 lenses at 300 nm UVB threshold (0.07 J/cm^2). Complete recovery at 2 weeks after exposure. Bar equals 1.75 mm.

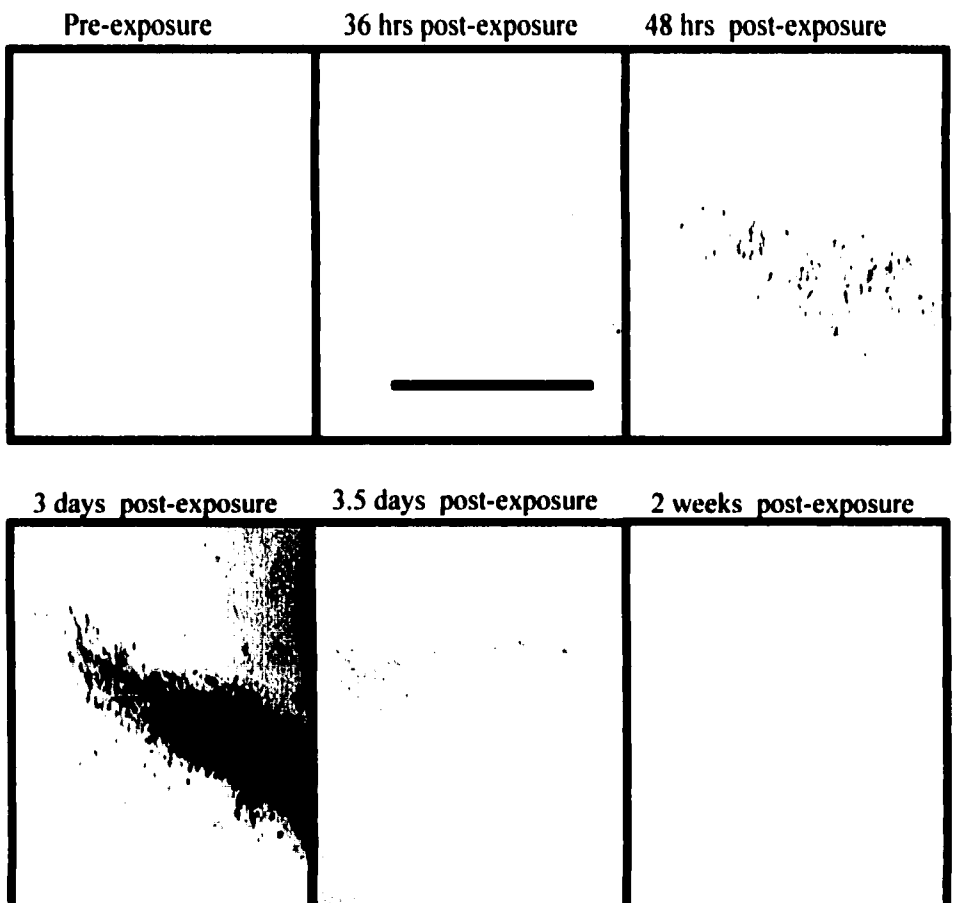

Figure 3.7. A representative illustration of morphological changes in exposed group 2 lenses at 300 nm UVB 2X threshold (0.14 J/cm^2). No complete recovery at 4 weeks after exposure. Bar equals 1.75 mm.

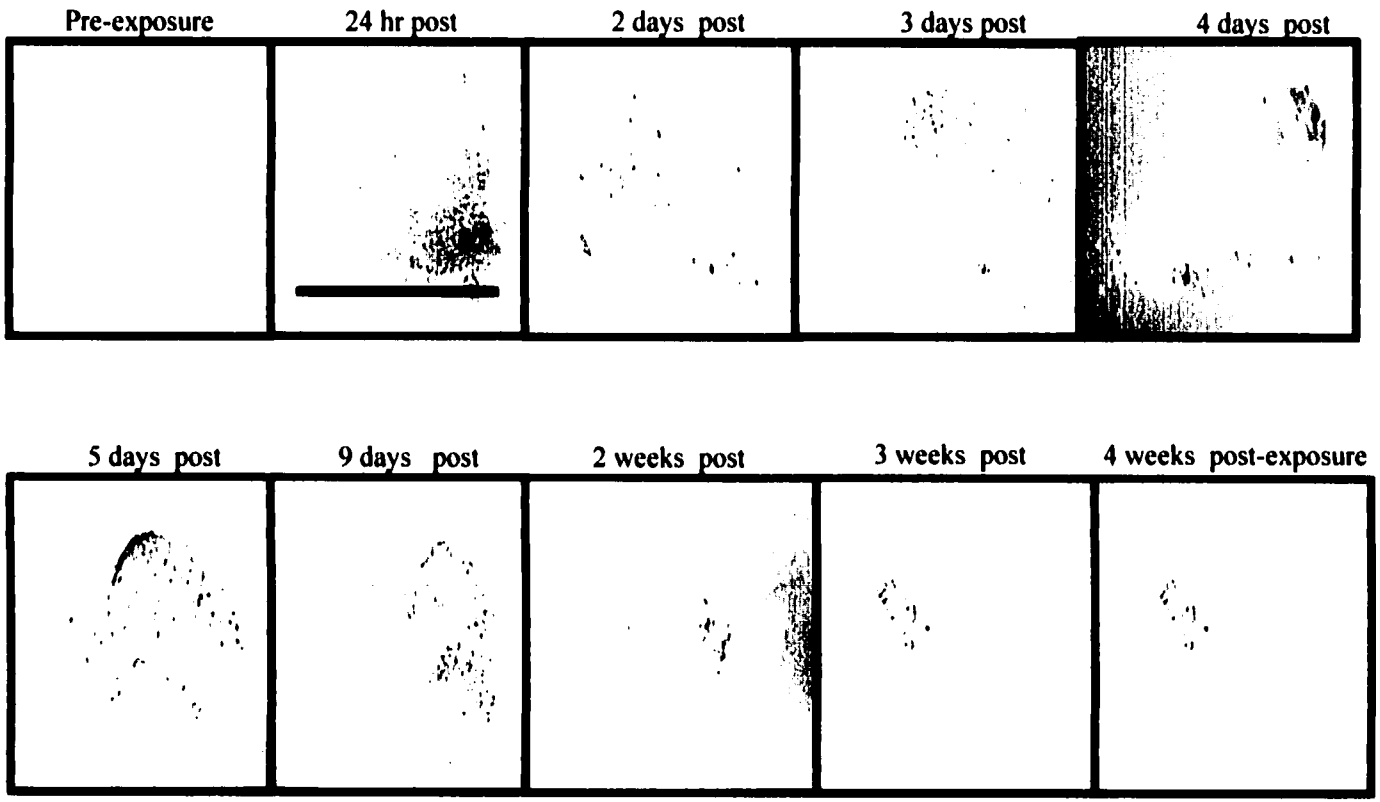

Figure 3.8. A representative illustration of morphological changes in group 3 lenses at 300 nm UVB 5X threshold (0.35 J/cm^2). No complete recovery 4 weeks after exposure. Bar equals 1.75 mm.

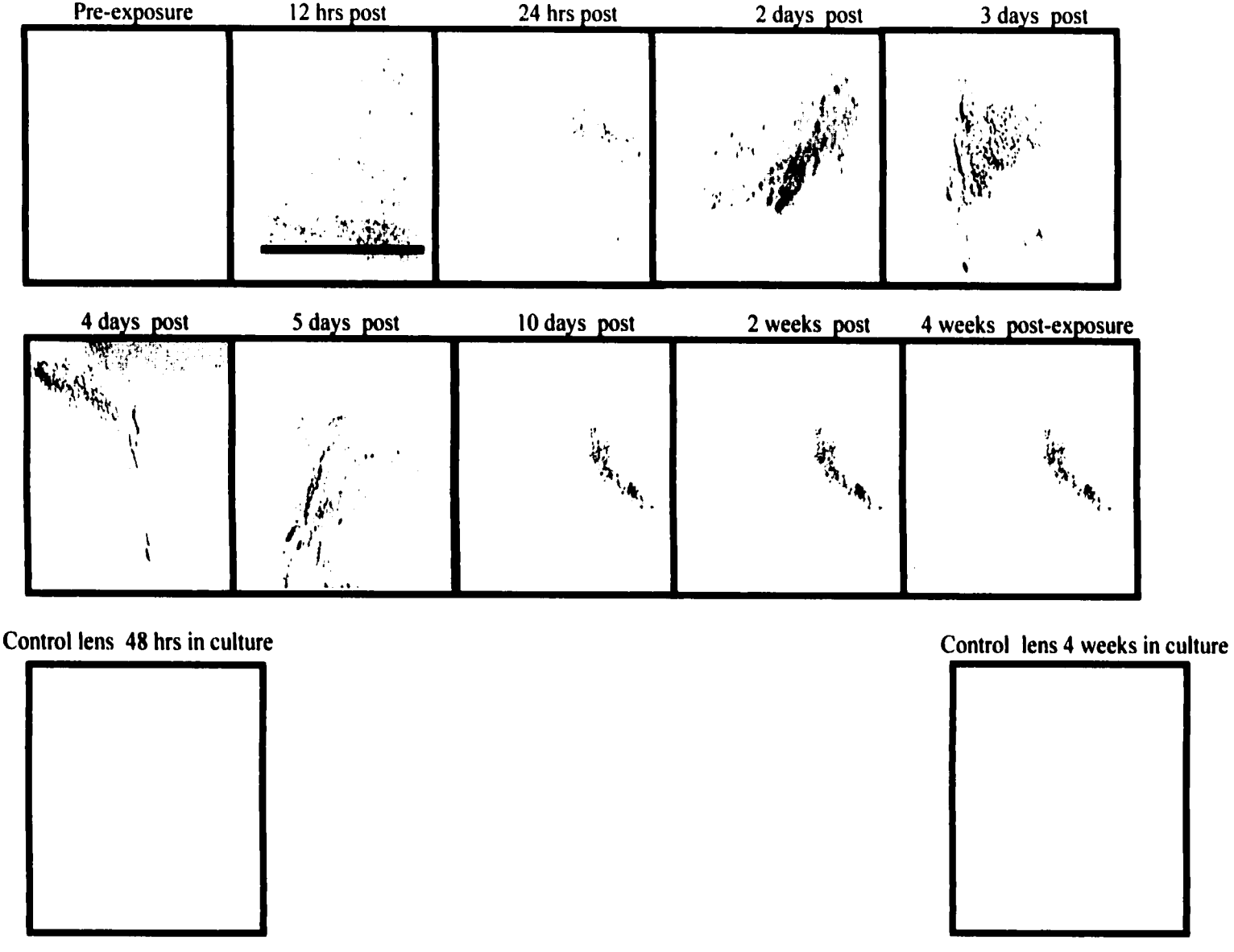

Figure 3.9. A representative illustration of morphological changes in group 4 lenses at 350 nm UVA 2X threshold (222.6 J/cm^2). No complete recovery 4 weeks after exposure. Bar equals 1.75 mm.

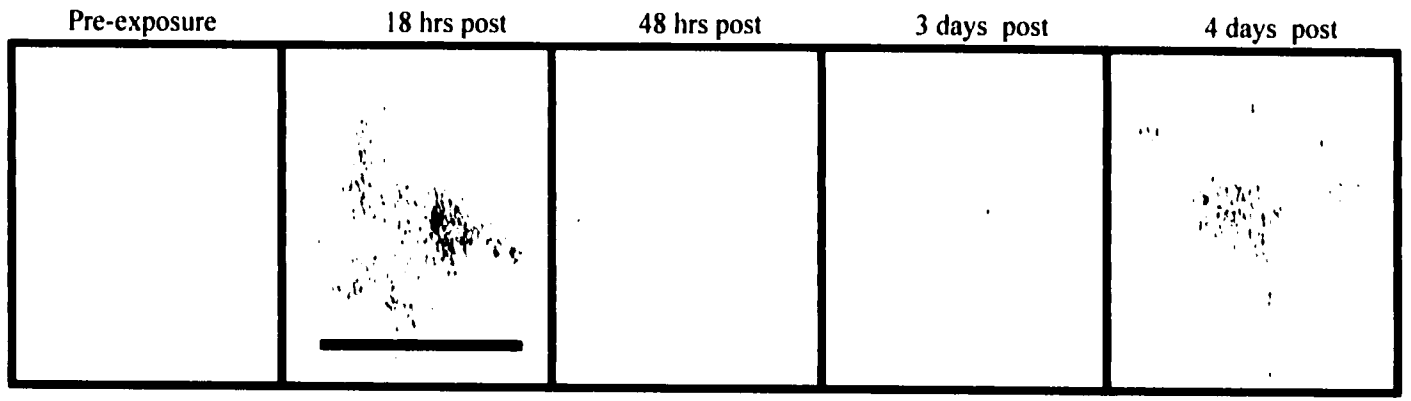

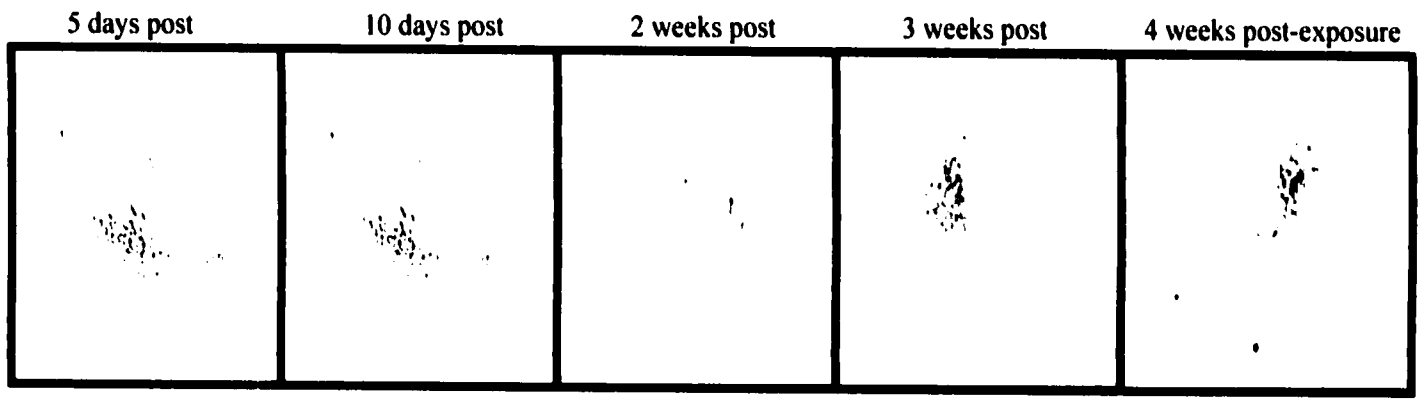

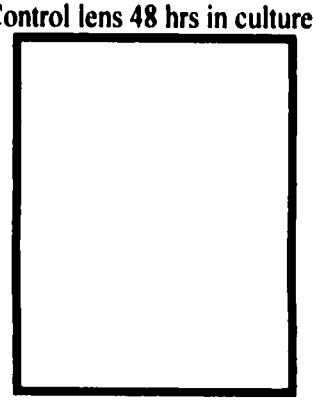

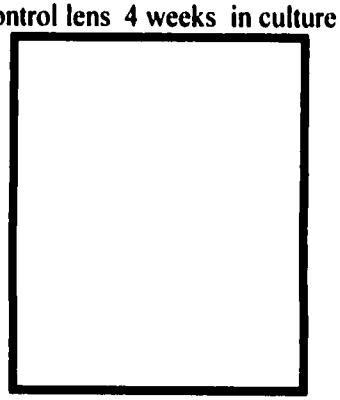

3.5 Discussion

Probit analysis is useful in that it enables the conversion of subjective, non-parametric data into parametric data (e.g. calculating 50^{th} percentile), thus allowing for the derivation of ED_{50} (median effective dose), which represents 50% probability of a defined UV radiant exposure causing photodamage. Simply stated, the ED_{50} or ED50 is the dose that will produce a response in half the population (Finney, 1971) of the exposed lenses. The action spectrum of UVR on the cultured intact crystalline lens gives the relative effectiveness per incident photon at each waveband for a single UV exposure. Biological effects of solar radiation on the lens epithelium would result from many exposures to both UVB and UVA radiation over decades (Andley et al., 1994). Figure 3.5 illustrates the derived action spectrum for *in vitro* UVR cataract formation for porcine lenses in the current study. Pitts et al., (1977a) reported that the action spectrum for UV-induced lens opacities in rabbits *in vivo* begins at 295 nm and extends to 320 nm. Radiation at 300 nm, using a 6.6 nm full bandpass, was found to be 30 times as effective as 315 nm radiation in producing lens opacities *in vivo*.

The *in vitro* action spectrum obtained in this study shows a similar trend to the *in vivo* data of Pitts et al., (1977a) that extended from 295 to 395 nm. Because of the absence of corneal absorption, it was possible to induce lenticular opacity with shorter wavelengths down to 270 nm in the present study. This was done so that future *in vitro* UV lens damage investigations may extend below 290 nm. Therefore, the data in the present study involved wavelengths from 270 to 370 nm at 5 or 10 nm intervals. The limit at the longer UV wavelengths was at 370 nm in the present study because no observable damage could be induced with the highest radiant exposures at the 370 nm waveband.

This tends to agree with Andley et al., (1994) who reported that the highest dose at the 405 nm waveband in their study produced no adverse effect on lens epithelial cells. Also, using 162 J/cm^2 radiant exposure at 365 nm waveband, which was the highest dose in their study, Pitts et al., (1977a) could not achieve any lenticular opacities *in vivo* in rabbit.

By comparison, at 300 nm, the present study found 0.069 J/cm^2 as threshold, while Pitts et al., (1977a) found 0.15 J/cm^2, and Andley et al., (1994) and Andley and Weber (1995) found 0.068 J/cm^2 and 0.052 J/cm^2 at 302 nm respectively, using rabbit and human lens epithelial cells. Data in the present study showed radiation at 295 nm waveband to be 25 times more effective than 315 nm radiation in producing UV induced lens anterior subcapsular lesions (Table 4.2), while the data of Pitts et al., (1977a) showed that 295 nm radiation was 6X more effective than 315 nm radiation. The data of Andley et al., (1994) and Andley and Weber (1995) found the radiation at 297 nm to be 171 and 261 times more effective than the 313 nm radiation used in their respective studies with rabbit and human lens epithelial cells. The difference in relative effectivity is not surprising because of the absence of corneal absorption in the *in vitro* conditions. Moreover, in isolated epithelial cells, the influence of overlying capsule, underlying cortex and adjacent cells are absent or minimal with respect to the impact of the radiation. The *in vitro* radiant exposure values in this study are 29X lower at 295 nm, ~2X lower at 300 nm, ~3X at 305 nm, ~3X at 310 nm, 6X at 315 nm, ~4X at 320 nm, than *in vivo* data reported by Pitts et al., (1977a) for UV-induced lens opacities in rabbits. Beginning from approximately 330 nm, both the *in vitro* and *in vivo* thresholds are similarly high. This may be due to the fact that the cornea transmits all UV wavelengths above ~325 nm.

The data in the current study showed that very high radiant exposure is needed from wavelengths above ~325 nm to induce subcapsular lesions *in vitro*; this agrees fairly well with Pitts (1978) who mentioned that radiant exposures above 320 nm need to be quite high to have an effect for *in vivo* experiments. The increased radiant exposure required at longer wavelengths to produce lenticular damage is not surprising due to the lower relative effectiveness of longer UV wavelengths (Table 3.4). Although different endpoints were used in the current study compared to those of Pitts et al., (1977a and 1977b); Andley et al., (1994); and Andley and Weber (1995) the present study is generally in agreement with the wavelengths of UVR that are most effective at inducing cataractous changes in the crystalline lens *in vivo* (Pitts et al., 1977a and b). The *in vitro* action spectrum in the present study begins at 270 nm and extends to about 365 nm while the *in vivo* action spectrum begins at 295 nm and extends to about 335 nm (Pitts et al., 1977b). Pitts et al., (1977b) found the lens and cornea curves to be relatively parallel from 300 nm up to about 320 nm. The present study found the threshold radiant exposure at 300 and 305 nm wavebands to be similar to values reported for corneal damage (Pitts et al., 1977b). This similarity between lenticular and corneal UV thresholds is not surprising since both the cornea and the lens derive embryologically from the surface ectoderm.

The relatively low radiant exposures in the 270 nm to 315 nm wavelength range might imply that the most effective wavelength range for producing UV cataract *in vitro* was from 270 to 315 nm. Looking at the trend of the action spectrum (Figure 3.5), it would be expected that wavelengths below 285 nm should be more effective with lower thresholds because the shorter the UV wavelength the higher the photon energy. However, there was a fair rise in radiant exposure below 285 nm (Figure 3.5), which

might indicate that a different mechanism is responsible for UVR lenticular toxicity below 285 nm. Another possible explanation is that UVR does not affect crystalline lens biomolecules in the same way for each waveband (Pitts, 1978). The action spectrum curve shows that 285 nm is the most effective wavelength for UV toxicity on porcine lens. This is relatively close to 280 nm, the shorter absorption maximum of human crystalline lens which has been reported to demonstrate absorption maxima at 280 and 370 nm (Maisel, 1985). At the long UV wavelengths, 365 nm appears to be more effective than 360 nm in causing cataract. These might indicate that the porcine lens has absorption maxima at 365 nm and 285 nm for longer and shorter UV wavelengths, respectively. The inability to obtain UV induced damage at 370 nm might indicate that the porcine crystalline lens transmits all UV wavelengths from 370 nm and above. The present study has established the *in vitro* UV action spectrum for cultured porcine lens using gross morphological changes (anterior subcapsular opacities) as damage criteria. However, extrapolations from the data can be applied to the study of *in vitro* UV-induced cataracts using lenses from other animal species.

In terms of recovery from UV damage, the present study confirms the findings by Pitts et al., (1977a and b) that radiant exposure at two times threshold level results in permanent opacity (Figure 3.7). Also, at two times UVA threshold exposures, there was no full recovery (Figure 3.9), confirming that UVA is cataractogenic. At five times UVB threshold exposure, the photodamage gave rise to prominence of the suture, which might be an indication of permanent opacity with no chance of recovery (Figure 3.8). Data in the present study support the theory that repair would generally occur for UVR induced cataract at threshold and subthreshold radiant energy levels (Figure 3.6). This may tempt

one to speculate that the temporary blurring of vision often experienced due to UVR induced photokeratoconjunctivitis may arise from not only the cornea but also from the lens.

Chapter 4

Application of a novel fluorometric bioassay methodology and laser scanning system for UV cataractogenesis study

4.1 Abstract

This study investigated the feasibility of using a new nontoxic fluorometric bioassay approach to monitor induced UV damage in cultured porcine crystalline lenses. In an attempt to validate this new bioassay comprising alamarBlue™ and 5-carboxyfluorescein diacetate, acetoxymethyl ester (CFDA-AM), a scanning laser monitoring system was employed to assess the optical quality of the same set of lenses following UV exposure. Whole, aseptically dissected, porcine lenses were cultured in modified M199 medium supplemented with 1% penicillin/streptomycin (100 units/mL) and 4% porcine serum. After one week of preincubation in 37°C, 4% CO_2, 96% air, baseline (pre-exposure) fluorescence and optical quality measurements were taken. The lenses were then irradiated with determined levels of broadband UVB radiant exposures in a custom built UV irradiation system with 5% CO_2 and 95% membrane filtered air. During the irradiation, temperature ranged from 33 to 36°C, with 62% relative humidity. The control lenses were protected from UV radiation. After irradiation, lenses were further incubated for 4 weeks, with fluorescence and optical measurements carried out every 48h in the first 9 days post exposure and then once each week. For fluorometry, both treated and control lenses were transferred into a 24-well plate with one lens per well. Each lens was immersed in a mixture of the assay solution and the basal medium for 50 minutes each

time, and readings taken with a fluorescence plate reader. For optical quality assessments, each lens was transferred to a custom-designed lens container and placed in the scanning laser monitor. Analyses based on each energy level showed a statistically significant difference between baseline and follow-up measurements ($p < 0.05$) of cellular metabolism, cell membrane integrity, and optical quality as indicated by the fluorometric bioassay and SLM techniques respectively. UV-induced damage was obtained at the 0.038 J/cm^2 but not at the 0.019 J/cm^2 energy level, suggesting the threshold for *in vitro* broadband UVB energy for cataractogenesis to be >0.019 J/cm^2 and < 0.038 J/cm^2.

4.2 Introduction

Cataract as a major cause of blindness worldwide constitutes a public and occupational health concern because, apart from environmental exposure, many industrial operations use UV radiation in their process. The number of blind people in the world and the proportion due to cataract is increasing due to population growth and increasing longevity (Foster, 1999). There is currently an estimated backlog of 16-20 million unoperated cases globally (Thylefors, 1998). The furtherance of UV cataract research is essential due to the following reasons: First, cataract stands out as the first priority among major causes of preventable blindness, and the alarming indication in the literature of potential doubling of the world's blindness burden by 2020. Second, the role of UVB and/or UVA in the pathogenesis of human cataracts is still controversial. Third, approximately 5000 cataract surgeries per million people per year are carried out in the United States, while the figures are ~200, 500-1500, ~2000, and ~3000 for Africa, Latin America, India, and Europe, respectively (Thylefors, 1998). Recent reports indicate that there are approximately 20

million people blind from cataract in the world, the majority of whom do not have access to affordable cataract surgery (Foster, 1999). Even for those who have access to cataract surgery, it has been reported that posterior capsular opacification, a common complication of cataract surgery, occurs in up to 50% of patients by 2 to 3 years after their surgery (Spalton, 1999). Thus, cataract prevention or delay in progression would represent a major achievement for human welfare.

It cannot be overemphasized that cataract still represents the leading cause of blindness throughout the world. Therefore more research effort is necessary in furthering the understanding of the biological basis of UV radiation effects on lens morphology, function, and pathology. From the literature, it is evident that countries that are plagued with high cataract prevalence are underserved with cataract surgical personnel and facilities. This further underscores the need to intensify basic research in UV cataractogenesis and preventive modalities. Therefore, the present study was undertaken to investigate the feasibility of using two fluorescent dyes, alamarBlue™ and 5-carboxyfluorescein diacetate, acetoxymethyl ester (CFDA-AM) to study pathogenesis of UV-induced cataract at the cellular level. The alamarBlue™ assay has been used in studies of lymphocyte proliferation (Ahmed et al., 1994), and to quantify the phototoxicity of fluoranthene to a rainbow trout gill cell line (Schirmer et al., 1997; 1998). These studies (Ahmed et al., 1994; Schirmer et al., 1997; 1998) reported that alamarBlue™ is a sensitive assay to monitor changes in intracellular mitochondrial integrity, which is a measure of cellular viability. The CFDA-AM fluorescent assay is a good indirect measure of plasma membrane integrity (O'Connor et al., 1991; Schirmer et al., 1997), and an accurate method for quantifying cells growth *in vitro* (Hanthamrongwit

et al., 1994). The secondary goal was to use the established scanning laser monitor approach to validate this novel *in vitro* dual fluorometric bioassay methodology in monitoring UV damage on cultured porcine lens.

4.3 Materials and Methods

Whole aseptically dissected porcine lenses were cultured in modified M199 (no phenol red), 1% antibiotics (penicillin/streptomycin 100 units/mL) and 4% porcine serum, with sodium bicarbonate and HEPES as buffers. All culture ingredients were purchased from the Sigma Chemical Company except otherwise stated. Figure 4.1A illustrates the pre- and post-UV exposure protocol for the study (5 week) duration. The lenses were preincubated at 37°C, 4%CO_2, 96% air for one week pre-exposure. At one week, the fluorescence levels of the lenses were measured with a bioassay containing alamarBlue™ and 5-carboxyfluorescein diacetate-acetoxymethyl ester (CFDA-AM) dyes. The optical quality measurements were taken as well pre-exposure to UV. The measurements at one week were taken as baseline for control and exposed lenses.

The lenses were irradiated with predetermined actual energy levels at 0.96, 0.48, 0.24, and 0.12 J/cm^2 of broadband UVB exposures in a custom built UV irradiation system (Figure 4.1B) with 5% CO_2 and 95% membrane filtered air. For comparative purposes to other studies, it was necessary to calculate the biologically effective UVB (290 – 320 nm) doses of the four radiant energy levels (i.e., 0.96, 0.48, 0.24, and 0.12 J/cm^2) utilized in this study based on an 8 hr exposure. The calculation was carried out using the American Conference of Governmental Industrial Hygienists (ACGIH) spectral weighting functions with the following formula: $^{320}\Sigma_{290}\, H_\lambda \times \Delta_\lambda \times S_\lambda$, where H_λ is the

actual radiant exposure (J/cm^2) at a specific wavelength as obtained from spectroradiometer, Δ_λ is the wavelength interval (nm), and S_λ is the UVR spectral weighting function or relative spectral effectiveness (unitless). Therefore, the calculated biologically effective radiant energy level, to be used in subsequent discussion were 0.152, 0.076, 0.038, and 0.019 J/cm^2 respectively (Table 4.1). The UV fluorescent tubes were purchased from Microlites Scientific (Scarborough, Ontario, Canada). A sterile sheet of cellulose acetate measured to be opaque to wavelengths below 290 nm was placed on top of the containers holding the lenses during exposure to filter out all the wavelengths below 290 nm. The spectral distribution of the UVB fluorescent tubes used (Figure 4.2) extends from 290 nm to about 370 nm wavelengths. However, since it was found that the contribution of the wavelengths within the 320 to 370 nm waveband was only 0.1%, this was ignored.

During the irradiation, temperature ranged from 33 to 36°C with 62% relative humidity. Before irradiation, the spectral output of the UVB source (with cellulose acetate sheet placed on top of the integrating sphere) was measured with a calibrated Instaspec II diode-array spectroradiometer (Oriel Corporation, Stratford, CT., USA). Control lenses were protected from UV radiation by covering their containers with a sterile plastic sheet opaque to UV and visible radiation. Lenses were further incubated for 4 weeks post-irradiation, with fluorescence and optical quality measurements carried out every 48h in the first 9 days, and then once each week thereafter. For fluorescence measurements, both treated and control lenses were transferred into a 24-well cell culture plate, with one lens per well. Each lens was immersed in a mixture of the assay and basal medium and incubated for 50 minutes. Measurements were then taken with a CytoFluor™

fluorescence plate reader (PerSeptive Biosystems Inc., Framingham, MA, USA). The optical quality measurements were obtained approximately 8 hour after the fluorescence measurements. This was to allow the assay dyes to diffuse out of the lenses. Each lens was transferred to a two-compartment container filled with culture medium (with serum), and placed in the SLM for the optical quality assessment. It should be noted that the same sets of lenses were assessed using the assay technique and the scanning laser monitor at each energy level. Photomicrographs of lens samples were randomly obtained. Statistical analysis of individual radiant exposure was performed using repeated measures analysis of variance (MANOVA) with general linear model. P values, set at 0.05 significance level were calculated using F-test. Fifty-two exposed and 32 control lenses were used in this study.

Figure 4.1A. Flow chart illustrating the pre (baseline) and post-UV exposure protocols for 5 weeks.

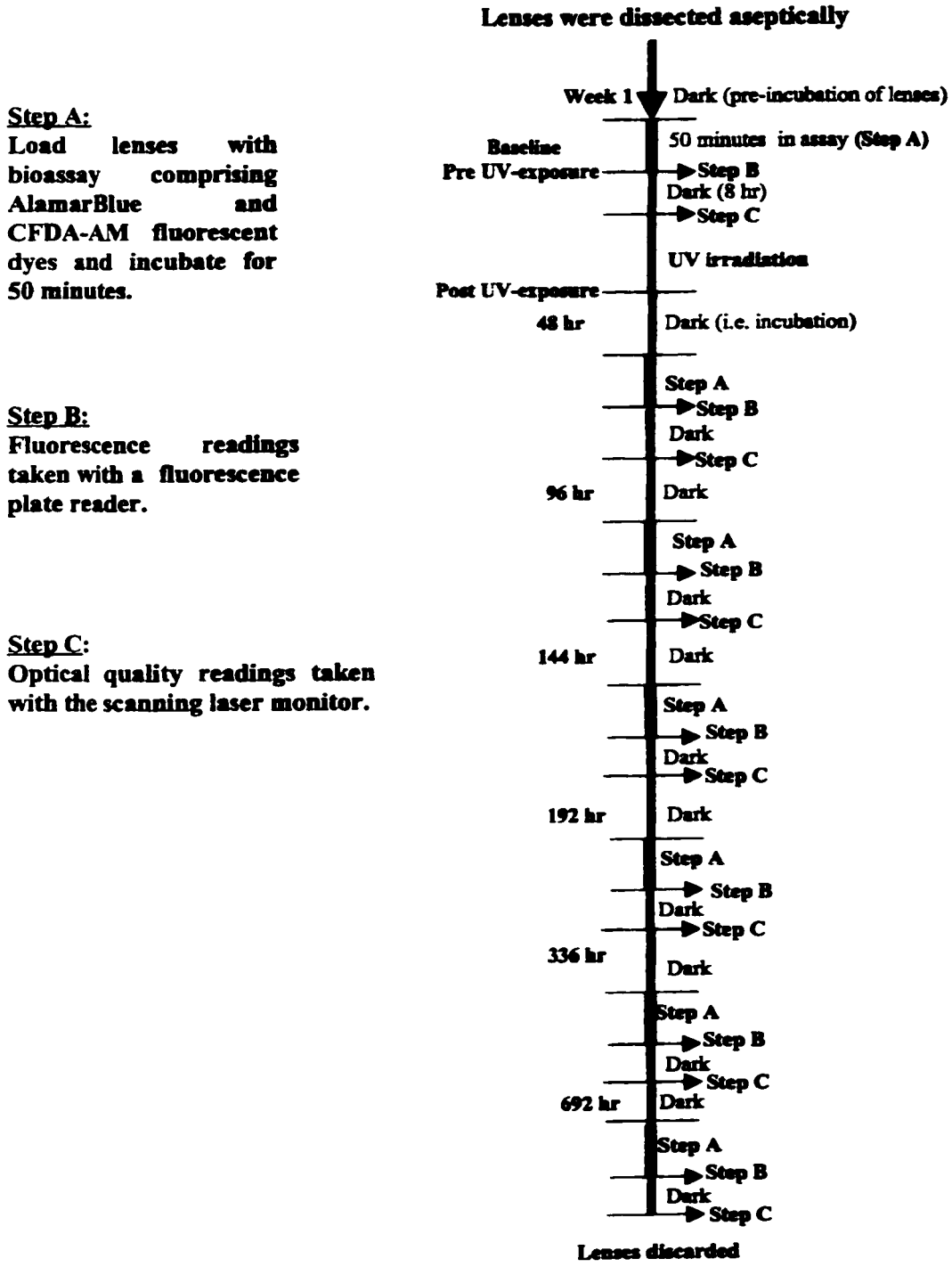

Figure 4.1B. Broadband UV exposure system.

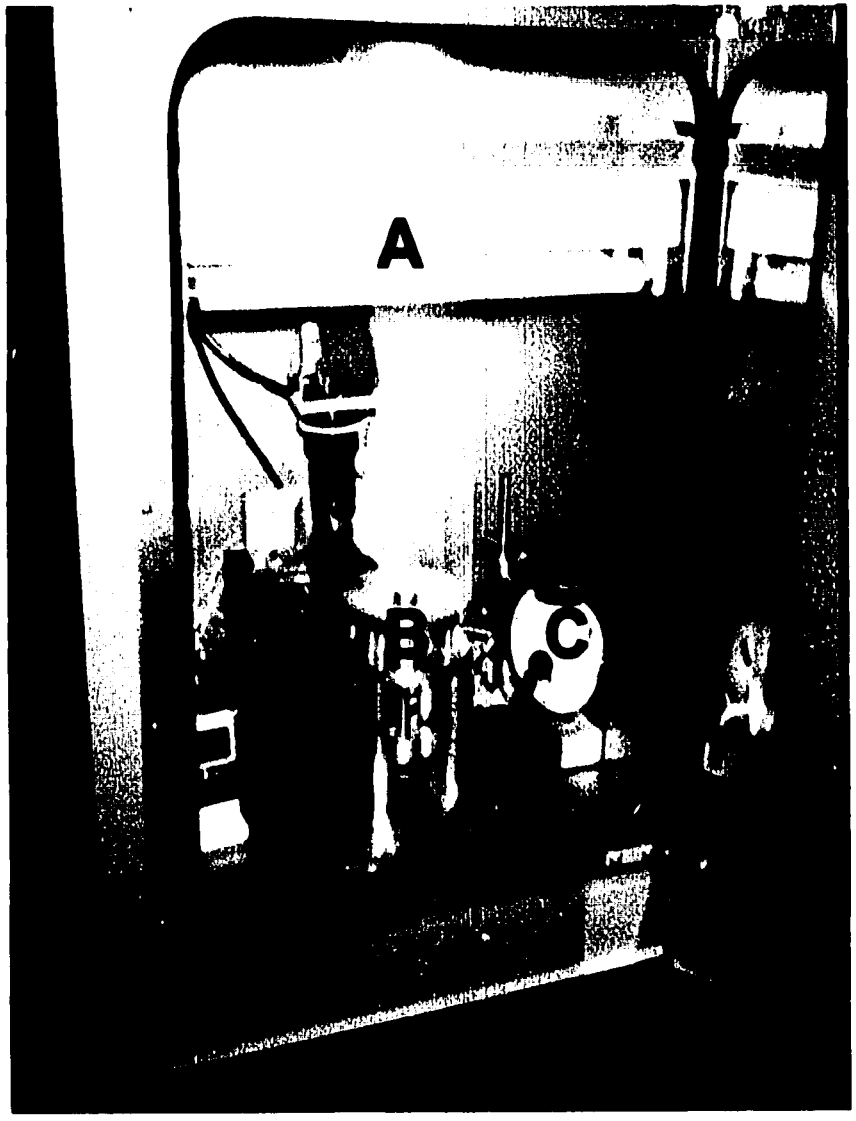

(A) UV Fluorescent fixture and tubes

(B) Rotatory base for holding lens containers during exposure

(C) Integrating sphere

(D) Fibre optic connecting the integrating sphere to the spectroradiometer

Figure 4.2. A representative plot of spectral emission of the UVB fluorescent tubes used for the broadband UVB exposure.

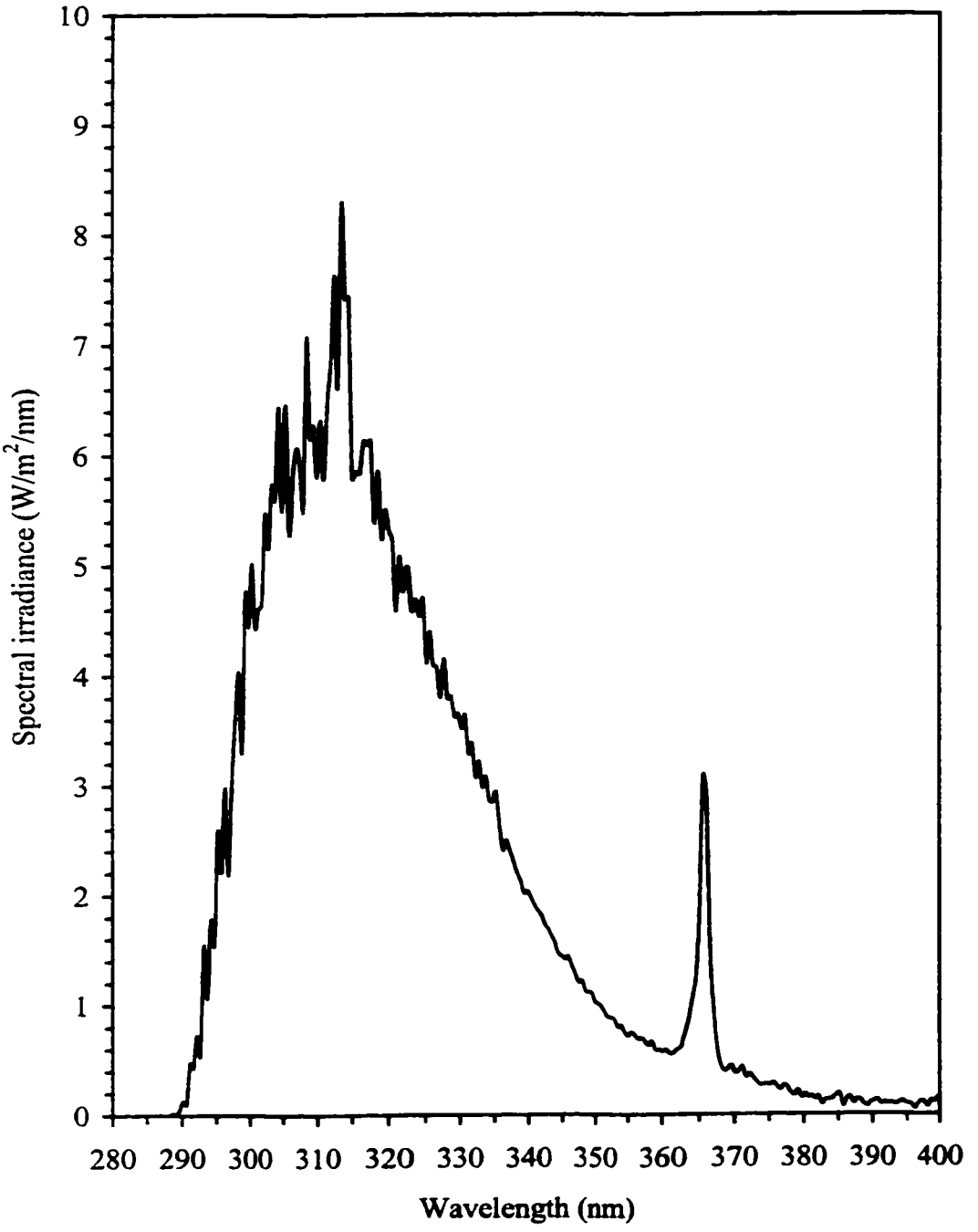

4.4 Results

4.4.1 Fluorometric Bioassay

Based on the fluorometric bioassay technique, a total of 11,760 (i.e. 5,880 for alamarBlue™ and 5,880 for CFDA-AM dyes) quantitative measurements were obtained, with each fluorescence measurement providing an average of 10 readings per scan, and each lens subjected to two scans (first scan for alamarBlue™, and the second scan for CFDA-AM assay readings, respectively) at least 7 times through the study duration. The control lenses did not show significant change in both the bioassay and the SLM measurements throughout the experiment duration (Tables 4.2 – 4.13). With the exception of the 0.019 J/cm^2 UVB energy level (Table 4.8), all the UVB energy levels (Tables 4.2, 4.4, & 4.6) caused significant decrease ($P < 0.05$) in the alamarBlue™ assay readings post-irradiation. Sometimes alamarBlue™ readings rebounded indicating a recovery trend from the UV damage but none returned to baseline readings (Figures 4.3). For the CFDA-AM assay, non-significant P values were obtained for 0.152 J/cm^2 at 48hr, 96hr, 336hr and 672hr; and for 0.076 J/cm^2 at 48hr post exposure (Tables 4.3 & 4.5). However, as shown in Table 4.7 with the same CFDA-AM assay, a significant decrease ($P < 0.05$) in fluorescence was obtained for the 0.038 J/cm^2 UVB exposure beginning from 48hr ($P = 0.0001$) with no indication of recovery at 672hr ($P = 0.0008$). Significantly higher ($P < 0.05$) fluorescence readings were obtained for 0.152 J/cm^2 at 144hr and 192hr (Table 4.3); and for 0.076 J/cm^2 at 96hr through 672hr (Table 4.5). As with alamarBlue™, the CFDA-AM fluorescence readings did not show any significant change compared to baseline readings at the 0.019 J/cm^2 UVB exposure level (Figures 4.3 & 4.4).

4.4.2 Optical Quality Monitoring

For the optical quality measurements, each scan by the SLM produced 23 measures of focal length in each lens, and each lens was scanned 7 times. Thus the SLM results are based on at least 13,524 quantitative optical measures for both exposed and control lenses. As in bioassay measurements, the optical quality measurements did not show any significant change compared to the baseline at the 0.019 J/cm^2 UVB exposure (Table 4.13; Figures 4.5 & 4.6). The 0.152 J/cm^2 UVB energy level caused a significant increase in average focal length at 192 hr, and an increase in focal length variability at 336 hr and 672 hr (Table 4.10). It should be noted that due to severe opacity induced by the 0.152 J/cm^2 UVB radiant exposure, some of the exposed lenses could not be scanned at certain times post-exposure, therefore, only 6 out of 11 exposed lenses could be used for statistical analysis at this particular energy level. For the 0.076 J/cm^2 UVB exposure, a significant decrease in average focal length was obtained at 48 hr and 96 hr, with a cross over to a significant increase at 144 hr and 336 hr, and recovery at 672 hr (Table 4.11).

The lenses exposed to 0.152 J/cm^2 UVB showed a consistent increase in AFL from 48 hr post exposure (Figure 4.5). The lenses exposed to 0.076 J/cm^2 UVB showed an upward trend in FLV from the 96 hr (Figure 4.6) however, the upward trend was only significant at the 336 hr post exposure (Table 4.11). The 0.038 J/cm^2 UVB energy level caused a significant decrease in AFL at 48 hr, and an increase at 96 hr (Figure 4.5) with recovery being shown from about 144 hr; the upward trend at 192 hr was not significantly different from baseline (Table 4.12). With respect to FLV, the 0.038 J/cm^2 UVB energy level caused a significant increase at 144 hr and 692 hr (Table 4.12). The error bars in the

Figures 4.3 to 4.6 represent S.E.M. Figure 4.7 shows a representation of one sample of photomicrographs.

Table 4.1. The direct UV radiant energy from the UVB source and calculated biologically effective dose with corresponding exposure duration for the different energy levels utilised in this study.

Radiant exposure (J/cm^2)		Exposure duration (seconds)
Direct energy	Biologically effective dose	
0.96	0.152	7272
0.48	0.076	3636
0.24	0.038	1818
0.12	0.019	909

Note: The biologically effective dose was calculated using the ACGIH biological spectral weighting function for respective (UVB) wavelengths from 290 to 320 nm.

Table 4.2. Descriptive statistics of alamarBlue™ fluorescence data for 0.152 J/cm^2 UVB radiant exposure (n= 11 for exposed lenses, and 7 for control lenses).

Measurement time (variable)	Fluorescence (Mean±STD)		Minimum value		Maximum value		*P* values	
	Exposed	Control	Exposed	Control	Exposed	Control		
Baseline	8568.2 ± 1169	8718.6 ± 656	6863	7488	10239	9478	Exposed	Control
Hour48	5858.1 ± 681	8492.6 ± 724	4831	7214	6996	9264	0.0001	0.514
Hour96	5838.8 ± 608	8342.1 ± 915	5044	7091	6833	9739	0.0001	0.378
Hour144	5592.4 ± 464	8130.4 ± 818	4874	6880	6621	8859	0.0001	0.058
Hour192	7354.7 ± 1341	9057.6 ± 1129	5280	7323	10077	10467	0.0060	0.259
Hour336 (wk2)	6502.3 ± 512	8757.1 ± 529	5547	7933	7397	9595	0.0001	0.895
Hour672 (wk4)	7416.1 ± 1126	9244.0 ± 1029	5588	8206	8829	10406	0.0200	0.155

Note: The *P* value set at 0.05 significance level is the comparison of baseline to subsequent measurements post-UV irradiation.

Table 4.3. Descriptive statistics of CFDA-AM fluorescence data for 0.152 J/cm^2 UVB radiant exposure (n= 11 for exposed lenses, and 7 for control lenses).

Measurement time (variable)	Fluorescence (Mean±STD)		Minimum value		Maximum value		*P* values	
	Exposed	Control	Exposed	Control	Exposed	Control	Exposed	Control
Baseline	36204.4 ± 4431	36729.7 ± 5910	29255	29650	44690	45366		
Hour48	43091.4 ± 10642	39699.7 ± 5853	32668	32883	64262	51273	0.056	0.250
Hour96	36920.5 ± 5343	39434.0 ± 5582	27918	31764	46804	48637	0.716	0.330
Hour144	41965.9 ± 3591	42998.3 ± 5439	36275	35849	46989	51784	0.003*	0.052
Hour192	42901.7 ± 5091	39993.9 ± 17311	36337	36703	50276	56119	0.007*	0.680
Hour336 (wk2)	38741.9 ± 5221	40855.3 ± 8161	29911	32993	44349	54282	0.081	0.070
Hour672 (wk4)	33053.0 ± 2854	33625.3 ± 5681	28813	26187	38313	40242	0.102	0.300

Note: The *P* value set at 0.05 significance level is the comparison of baseline to subsequent measurements post-UV irradiation. *P* value with asterisk (*) indicates that fluorescence measurement at the time interval was higher than the baseline measurement in the group of lenses.

Table 4.4. Descriptive statistics of alamarBlue™ fluorescence data for 0.076 J/cm^2 UVB radiant exposure (n= 16 for exposed lenses, and 9 for control lenses).

Measurement time (variable)	Fluorescence (Mean±STD)		Minimum value		Maximum value		*P* values	
	Exposed	Control	Exposed	Control	Exposed	Control		
Baseline	9535.4 ± 1042	9372.30 ± 1128	7584	8125	11416	12021	Exposed	Control
Hour48	8534.6 ± 1144	10827.0 ± 1678	6903	9538	10863	14788	0.0290	0.086
Hour96	7352.7 ± 742	9998.10 ± 572	6363	9346	8822	11149	0.0001	0.164
Hour144	8066.9 ± 1043	10276.4 ± 1062	6155	9110	9862	12414	0.0001	0.140
Hour192	7935.6 ± 1733	10042.1 ± 1200	5613	8664	11958	12745	0.0003	0.069
Hour336 (wk2)	8097.6 ± 1085	9673.70 ± 1613	6430	7035	9813	11515	0.0001	0.513
Hour672 (wk4)	7154.1 ± 873	8456.10 ± 1146	5628	6589	9014	9989	0.0001	0.067

Note: The *P* value set at 0.05 significance level is the comparison of baseline to subsequent measurements post-UV irradiation.

Table 4.5. Descriptive statistics of CFDA-AM fluorescence data for 0.076 J/cm^2 UVB radiant exposure (n= 16 for exposed lenses, and 9 for control lenses).

Measurement time (variable)	Fluorescence (Mean±STD)		Minimum value		Maximum value		*P* values	
	Exposed	Control	Exposed	Control	Exposed	Control		
Baseline	32342.1 ± 3177	33940.9 ± 4903	23162	28925	35730	41679	Exposed	Control
Hour48	37510.6 ± 13743	37592.3 ± 11643	17827	21243	63976	56419	0.1530	0.190
Hour96	37299.3 ± 3222	36382.8 ± 4803	31110	30588	42017	43602	0.0003*	0.344
Hour144	36297.1 ± 7053	37738.6 ± 5343	26714	30908	54759	46517	0.0270*	0.151
Hour192	44452.1 ± 9275	39124.6 ± 12084	33577	22678	66136	57779	0.0002*	0.158
Hour336 (wk2)	37351.5 ± 6443	36651.4 ± 6269	28226	28814	52707	47130	0.0070*	0.081
Hour672 (wk4)	38628.8 ± 6608	38234.8 ± 8919	28615	24254	53138	51968	0.0060*	0.106

Note: The *P* value set at 0.05 significance level is the comparison of baseline to subsequent measurements post-UV irradiation. *P* value with asterisk (*) indicates that fluorescence measurement at the time interval was higher than the baseline measurement in the group of lenses.

Table 4.6. Descriptive statistics of alamarBlue™ fluorescence data for 0.038 J/cm^2 UVB radiant exposure (n= 12 for exposed lenses, and 7 for control lenses).

Measurement time (variable)	Fluorescence (Mean±STD)		Minimum value		Maximum value		*P* values	
	Exposed	Control	Exposed	Control	Exposed	Control		
Baseline	9672.2 ± 1160	8884.3 ± 939	8161	7308	11586	10202	Exposed	Control
Hour48	8597.1 ± 1161	9350.7 ± 669	6672	8492	10751	10178	0.0088	0.262
Hour96	7981.9 ± 1165	9976.7 ± 1726	6780	7704	10354	12457	0.0114	0.142
Hour144	8216.5 ± 1104	9040.9 ± 984	6407	7991	10473	10687	0.0203	0.806
Hour192	8033.5 ± 1072	9836.7 ± 1143	6597	8570	9983	11933	0.0068	0.178
Hour336 (wk2)	8450.9 ± 1265	9376.4 ± 1595	6708	7499	10854	12573	0.0678	0.486
Hour672 (wk4)	6412.3 ± 1092	8573.0 ± 552	4554	7585	8673	9218	0.0001	0.529

Note: The *P* value set at 0.05 significance level is the comparison of baseline to subsequent measurements post-UV irradiation.

Table 4.7. Descriptive statistics of CFDA-AM fluorescence data for 0.038 J/cm^2 UVB radiant exposure (n= 12 for exposed lenses, and 7 for control lenses).

Measurement time (variable)	Fluorescence (Mean±STD)		Minimum value		Maximum value		*P* values	
	Exposed	Control	Exposed	Control	Exposed	Control		
Baseline	53717.5 ± 7337	47228.9 ± 8430	39481	35365	69932	58767	Exposed	Control
Hour48	44582.6 ± 5725	44076.3 ± 7381	35995	36224	59419	53648	0.0001	0.08
Hour96	47128.3 ± 8105	49579.3 ± 8736	33075	39514	60470	65473	0.0342	0.29
Hour144	45484.6 ± 5415	46684.1 ± 7366	39011	36367	56387	56005	0.0013	0.80
Hour192	46352.8 ± 8786	43017.3 ± 8458	32554	34012	67412	59537	0.0064	0.15
Hour336 (wk2)	44886.8 ± 4213	43200.1 ± 7341	38098	36240	51019	56095	0.0038	0.06
Hour672 (wk4)	39634.3 ± 10406	42939.0 ± 5550	17796	36479	57731	50974	0.0008	0.06

Note: The *P* value set at 0.05 significance level is the comparison of baseline to subsequent measurements post-UV irradiation.

Table 4.8. Descriptive statistics of alamarBlue™ fluorescence data for 0.019 J/cm^2 UVB radiant exposure (n= 13 for exposed lenses, and 9 for control lenses).

Measurement time (variable)	Fluorescence (Mean±STD)		Minimum value		Maximum value		*P* values	
	Exposed	Control	Exposed	Control	Exposed	Control		
Baseline	10284.6 ± 1244	10259.3 ± 1651	8646	8509	13252	13033	Exposed	Control
Hour48	9495.90 ± 990	9777.90 ± 1046	7838	8417	10962	11064	0.13	0.45
Hour96	9957.40 ± 2182	10186.2 ± 1426	7143	8095	14406	12766	0.61	0.93
Hour144	9453.00 ± 1039	9377.30 ± 1294	8075	6987	11156	11296	0.07	0.18
Hour192	9820.20 ± 967	10081.2 ± 1380	8430	7812	11383	12451	0.34	0.85
Hour336 (wk2)	9893.80 ± 1647	10225.8 ± 1018	7678	8503	13469	11883	0.27	0.97
Hour672 (wk4)	9636.50 ± 1269	9751.20 ± 1259	7715	7817	11728	11192	0.23	0.44

Note: The *P* value set at 0.05 significance level is the comparison of baseline to subsequent measurements post-UV irradiation.

Table 4.9. Descriptive statistics of CFDA-AM fluorescence data for 0.019 J/cm^2 UVB radiant exposure (n= 13 for exposed lenses, and 9 for control lenses).

Measurement time (variable)	Fluorescence (Mean±STD)		Minimum value		Maximum value		*P* values	
	Exposed	Control	Exposed	Control	Exposed	Control		
Baseline	40252.3 ± 7289	43105.9 ± 5916	30983	33648	52188	51127	Exposed	Control
Hour48	41423.7 ± 4170	38915.7 ± 4826	34155	30628	47464	44537	0.51	0.08
Hour96	44249.1 ± 10236	45336.7 ± 8254	31258	35246	62416	58285	0.07	0.38
Hour144	43653.5 ± 9364	42331.7 ± 6373	32005	34665	56729	50786	0.06	0.76
Hour192	39794.1 ± 4894	39723.7 ± 7462	33126	28565	46976	50519	0.80	0.08
Hour336 (wk2)	42491.1 ± 6379	39485.0 ± 3062	31561	35613	53849	43390	0.33	0.12
Hour672 (wk4)	41022.3 ± 5301	41523.7 ± 2999	34505	37464	51782	46062	0.76	0.52

Note: The *P* value set at 0.05 significance level is the comparison of baseline to subsequent measurements post-UV irradiation.

Table 4.10. Summary of the optical quality assessment data for 0.152 J/cm^2 radiant exposure. Sample size (n) equals 11 for exposed, and 7 for control lenses, respectively.

Measurement time (variable)	mean AFL (FLV) in mm		*P* values for mean AFL		*P* values for mean FLV	
	Exposed	Control	Exposed	Control	Exposed	control
Baseline	29.5 (0.67)	29.0 (0.51)				
Hour48	30.0 (1.04)	29.6 (0.50)	0.890	0.282	0.399	0.925
Hour96	30.0 (1.02)	29.1 (0.50)	0.400	0.725	0.590	0.819
Hour144	30.5 (0.98)	29.0 (0.50)	0.870	0.927	0.931	0.970
Hour192	31.6 (1.75)	28.6 (0.61)	0.026	0.529	0.083	0.061
Hour336 (wk2)	32.7 (1.89)	28.2 (0.52)	0.047	0.127	0.008	0.851
Hour692 (wk4)	33.1 (1.97)	29.0 (0.58)	0.031	0.826	0.050	0.185

Note: Mean AFL is the mean of the average focal lengths of all the lenses, and mean FLV in parentheses is the average of the focal length variability (i.e. S.E.Ms of the individual average focal length) of all lenses. Baseline measurements denote measurements prior to UV-irradiation. Data from only 6 out of 11 exposed lenses could not be used for analysis due to severe opacity in some lenses which rendered the lenses unscannable with the scanning laser monitor (SLM).

Table 4.11. Summary of the optical quality assessment data for 0.076 J/cm^2 radiant exposure (n = 16 for exposed, and 9 for control lenses, respectively).

Measurement time (variable)	mean AFL (FLV) in mm		*P* values for mean AFL		*P* values for mean FLV	
	Exposed	Control	Exposed	Control	Exposed	control
Baseline	28.9 (0.59)	28.8 (0.51)				
Hour48	28.3 (0.58)	28.2 (0.46)	0.024	0.244	0.245	0.325
Hour96	28.5 (0.73)	28.9 (0.54)	0.016	0.939	0.382	0.649
Hour144	29.8 (0.88)	28.9 (0.49)	0.003	0.973	0.124	0.758
Hour192	30.1 (0.96)	28.5 (0.57)	0.077	0.441	0.105	0.334
Hour336 (wk2)	30.5 (0.88)	28.8 (0.50)	0.003	1.000	0.016	0.913
Hour692 (wk4)	30.0 (0.93)	29.6 (0.52)	0.123	0.217	0.060	0.930

Note: Sample size for exposed lenses dropped to 15 at wk2 and wk4 due severe opacity in one lens which rendered the lens unscannable with SLM.

Table 4.12. Summary of the optical quality assessment data for 0.038 J/cm^2 radiant exposure (n = 12 for exposed, and 7 for control lenses, respectively).

Measurement time (variable)	mean AFL (FLV) in mm		*P* values for mean AFL		*P* values for mean FLV	
	Exposed	Control	Exposed	Control	Exposed	control
Baseline	30.2 (0.53)	29.7 (0.52)				
Hour48	28.9 (0.82)	29.7 (0.64)	0.005	0.958	0.059	0.260
Hour96	30.9 (0.89)	29.3 (0.65)	0.028	0.529	0.151	0.237
Hour144	30.2 (0.94)	29.5 (0.56)	0.571	0.618	0.011	0.702
Hour192	31.9 (1.04)	29.5 (0.60)	0.281	0.702	0.105	0.314
Hour336 (wk2)	30.1 (0.82)	29.4 (0.70)	0.178	0.538	0.112	0.141
Hour692 (wk4)	30.2 (0.80)	29.4 (0.50)	0.485	0.780	0.025	0.795

Note: Sample size (n) for exposed lenses dropped to 11 at hr144 and hr192, and to 8 at wk2, and to 7 at wk4 due severe opacity in some lenses which rendered the lenses unscannable with the SLM. The *P* value set at 0.05 significance level is the comparison of baseline to subsequent measurements post-UV irradiation.

Table 4.13. Summary of the optical quality assessment data for 0.019 J/cm^2 radiant exposure (n = 13 for exposed, and 9 for control lenses, respectively).

Measurement time (variable)	mean AFL (FLV) in mm		*P* values for mean AFL		*P* values for mean FLV	
	Exposed	Control	Exposed	Control	Exposed	control
Baseline	29.0 (0.51)	28.5 (0.38)				
Hour48	29.3 (0.54)	28.1 (0.46)	0.366	0.121	0.532	0.118
Hour96	29.3 (0.54)	28.1 (0.42)	0.319	0.250	0.452	0.217
Hour144	28.6 (0.49)	28.3 (0.44)	0.203	0.598	0.567	0.168
Hour192	29.0 (0.51)	28.3 (0.47)	1.000	0.720	0.954	0.054
Hour336 (wk2)	28.9 (0.53)	28.3 (0.42)	0.650	0.628	0.620	0.233
Hour692 (wk4)	28.5 (0.57)	28.0 (0.44)	0.109	0.074	0.200	0.080

Note: The *P* value set at 0.05 significance level is the comparison of baseline to subsequent measurements post-UV irradiation.

Figure 4.3. Level of UVB damage as a function of radiant exposure and time compared to baseline measurements as indicated by the alamarBlue assay.

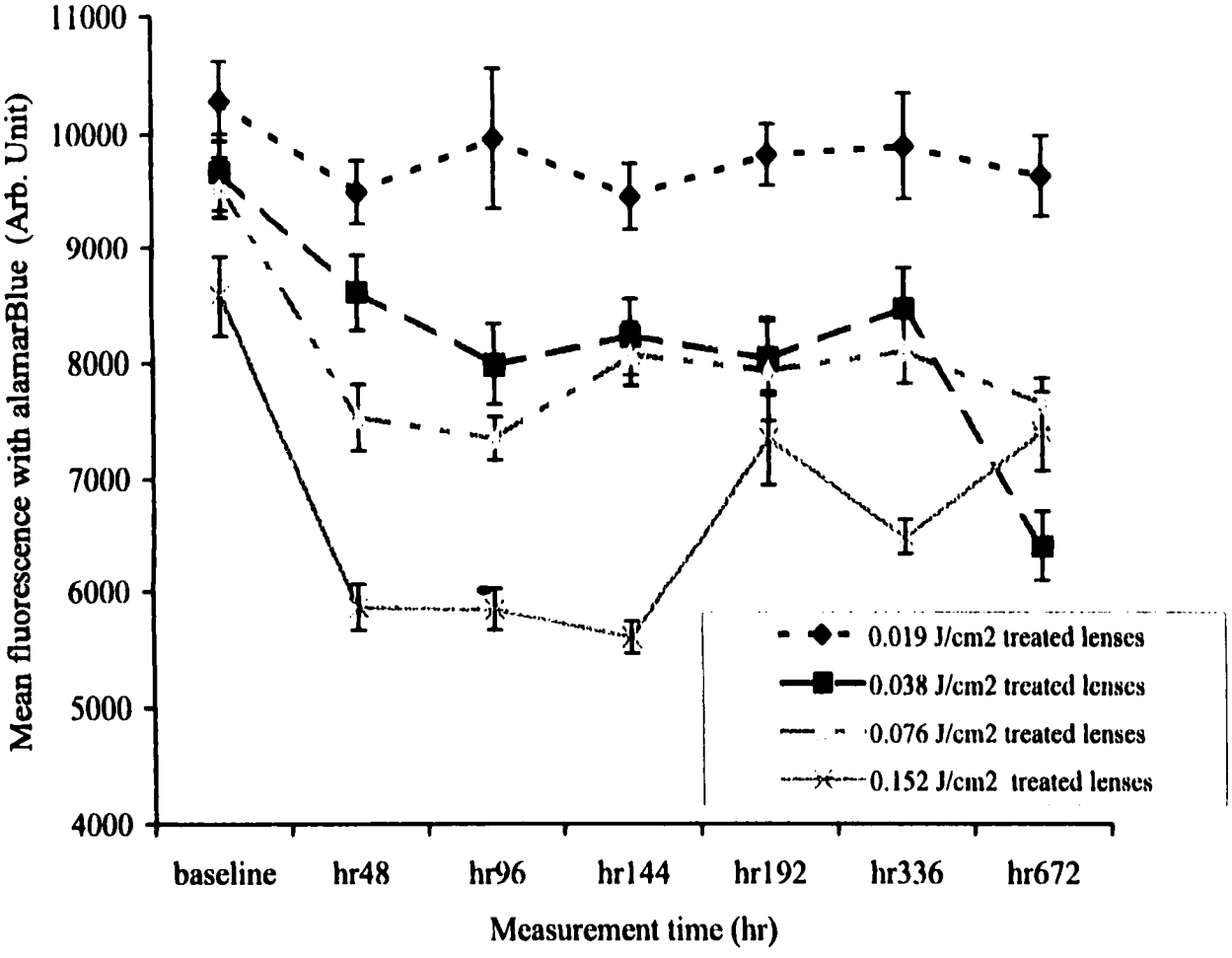

Figure 4.4. Level of UVB damage as a function of radiant exposure and time compared to baseline measurements as indicated by the CFDA-AM assay

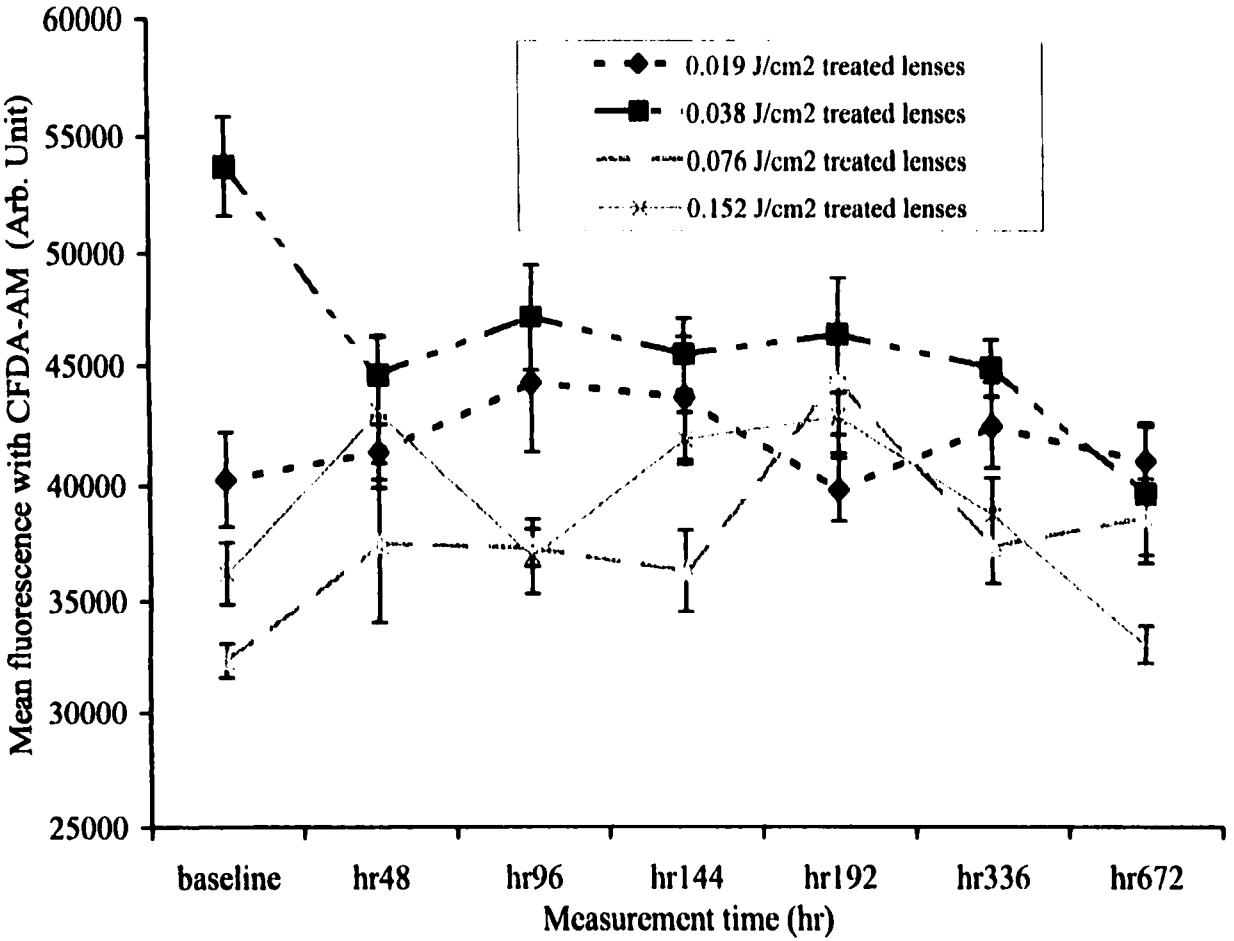

Figure 4.5. Level of UVB damage as a function of radiant exposure and time compared to baseline measurements as indicated by the mean focal length.

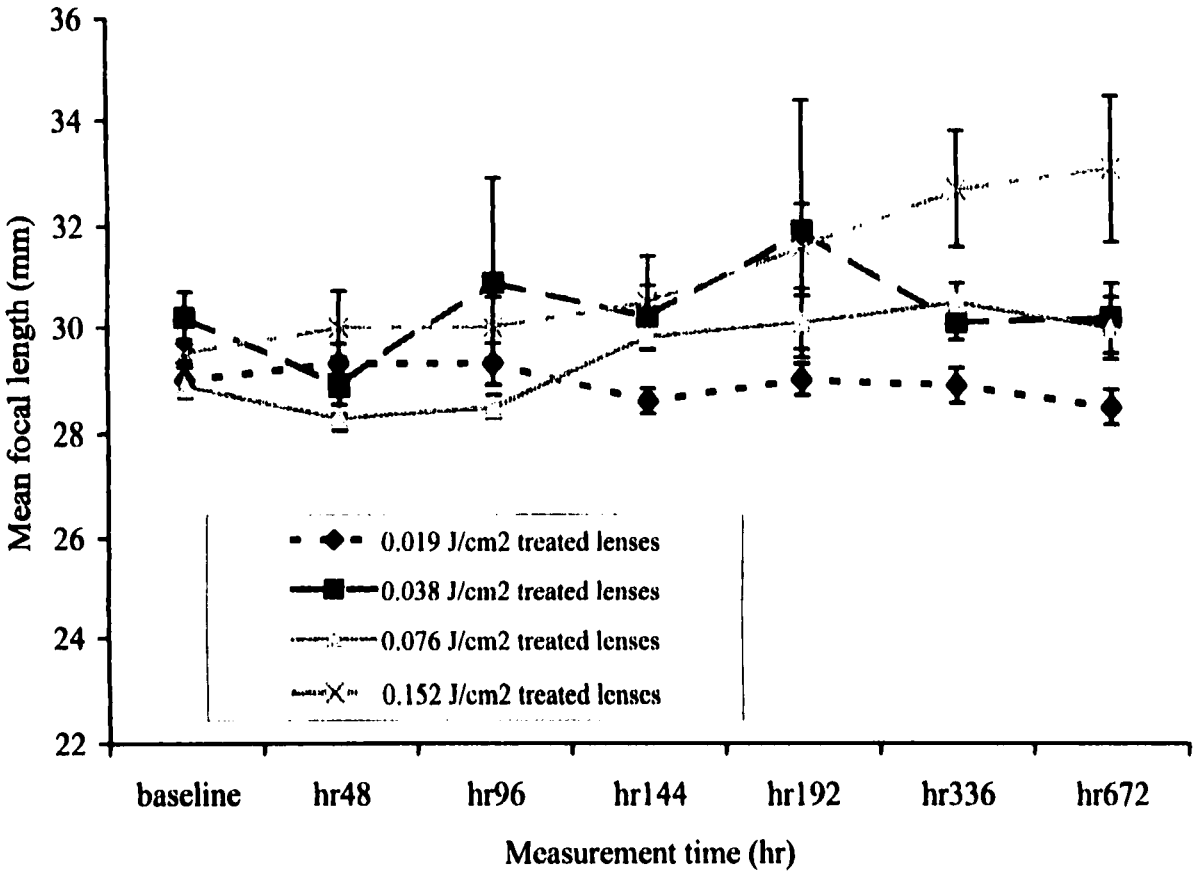

Figure 4.6. Level of UVB damage as a function of radiant exposure and time compared to baseline measurements as indicated by the mean focal length variability.

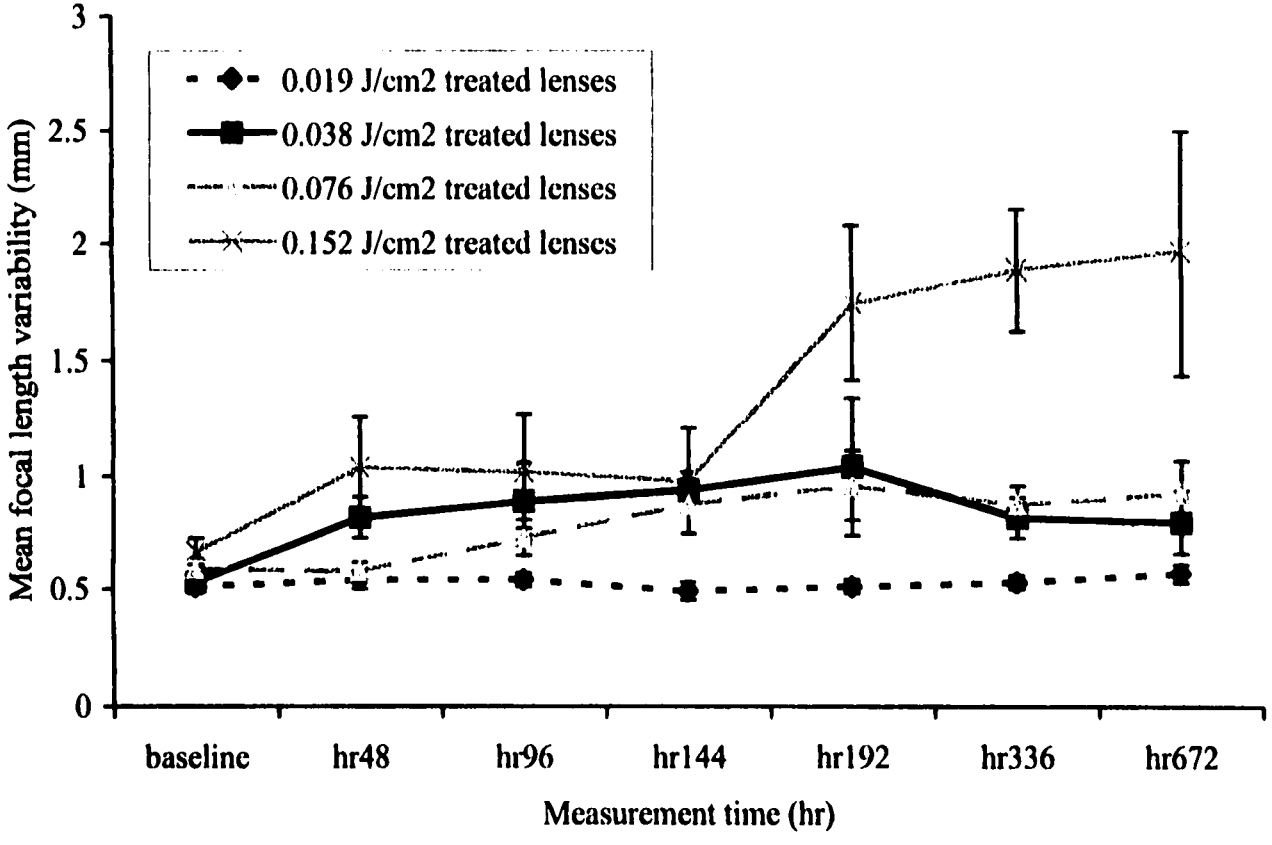

Figure 4.7. Representative pre and post-treatment photomicrographs showing morphological changes of lenses with 0.076 J/cm^2 UVB. (A) pre-exposure; (B) 48hr post-exposure (some vacuoles and discrete dot opacities at the anterior subcapsular; (C) 2 week post-exposure (vacuoles have coalesced and equatorial opacities now formed. Not to scale.

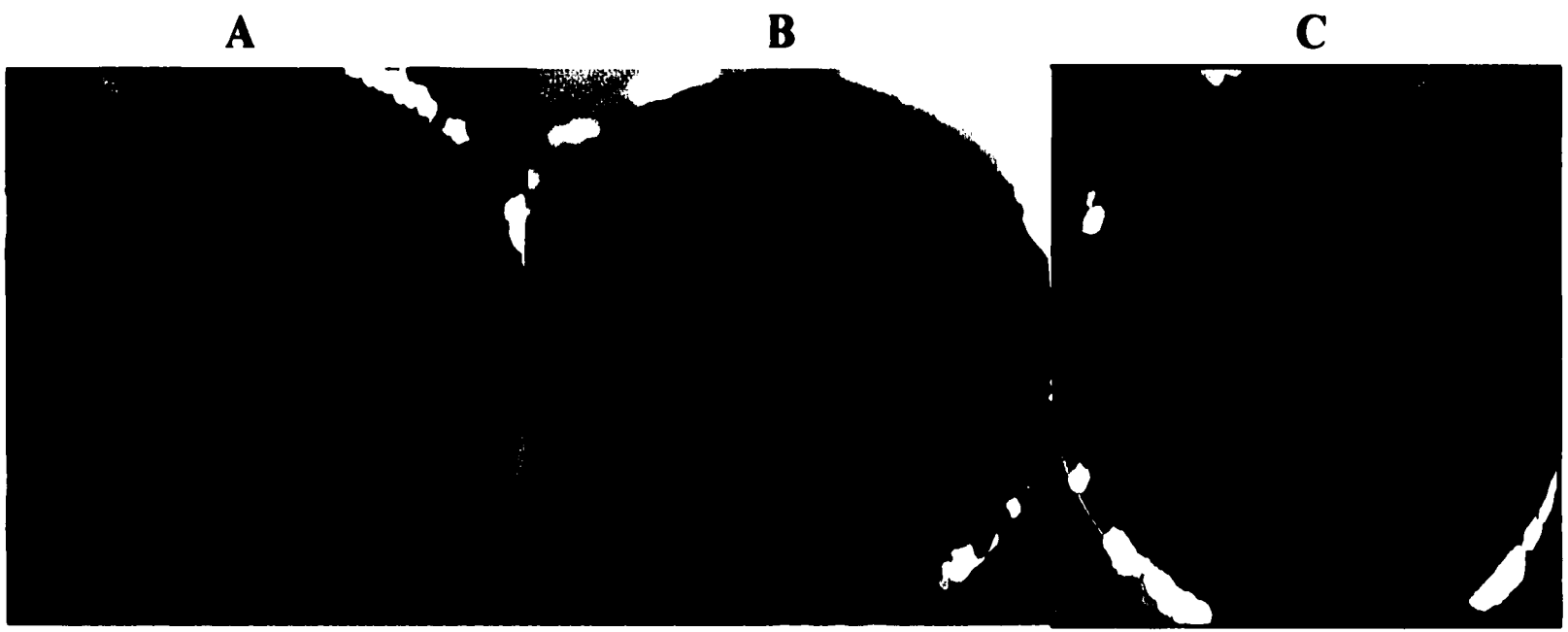

4.5 Discussion

The main objective of this study was to determine if the CFDA-AM and alamarBlue™ fluorescence indicator dyes in a combined assay would be a valid and repeatable cell biology approach to detect and monitor UV damage in organ cultured crystalline lens. The assay measurements and monitoring of the UVB induced damage on the lenses were done using a protocol that is similar to the one developed by Schirmer et al., (1997). The assay measurements were supplemented by the assessment of the relative changes in the average focal length and focal length variability of the lenses using the computer controlled scanning laser monitor developed by Sivak et al., (1986).

The CFDA-AM assay measurements showed a fair indication of the lens epithelial cell plasma membrane compromise at 48 hr post-exposure with both 0.152 J/cm^2 and 0.076 J/cm^2 UVB radiant exposures compared to control lenses (Tables 4.3 and 4.5). However, the lenses exposed to 0.152 J/cm^2 UVB showed an early recovery tendency at about 96 hr (Table 4.3). Beginning from 96 – 144 hr, significant change in cell plasma membrane integrity was obtained in lenses exposed to 0.152 J/cm^2 and 0.076 J/cm^2 UVB energy levels with an indication of recovery in 0.152 J/cm^2 UVB treated lenses, while the 0.076 J/cm^2 UVB treated lenses did not show recovery. Surprisingly, while lenses treated with 0.152 J/cm^2 and 0.076 J/cm^2 UVB radiant exposures showed an upward trend (Tables 4.3 and 4.5) in mean fluorescence (MF), those treated with 0.038 J/cm^2 UVB radiant exposure showed a consistently significant decrease ($P < 0.05$) in MF beginning from about 48 hr post-exposure with no sign of recovery through the study duration (Table 4.7 and Figure 4.3). The results obtained for 0.038 J/cm^2 UVB treated lenses was

in line with expectation, because a decrease in fluorescence readings is a direct measure of decline in cellular esterase activity due to loss of appropriate cellular milieu (Schirmer et al., 1997) from the UVB exposure. Also, substantially suprathreshold or high UVB radiant energy might induce UV damage via a passive diffusion process and there is an additional fluorescent component from the possible UVB-induced generation of intrinsic fluorogenic products (fluorogens or fluorescent chromophores) in the exposed crystalline lenses. This may imply that the increase in lenticular fluorescence post- exposure in the 0.152 J/cm^2 and 0.076 J/cm^2 UVB treated lenses might be accounted for possibly by the UVB-induced production of the fluorescent chromophore in the lens, and not just the CFDA-AM enhanced fluorescence. This explanation is supported by the fact that only viable epithelial cells can deacetylate the non-fluorescent CFDA-AM to carboxyfluorescein (which is fluorescent) and accumulates inside the cells for the fluorescence reading at each measurement time.

Studies that have shown the existence of fluorescent chromophores in the lens include that of Lerman and Borkman (1978) who demonstrated the presence of a fluorescent region (approximately 420-435 nm excitation and 500-520 nm emission) which becomes apparent in human crystalline lenses after the first decade of life. They explained that fluorogens in the human lens tend to increase with age. Of interest is that the emission wavelength region (500-520nm) of the fluorogens reported by Lerman and Borkman (1978) is close to the emission wavelength of CFDA-AM (530 nm). Therefore, the fluorescence reading obtained at high UVB exposure levels might be a combination of the fluorescence from both the CFDA-AM/esterase cleavage and the lens fluorescent chromophores. It has been shown that the generation of fluorogens (Lerman et al., 1976;

Lerman and Borkman, 1978; Zigman et al., 1977) is a sign of aging in the lens. More recently, Aquilina et al., (1997) demonstrated that 3-OH-kynurenine (3-HK) oxidation products can bind to lens protein causing macromolecular changes that occur with age such as protein aggregation, pigmentation, and fluorescence formation. The results in the current study suggest that, 0.038 J/cm^2 UVB radiant exposure might be the *in vitro* threshold for UVB acceleration of fluorogen generation in the lens. Overall, these results show that the CFDA-AM assay is a convenient method for quantifying UVB toxicity on lens plasma membrane integrity.

The results of the alamarBlue™ assay measurements show that UVB irradiation of lenses with 0.152 J/cm^2, 0.076 J/cm^2 and 0.038 J/cm^2 UVB radiant exposures induce significant reduction in the lens epithelial cellular metabolic activity beginning from 48 hr post-exposure and no indication of recovery from the UV damage (Tables 4.2; 4.4 and 4.6). The alamarBlue™ assay measurements show that the free radicals generated by UVB photochemical reaction in the lens cells at 0.038 – 1.52 J/cm^2 UVB radiant exposures could inhibit mitochondrial function in the lens epithelial cells. Comparing both CFDA-AM assay results (Table 4.5) to the alamarBlue™ results (Table 4.4) at the 48 hr assessment of the 0.076 J/cm^2 UVB treated lenses, it appears the impairment effect of UVB on cellular metabolic activity precedes plasma membrane damage. This study presents a quantitative evaluation of UV effect on mitochondrial function in the lens. The CFDA-AM results (Figure 4.4) indicate that UVB enhances aging of cell membranes, an event in cataract formation.

As with the assay results, all lenses except those treated with 0.019J/cm^2 UVB demonstrated significant increases or decreases in mean focal length and focal length

variability (sharpness of focus) relative to both baseline and control measurements. The average focal length of the lenses treated with 0.152 J/cm^2 did not demonstrate recovery from UV damage. The significant increase/increase in mean focal length of lenses treated with 0.038 and 0.076 J/cm^2 exposures exhibited recovery (Tables 4.11 and 4.12). It was deemed necessary to compare between the assay and optical measurements. To do this, the 0.076 J/cm^2 next to the highest exposure level used in this study was chosen. Therefore taking the 0.076 J/cm^2 data, it is shown in Tables 4.4, 4.5 and 4.11 that cellular and optical changes caused by UVB exposure commenced at about the same times post-exposure. No significant change in the plasma membrane integrity was shown until 96 hr post-exposure (Table 4.5). This delay may indicate that UVB damage of lens plasma membranes is preceded by perturbation of the lens epithelial cell mitochondrial and optical function. However, the optical changes showed recovery, but the cellular damage did not show any recovery through the duration of the study.

The increased focal lengths observed in some lenses could be a result of reduced refractive index caused probably by a UVB induced disruption of the normal water balance within the lens (Stuart et al., 1991). Widmark (1892) noted the disruption in water balance in UV damaged lenses when he described morphological signs of water imbalance through microscopic analysis. The findings of the current study show that relatively low dose of UVB radiation does not cause permanent damage in the lens cellular and optical integrity. Stuart et al., (1991) found that cultured bovine lenses treated with UVB radiant exposures ranging from 0.03 to 0.05 J/cm^2 demonstrated only temporary UV damage. The results of the current study suggest in vitro UVB lens damage to be between 0.019 and 0.038 J/cm^2, and show that the recovery from UV damage by

porcine lenses is similar to what has been reported for other experimental animal models for *in vivo* and *in vitro* conditions (Pitts et al., 1977b; Stuart et al., 1991).

Some photomicrographs were randomly taken during the course of this study. Comparing the morphological data in the present *in vitro* study with *in vivo* and *in situ* conditions, the findings support the view of Jose (1986) that if the lens anterior epithelium is disrupted metabolically or morphologically by UVB, its interaction with the bow fibres in turn may be altered or eliminated. The normal lens epithelium-bow interaction involves the epithelial cells becoming elongated fibres, and during the elongation, nuclei are transformed and the DNA is degraded (Trevithick et al., 1987). Jose (1982), noted that such disruption might occur if the genome of the epithelial cells were damaged by UVB. This could cause metaplasia of the epithelium and cortical fibres especially in the bow region thereby producing the characteristic UV radiation induced cortical opacification in the lens equatorial region (Schein et al., 1994). Equatorial opacities would normally not affect vision, but vision may become threatened when capsular wrinkling and cortical fibre plaques encroach on the visual axis. These plaques may be due to unrepaired coalesced vacuoles. Figure 4.7 is presented to illustrate the above point. This figure shows the microscopically visible experimentally induced UVB equatorial opacification. This equatorial opacification was thought to have resulted from the coalesced small vacuoles observed at about 48 hour post-exposure (note: time of first observation of vacuoles depends on the amount of UVB radiant exposure). The specific mechanisms for equatorial opacification by UVB as shown in this study remain to be confirmed. Jose and Pitts (1985) hypothesised that chronic UV damage to the lens epithelium may disrupt normal differentiation into non-nucleated fibres at the bow. Jose

(1986) speculated that UV exposure of lens epithelium might cause loss of DNA cues required for normal differentiation that pass from the epithelium to the fibres. Consequently, the epithelial cells and nucleated fibre cells fail to differentiate normally. Thus, the nucleated fibre cells neither lose their nuclei nor do they elongate toward the locus of the anterior-posterior sutures (Jose, 1986). Instead the cells may migrate and aggregate in areas within the lens cortex, which may act as a light-scattering element (Cullen et al., 1994). Zigman (1995) mentioned that lens anomalies occur initially in the epithelial cells, followed by anterior outer cortical fibre damage, and subsequently anterior cortical opacity. The observation of radial equatorial opacification may explain why cortical spokes are often clinically observed in the lens of older persons around the age of 60 years who might have had some exposure to UVB (Schein et al., 1994; West et al. 1998). These points demonstrate that photomicrography could be used for assessing UVB induced lens damage experimentally. However, it is a qualitative approach compared to the bioassay and SLM methods as presented in the current study.

In summary, in terms of quantifying UV damage and recovery, these experimental results show a fair correlation between the assay and SLM methods, thus confirming that alamarBlue™ and CFDA-AM assay would be a reliable and convenient *in vitro* cell biology methodology to study how UVB causes damage to the lens epithelial enzymes, mitochondrial function and lens membrane integrity. The significance of the assay method presented in the current study for UV cataract investigation, is that alamarBlue™ fluorescent dye measures UV damage to lens cellular metabolism, while CFDA-AM fluorescent dye measures UV damage to lens membranes, respectively.

Chapter 5

Relative phototoxicity of broadband UVA and UVB radiation on organ cultured porcine crystalline lens

5.1 Abstract

The relative phototoxicity of broadband ultraviolet A (UVA) alone, and UVA plus UVB combined, was investigated by analyzing changes in cellular integrity as measured with fluorescence dye assay and optical quality, in terms of focal length and focal length variability (i.e. sharpness of lens focus) of the cultured porcine crystalline lens. The fluorescence capability of the lenses was measured using a dual bioassay approach, which incorporated the use of two cell culture fluorescent dyes (carboxyfluorescein-diacetate-acetoxymethyl ester [CFDA-AM] and alamarBlue™). The lens optical integrity was assessed using a scanning laser system. Lenses aseptically dissected from pig eyes were kept in culture medium comprising modified M199, 1% penicillin/streptomycin (100 units/mL) and 4% porcine serum. After one week of preincubation in 37°C, 4% CO_2, 96% air, the lenses were exposed to predetermined broadband UVA and UVB energy levels. Prior to UV exposure, baseline cellular and optical function measurements were taken. Lenses treated with 86 J/cm^2 of UVA alone showed a significant ($P < 0.05$) decrease in cellular metabolism and loss of optical integrity at 48 hr post exposure, but recovered from the UVA damage. The lenses treated with 43 J/cm^2 UVA alone did not show any significant damage compared to baseline and control measurements. Lenses treated with radiant exposure of both 15.63 J/cm^2 UVA and 0.019 J/cm^2 UVB experienced a significant decrease ($P < 0.05$) in cellular and optical function, but some recovery was

achieved in terms of plasma membrane integrity (no recovery was shown in terms of cellular metabolic activity and sharpness of focus). These findings show that a relatively high UVA dose alone can induce lenticular damage, while relatively low UVA combined with relatively low UVB radiant energy can exhibit synergistic adverse UV effects. These results confirm that UVA is also cataractogenic.

5.2 Introduction

Evidence is mounting in the literature to the view that ultraviolet A (UVA) radiation contributes to cataract formation. Environmentally, atmospheric ozone does not absorb solar UVA radiation, but scattering of UVA by other atmospheric molecules such as N_2 and O_2 is significant (Frederick and Alberts, 1992). Some occupational, therapeutic and recreational conditions predispose individuals to UVA exposure as well. Zigman (1983) reported that the irradiance levels of solar UVA peaked at 365 nm to be 50 W/m^2 at Woods Hole, Massachusetts, U.S.A. in July, and 80 W/m^2 in January in Sarasota, Florida. Hietanem (1991) found irradiance levels of broadband UVA (320-400 nm) in Helsinki, Finland ranged from 18 W/m^2 in March to 48 W/m^2 in August. In comparison with Hietanem's (1991) data, the data reported in Figure 1.1 in section 1.2.3 of this thesis, showed the levels of broadband solar UVA (320-400 nm) to be 48.77 W/m^2 on June 18, 1999 in Waterloo, Ontario, Canada. The solar broadband UVB irradiance level on the same day in Figure 1.1 was 2.76-W/m^2, which is substantially higher than the values ranging between 0.065 to 0.2955 W/m^2 reported by Green et al., (1974) and Merchikunnel et al., (1983). From the foregoing, it is apparent that terrestrial UVA irradiance levels can influence the development of cataracts in human and other animals.

The mechanisms by which UVA radiation could cause damage to the crystalline lens or to the ability of the lens to recover from such damage are not yet clear (Pitts, 1988). According to Grothus-Draper's law, some amount of radiation must be absorbed by a tissue for damage to be elicited. Pirie (1971), proposed that low-power, long term exposure to UVR was the cause of brown nuclear cataract in humans, and Zigman and Vaughan (1974) observed cataracts in mice raised under elevated near-ultraviolet irradiance levels. They found that subcapsular and cortical punctate lenticular opacities appeared after 35 weeks after 12 hour daily exposure to of 4.5 W/m^2 UVB from black-light fluorescent tubes (Zigman and Vaughan, 1974). The role of solar UVA cataractogenesis proposed by Zigman (1983) has been challenged. Using different research protocols, the studies by Bachem, (1956), Pitts et al., (1977 a and b), and Jose and Pitts, (1985) concluded that UVB radiation between 295 and 315 nm induces anterior lenticular opacities, but that exposure to UVA radiation between 320 and 400 nm does not cause cataracts. Jose (1986) offered an explanation by noting that Zigman and Vaughan (1974) used a black light fluorescent tube that emitted a small amount of UVB radiation which might have caused the observed opacities.

In common with the human lens, the porcine lens contains low-molecular weight compounds with maximal absorption at approximately 360 nm and 265 nm (Cooper and Robson, 1969; van Heyningen, 1971). Therefore, it is expected that lenticular damage from UV radiation in the porcine lens would be similar to damage in human lenses and to that reported previously in other species such as rabbit (Pitts et al., 1977b) and cow (Stuart et al., [1991]; Dovrat and Weinreb, 1995 and 1999). In most reported *in vitro* studies, the damage observed in the lens included microscopically visible opacities,

decreased ATP, morphological defects in epithelial cells, loss of enzyme activities (such as catalase, NaK-ATPase), cytoskeletal actin breakdown, and cationic imbalances. There is great variability in the values for damage thresholds (Zigman, 1995). It has been calculated that only approximately 3% of the total solar UV radiation reaching the surface of the lens is UVB, and this might be sufficient to induce cataract (Zigman, 1995) because UVB contains more photon energy than UVA.

Barron et al., (1987), and Giblin (1998) showed that UVA causes nuclear light scattering in the guinea pig and knockout mouse. Linetsky and Ortwerth (1995) showed that UVA irradiation of older yellow human lens proteins caused the formation of free radicals. A recent *in vitro* study by Dovrat and Weinreb (1999) showed that exposure of organ cultured bovine lenses to 33 J/cm^2 UVA peaked at 365 nm and caused reversible damage to both the lens optics and NaK-ATPase activity. The present study was undertaken to investigate if the UVA radiation alone or combined with an experimentally determined subthreshold UVB level would have an effect on crystalline lens optics, plasma membranes and cellular metabolic activity.

5.3 Materials and Methods

5.3.1 Organ Culture and UV Exposure

Fresh eyes from 6-8 month old pigs were obtained from a local slaughterhouse approximately 1 hr post-mortem and held at room temperature until dissection, which was usually performed from 2 to 4 hr post-mortem. Visually clear lenses were aseptically dissected from the globe, with the adhering vitreous and ciliary body removed. The lens

was placed in a custom designed two-compartment glass chamber containing modified M199 culture medium with Earl's salts, without phenol red (phenol red is known to absorb UV radiation), plus 4% porcine serum (SIGMA Chemical), antibiotics (100 units/mL penicillin and 0.1 mg/mL streptomycin) and L-glutamine (0.1 g). The lenses were first maintained in organ culture for 168 hour (1 week) and only lenses without visible haze or opacities after the preincubation period were selected for the experiment. The reason for the one week preincubation was that it took 5-7 days for the lenses to attain homeostasis in the culture. The lenses randomly assigned to control and exposed groups were maintained in a water-jacketed incubator at 37°C, 4% CO_2, 96% air atmosphere, except during the UV irradiation period during which time they were kept in a custom built UV irradiation system with controlled temperature and humidity. Lenses were placed with the anterior surface facing up throughout the duration of the study. Both lens surfaces were bathed in a total of 25 mL of the culture medium which was replaced with sterile medium every 48 hr. The UV irradiation system had a membrane filtered air supply to keep the atmospheric condition of 4% CO_2 and 96% air. The relative humidity and temperature during irradiation were kept at 62% and 33°C to avoid heat effect. At one week of incubation, before exposing the lenses assigned for UV treatment, baseline fluorescence and optical quality measurements were taken using a fluorometric bioassay and optical laser scanning methods, respectively as described in chapter 4.

Approximately 12 hr after the baseline measurements, the treated lenses were exposed to broadband 86 J/cm^2 UVA (group 1); broadband 43 J/cm^2 UVA (group 2); and broadband 0.019 UVB combined synergistically with broadband 15.63 J/cm^2 UVA (group 3). The experiments for the different groups were conducted at different times.

Before irradiation, the culture medium was removed from the top of the lens in culture chamber so that just enough (approximately 1 mm) was left to cover the lens to prevent drying, but not enough to interfere with the process of irradiating the lens. For the 86 and 43 J/cm^2 UVA exposures, the UV source to the lens anterior surface was 15 cm, and exposure duration was 12 hr 30 seconds for 86 J/cm^2 UVA and 6 hr 15 seconds for 43 J/cm^2 UVA. Zigman (1995) reported in his review that the average UVA threshold for *in vitro* irradiated rabbit and squirrel lenses was 40 J/cm^2. Dovrat and Weinreb (1995) found no recovery of optical and enzyme activity with 44.8 J/cm^2 UVA irradiation of bovine lenses *in vitro*. Since there is no data for porcine lenses, it was decided to use 43 J/cm^2 UVA as the lower exposure level and double it for the higher UVA exposure in the present study.

For the synergism study, the lenses were exposed for $20x10^3$ seconds in order to obtain a maximum of 0.12 J/cm^2 UVB (biological effective dose equals 0.019 J/cm^2). This duration gave a simultaneous radiant exposure of 15.63 J/cm^2 UVA. The distance from the UV source to the anterior lens surface was 9 cm for the synergism experiment. It was decided to limit the duration of UVA exposure to the duration required for 0.019 J/cm^2 UVB because this UVB energy level has been found in earlier work (reported in chapter 4 of this thesis) not to cause apparent UVB lens-damage. Since the average UVA threshold for *in vitro* exposure is reported to be 40 J/cm^2 (Zigman, 1995), any damage observed with simultaneous UVA exposure must be due to UVB and UVA combined effect (synergism). A piece of cheesecloth was used to screen the UVB fluorescent tube in order to reduce UVB irradiance so as to achieve a sufficient UVA exposure. In order to prevent exposure to wavelengths below 290 nm, a cellulose acetate sheet measured to be

opaque to UV wavelengths below 290 nm, was placed on top of the lens containers during exposure. For comparative purposes, it was necessary to calculate the biologically effective UVB dose utilized for group 3 lenses. The calculation was carried out using ACGIH spectral weighting functions as described in chapter 4. As reported in chapter 4, the calculated UVB effective dose of 0.12 J/cm^2 UVB (actual energy) from the experimental UVB source was equivalent to 0.019 J/cm^2. Hence, for comparative purposes in subsequent discussions, 0.019 J/cm^2 UVB will be used. The UVA and UVB irradiation was achieved with 1 UVB and 3 UVA fluorescent tubes (Southern New England Ultraviolet Co., Branford, CT, USA; purchased from Microlites Scientific, Scarborough, Ontario, Canada). The spectral output of the UVB tubes is the same as described in chapter 4. The UVA fluorescent (black light) tubes produced a broadband emission from 350 nm to 410 nm, peaking at 365 nm. The spectral output distribution of the UVA fluorescent tubes is shown in Figure 5.1. The UVA fluorescent tubes did not emit any UVB wavelengths.

Before each irradiation procedure, the spectral output of the UVA and UVB sources were measured with an InstaSpec II photodiode array spectroradiometer (Oriel Corporation, Stratford, CT, USA) calibrated with a 1 kW quartz halogen lamp. The experimental UVA source produced an irradiance of 19.41 W/m^2 (1.941 mW/cm^2) for the exposure of groups 1 and 2 lenses. In comparison to Zigman et al., (1992) who used 2.5 mW/cm^2 in their study of UVA effects on lens actin, the UVA provided by the irradiation system in the present study is at subsolar level. For exposure of group 3 lenses the UVB/UVA source produced an irradiance of 0.06 W/m^2 UVB and 7.815 W/m^2 UVA, respectively. During the exposure, the lenses were oriented so that the anterior surface

faced the incident UV irradiation. Control lenses were protected from UV radiation by covering their containers with a black plastic sheet measured to be opaque to UV and visible radiation.

5.3.2 Cellular and Optical Integrity Assessment

All lenses were kept sterile and further incubated for 4 weeks post-irradiation, with the fluorescence and optical quality measurements carried out every 48 hr in the first 9 days, and then weekly. Fluorometric bioassay and optical measurements were the same as described in chapter 4. Statistical analysis for the different groups of lenses was performed using repeated measures analysis of variance. Probability values, set at the 0.05 significance level, were calculated using the F-test.

Figure 5.1. A representative plot of spectral output of the UVA fluorescent tubes used for the UVA exposures.

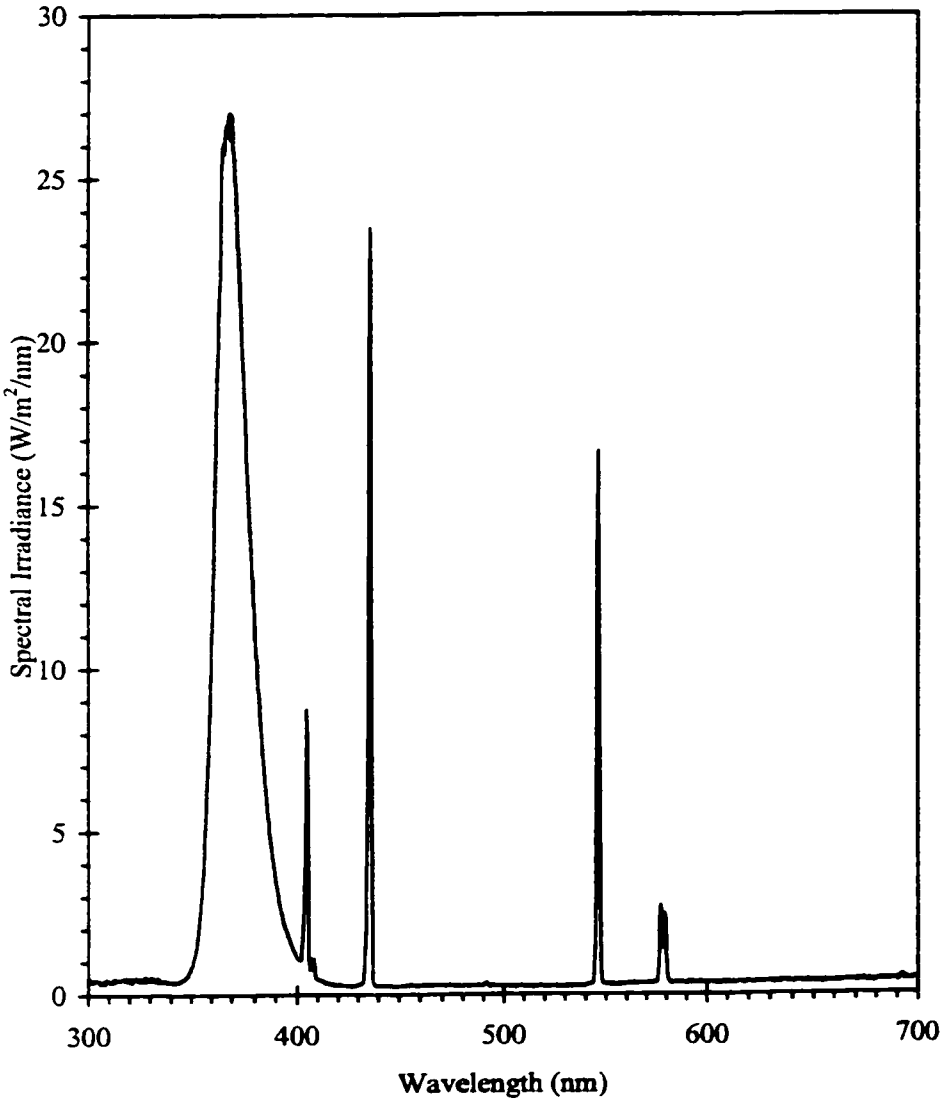

5.4 Results

5.4.1 Single UVA Exposure Experiment

A total of 12 control and 19 treated lenses were used in this experiment. Both the control and treated lenses were maintained in culture medium for a period of 672 hours except during measurements, UV irradiation (for treated lenses) and when changing the medium. The bioassay results are based on a total of 4,340 quantitative measures since each fluorescence measurement provides an average of 10 readings per scan, and each lens went through a cycle of 2 scans, one for alamarBlue™ and the second for CFDA-AM dyes at 7 different times. The optical quality results are based on 4,991 quantitative measures for the 31 lenses since each lens was scanned 7 times, and the SLM produced 23 measures of focal length each time. Figures 5.2 shows one representative plot of focal length profile of a porcine lens aged approximately 7 months.

Figure 5.2. A representative focal length profile for a single porcine lens. Equivalent focal length (mm) is shown on the horizontal axis. Eccentricity (mm) of laser beam position from optic axis (0.0) is shown on the vertical axis. The plus signs indicate where the beam crossed the axis at each eccentric position.

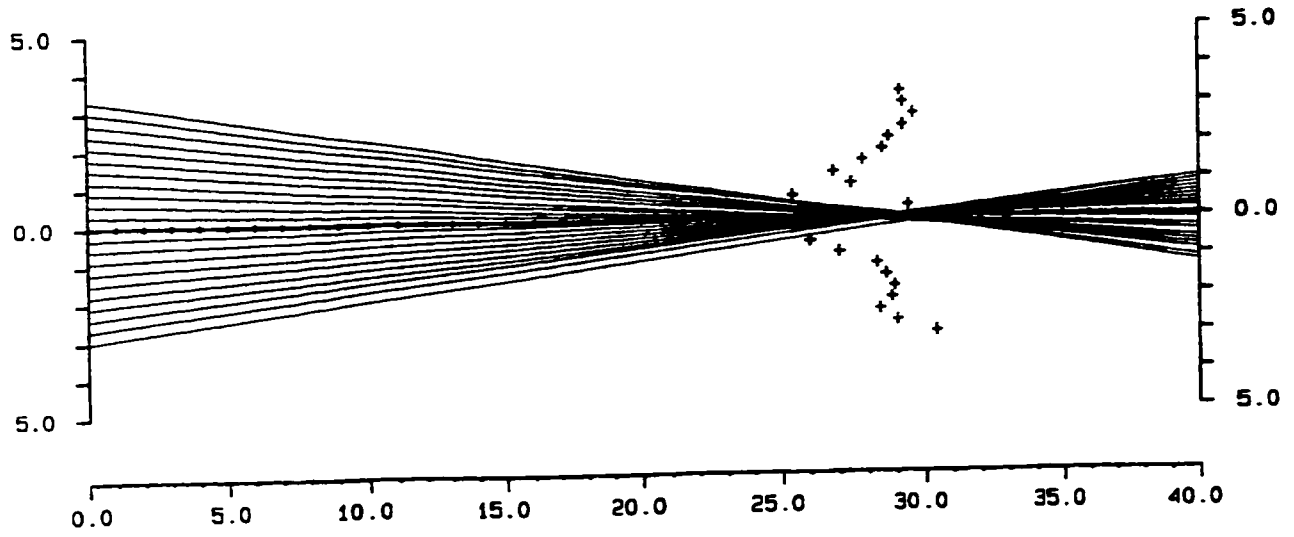

5.4.2 Lens Cellular Integrity Assessment

Lenses used for the 86 and 43 J/cm^2 UVA irradiation experiments had baseline mean fluorescence values ranging between 8277 (Table 5.4) and 11205 (Table 5.1) arbitrary fluorescence units (AFUs), as indicated by the alamarBlue™ assay and between 31957 (Table 5.5) and 51924 AFUs (Table 5.2) as indicated by the CFDA-AM assay. For clarity of presentation of the results, some collective data for all lenses are expressed graphically as mean fluorescence versus measurement time, with the error bars representing the standard error of the mean (S.E.M) (Figures 5.3 and 5.4). With the alamarBlue™ assay, the data in Tables 5.1 and 5.10 show that lenses treated with 86 J/cm^2 UVA exhibited some significant reduction in fluorescence (11%) at 48 hr (P = 0.013) and 10% at 96 hr (P = 0.036). These lenses demonstrated recovery from the UVA damage beginning from 114 hr (Table 5.1). Table 5.10 also shows that lenses treated with 43 J/cm^2 UVA demonstrated significant reduction in cellular metabolism of 8% at 48 hr (P = 0.042) with recovery commencing at 96 hr (Table 5.4). In terms of UVA damage of lens plasma membranes as indicated by the CFDA-AM assay, 86 J/cm^2 UVA irradiation led to a significant perturbation in esterase activity (P = 0.013) in the treated lenses at 48 hr, with quick recovery from 96 hr (Table 5.2). The lenses treated with 43 J/cm^2 UVA irradiation did not demonstrate any significant compromise in esterase activity (plasma membrane integrity) throughout the study duration.

5.4.3 Lens Optical Quality Assessment

The optical quality measurement results indicate the baseline mean focal lengths of both the control and treated lenses used for 86 and 43 J/cm^2 UVA irradiation ranged from 28.7 mm (Table 5.3) and 30.2 mm (Table 5.6) in control and treated lenses. The baseline mean focal length variability (FLV) ranged from 0.37 mm (Table 5.3) to 0.57 mm (Table 5.6) in all lenses. Some collective data for all lenses are expressed graphically as mean focal length variability (Figure 5.5) and mean focal lengths (Figure 5.6) over time with the error bars representing ± S.E.M of individual data point (not the focal length variability). The optical quality results, as indicated by the focal variability data, show that lenses treated with 86 J/cm^2 UVA exhibited a significant increase in FLV, as shown by a reduction in sharpness of focus beginning with 158% at 48 hr (P = 0.0002) with no recovery through to the end of the study (Tables 5.3 and 5.11). Table 5.11 shows that lenses treated with 43 J/cm^2 UVA did not demonstrate any significant reduction in lens sharpness of focus throughout the study period.

5.4.4 UVA/UVB Synergistic Irradiation

A total of 10 control and 15 exposed lenses were used in this experiment. The bioassay results here are based on a total of 3,500 quantitative measurements while the optical quality results are based on 4,025 quantitative measurements. The 15.63/0.019 J/cm^2 UVA / UVB synergistic irradiation produced significant reduction in cellular metabolic activity beginning from 48 hr (P = 0.0002) with no indication of recovery in the treated lenses (Table 5.7 and 5.10; Figure 5.7). However, lens plasma membrane damage was

only observed at 192 hr ($P = 0.04$) and 336 hr ($P = 0.0002$) with recovery at 672 hr (Table 5.8; Figure 5.8).

In terms of optical quality, the treated lenses demonstrated a significant increase in focal length variability (sharpness of focus) beginning from 96 hr ($P = 0.03$) post-irradiation with no recovery from the UV damage through to the end of study, while a significant change ($P = 0.012$) in mean focal length was observed only at 192 hr, which exhibited recovery by 336 hr ($P = 0.84$) (Table 5.9; Figures 5.9 and 5.10). This might explain why focal length variability (FLV) is more sensitive than average focal length (AFL).

Table 5.1. Descriptive statistics of alamarBlue™ fluorescence data for 86 J/cm^2 UVA radiant exposure (n= 10 for exposed lenses, and 6 for control lenses).

Measurement time (variable)	Fluorescence (Mean±STD)		Minimum value		Maximum value		*P* values	
	Exposed	Control	Exposed	Control	Exposed	Control		
Baseline	10789.3 ± 1101	11205.8 ± 935	8844	10015	12136	12337	Exposed	Control
Hour48	9625.7 ± 1254	9978.2 ± 927	7617	8659	11792	10888	0.013*	0.114
Hour96	9668.5 ± 456	10190.3 ± 499	8742	9588	10318	10956	0.036*	0.051
Hour144	9710.7 ± 943	10536.8 ± 901	8648	9332	11599	11756	0.055	0.091
Hour192	10359.9 ± 985	11183.7± 1130	9300	9875	11747	13012	0.330	0.977
Hour336 (wk2)	10322.3 ± 709	10916.2 ± 795	9313	9882	11301	12183	0.370	0.594
Hour672 (wk4)	10189.6 ± 734	10241.8 ± 496	9128	9589	11644	10935	0.220	0.122

Note: The *P* value set at 0.05 significance level is the comparison of baseline to subsequent measurements post-UV irradiation. *P* value with asterisk (*) indicates that fluorescence measurement at the time interval was significantly different from the baseline measurement in the group of lenses.

Table 5.2. Descriptive statistics of CFDA-AM fluorescence data for 86 J/cm^2 UVA radiant exposure (n= 10 for exposed lenses, and 6 for control lenses).

Measurement time (variable)	Fluorescence (Mean±STD)		Minimum value		Maximum value		*P* values	
	Exposed	Control	Exposed	Control	Exposed	Control		
Baseline	46805.7 ± 6120	44662.0 ± 6269	37024	35194	54395	51828	Exposed	Control
Hour48	39931.5 ± 4466	40249.3 ± 2130	34326	37231	49597	43275	0.013*	0.174
Hour96	48692.6 ± 6645	47424.7 ± 5554	37483	42185	58097	56158	0.508	0.238
Hour144	51924.8 ± 6030	50538.7 ± 7393	43410	41105	64608	56584	0.106	0.233
Hour192	45071.1 ± 6143	39579.3 ± 4923	36237	34972	52173	49217	0.567	0.127
Hour336 (wk2)	43318.4 ± 4375	42238.3 ± 6147	36506	30944	50291	47813	0.145	0.515
Hour672 (wk4)	38754.2 ± 5529	40267.7 ± 3175	33067	37502	47641	45489	0.012*	0.100

Note: The *P* value set at 0.05 significance level is the comparison of baseline to subsequent measurements post-UV irradiation. *P* value with asterisk (*) indicates that fluorescence measurement at the time interval was significantly different from the baseline measurement in the group of lenses.

Table 5.3. Summary of the optical quality assessment data for 86 J/cm^2 UVA radiant exposure (n = 10 for exposed lenses, and 6 for control lenses).

Measurement time (variable)	mean AFL (FLV) in mm		*P* values for mean AFL		*P* values for mean FLV	
	Exposed	Control	Exposed	Control	Exposed	control
Baseline	28.8 (0.41)	28.7 (0.37)				
Hour48	29.6 (1.06)	28.9 (0.41)	0.09	0.56	0.0002*	0.327
Hour96	28.9 (0.68)	28.4 (0.38)	0.88	0.49	0.007*	0.916
Hour144	28.4 (0.56)	28.2 (0.39)	0.17	0.30	0.025*	0.463
Hour192	29.2 (0.88)	28.6 (0.44)	0.21	0.75	0.002*	0.226
Hour336 (wk2)	29.3 (0.75)	29.2 (0.37)	0.18	0.54	0.003*	0.842
Hour692 (wk4)	28.9 (0.77)	29.1 (0.41)	0.95	0.57	0.002*	0.244

Note: The *P* value set at 0.05 significance level is the comparison of baseline to subsequent measurements post-UV irradiation. *P* value with asterisk (*) indicates that fluorescence measurement at the time interval was significantly different from the baseline measurement in the group of lenses.

Table 5.4. Descriptive statistics of alamarBlue™ fluorescence data for 43 J/cm^2 UVA radiant exposure (n= 9 for exposed lenses, and 6 for control lenses).

Measurement time (variable)	Fluorescence (Mean±STD)		Minimum value		Maximum value		*P* values	
	Exposed	Control	Exposed	Control	Exposed	Control		
Baseline	8981.2 ± 1116	9678.5 ± 1246	7337	7887	10680	11488	Exposed	Control
Hour48	8277.7 ± 649	9605.2 ± 769	7672	8486	9615	10400	0.042*	0.840
Hour96	9305.2 ± 801	9470.0 ± 1365	7642	7258	10247	11004	0.504	0.615
Hour144	10138.1 ± 1264	10337.0± 918	8479	9564	11671	11900	0.076	0.140
Hour192	8932.1 ± 841	9649.0 ± 1332	7662	8721	10356	12282	0.912	0.943
Hour336 (wk2)	8809.0 ± 1483	9653.0 ± 1840	7345	7685	11886	12003	0.741	0.968
Hour672 (wk4)	8381.7 ± 899	8466.8 ± 1277	6983	6948	9685	9857	0.312	0.100

Note: The *P* value set at 0.05 significance level is the comparison of baseline to subsequent measurements post-UV irradiation. *P* value with asterisk (*) indicates that fluorescence measurement at the time interval was significantly different from the baseline measurement in the group of lenses.

Table 5.5. Descriptive statistics of CFDA-AM fluorescence data for 43 J/cm^2 UVA radiant exposure (n= 9 for exposed lenses, and 6 for control lenses).

Measurement time (variable)	Fluorescence (Mean±STD)		Minimum value		Maximum value		*P* values	
	Exposed	Control	Exposed	Control	Exposed	Control		
Baseline	35211.8 ± 2190	35952.2 ± 4964	31789	30345	38967	43328	Exposed	Control
Hour48	38193.0 ± 4178	39463.2 ± 4182	33366	33714	43568	44499	0.098	0.111
Hour96	40086.1 ± 6519	41822.5 ± 9044	31753	31429	53680	55262	0.067	0.072
Hour144	35786.1 ± 4180	39466.8 ± 2075	31734	35638	44680	41593	0.750	0.175
Hour192	38521.7 ± 4729	39552.5 ± 6842	32161	31672	44294	48242	0.057	0.365
Hour336 (wk2)	31957.6 ± 2349	33525.5 ± 3927	27309	29520	35186	40310	0.039*	0.187
Hour672 (wk4)	36201.9 ± 4431	41616.3 ± 4936	30014	36513	44956	47807	0.620	0.082

Note: *P* value with asterisk (*) indicates that fluorescence measurement at the time interval was significantly different from the baseline measurement in the group of lenses.

Table 5.6. Summary of the optical quality assessment data for 43 J/cm^2 UVA radiant exposure (n = 9 for exposed, and 6 for control lenses).

Measurement time (variable)	mean AFL (FLV) in mm		*P* values for mean AFL		*P* values for mean FLV	
	Exposed	Control	Exposed	Control	Exposed	control
Baseline	30.2 (0.53)	30.1 (0.57)				
Hour48	30.3 (0.67)	29.3 (0.71)	0.981	0.060	0.159	0.359
Hour96	30.4 (0.62)	29.2 (0.66)	0.533	0.107	0.231	0.403
Hour144	30.0 (0.82)	29.4 (0.57)	0.440	0.204	0.065	0.998
Hour192	30.1 (0.66)	29.2 (0.70)	0.437	0.146	0.208	0.129
Hour336 (wk2)	30.5 (0.92)	29.9 (0.60)	0.552	0.566	0.133	0.833
Hour672 (wk4)	29.0 (0.83)	29.5 (0.71)	0.030*	0.140	0.076	0.161

Note: *P* value with asterisk (*) indicates that fluorescence measurement at the time interval was significantly different from the baseline measurement in the group of lenses.

Table 5.7. Descriptive statistics of alamarBlue™ fluorescence data for 15.63 J/cm^2 UVA and 0.019 J/cm^2 UVB synergistic radiant exposure (n= 15 for exposed lenses, and 10 for control lenses).

Measurement time (variable)	Fluorescence (Mean±STD)		Minimum value		Maximum value		*P* values	
	Exposed	Control	Exposed	Control	Exposed	Control		
Baseline	9388.6 ± 839	9471.6 ± 1244	7909	7583	10623	11114	Exposed	Control
Hour48	7819.3 ± 691	8808.2 ± 1159	6612	6518	8796	9671	0.0001*	0.084
Hour96	8158.3 ± 1051	9207.2 ± 1772	5753	5927	9703	11719	0.0003*	0.507
Hour144	8534.9 ± 1038	9079.1 ± 1150	7193	6681	10898	10854	0.0048*	0.079
Hour192	8219.1 ± 1351.	9558.6 ± 845	5737	8164	10716	11531	0.0072*	0.802
Hour336 (wk2)	8123.4 ± 1192	9365.4 ± 1202	5989	6688	10341	10711	0.0064*	0.709
Hour672 (wk4)	8212.8 ± 1116	8742.5 ± 1815	6024	5604	9910	11390	0.0052*	0.114

Note: The *P* value set at 0.05 significance level is the comparison of baseline to subsequent measurements post-UV irradiation. The *P* value with asterisk (*) indicates that fluorescence measurement at the time interval was significantly different from the baseline measurement in the group of lenses.

Table 5.8. Descriptive statistics of CFDA-AM fluorescence data for 15.63 J/cm^2 UVA and 0.019 J/cm^2 UVB synergistic radiant exposure (n= 15 for exposed lenses, and 10 for control lenses).

Measurement time (variable)	Fluorescence (Mean±STD)		Minimum value		Maximum value		*P* values	
	Exposed	Control	Exposed	Control	Exposed	Control		
Baseline	44019.1 ± 6663	41754.5 ± 4344	35405	34350	60050	48611	Exposed	Control
Hour48	45155.0 ± 5003	46465.6 ± 6119	32500	41304	52810	58215	0.5252	0.103
Hour96	43571.9 ± 8158	41442.0 ± 4750	33184	34686	60264	46619	0.7901	0.870
Hour144	42340.5 ± 6360	43140.5 ± 5967	35745	30350	54929	50956	0.4449	0.369
Hour192	39028.9 ± 6036	40287.1 ± 4111	28999	34444	49059	48755	0.0423*	0.548
Hour336 (wk2)	38249.7 ± 4376	39316.7 ± 4860	31743	29950	46479	46207	0.0002*	0.095
Hour672 (wk4)	37469.0 ± 11238	39920.1 ± 6205	28263	31959	50657	53319	0.1395	0.574

Note: The *P* value set at 0.05 significance level is the comparison of baseline to subsequent measurements post-UV irradiation. The *P* value with asterisk (*) indicates that fluorescence measurement at the time interval was significantly different from the baseline measurement in the group of lenses.

Table 5.9. Summary of the optical quality assessment data for 15.63 J/cm^2 UVA and 0.019 J/cm^2 UVB synergistic radiant exposure (n = 15 for exposed, and 10 for control lenses).

Measurement time (variable)	mean AFL (FLV) in mm		*P* values for mean AFL		*P* values for mean FLV	
	Exposed	Control	Exposed	Control	Exposed	control
Baseline	29.3 (0.43)	29.1 (0.42)				
Hour48	28.9 (0.51)	29.2 (0.43)	0.348	0.646	0.194	0.291
Hour96	28.9 (0.59)	28.7 (0.44)	0.252	1.000	0.027*	0.189
Hour144	28.9 (0.80)	28.6 (0.39)	0.209	0.438	0.005*	0.302
Hour192	28.6 (0.75)	28.4 (0.37)	0.012*	0.118	0.021*	0.077
Hour336 (wk2)	29.4 (0.89)	29.1 (0.46)	0.839	0.935	0.003*	0.379
Hour692 (wk4)	29.0 (0.75)	29.3 (0.43)	0.265	0.434	0.009*	0.693

Note: The *P* value set at 0.05 significance level is the comparison of baseline to subsequent measurements post-UV irradiation. The *P* value with asterisk (*) indicates that fluorescence measurement at the time interval was significantly different from the baseline measurement in the group of lenses.

Table 5.10. Percent reduction in lens cellular metabolism due to the UV radiant exposures as indicated by alamarBlue™ assay assessment in terms of pre (baseline) versus post-UV irradiation measurements.

Type/Radiant exposure (J/cm2)	Percent reduction in lens metabolism (% reduction compared to baseline measurement)					
	48hr	96hr	144hr	192hr	336hr	672hr
86 UVA only (n=10)	11*	10*	10	4	4	6
43 UVA only (n=9)	8*	0	0	1	2	7
15.63 UVA / 0.02 UVB: synergism (n=15)	7*	13*	10*	12*	13*	13*

Note: Asterisk (*) means that the reduction in lens cellular metabolic activity at the time of assessment is significant ($p < 0.05$) compared to the baseline measurements.

Table 5.11. Percent reduction in lens optical integrity due to the different UV radiant exposures as indicated by increase in focal length variability (decrease in sharpness of focus), in terms of pre (baseline) versus post-UV irradiation measurements.

Type of / Radiant exposure (J/cm2)	Percent Increase in FLV (% increase compared to the baseline measurement)					
	48hr	96hr	144hr	192hr	336hr	672hr
86 UVA only (n=10)	158*	65*	36*	115*	82*	88*
43 UVA only (n=9)	26	16	54	24	73	56
15.63 UVA / 0.02 UVB: synergism (n=15)	18	37*	86*	74*	100*	73*

Note: Reduction in average focal length (AFL) could not be used as an indicator of diminishing lens viability because SLM studies have shown that compromise in lens optical integrity could be demonstrated in higher or lower values of AFL compared to the baseline. However, focal length variability (FLV) seems to be a good indicator since increase in FLV mostly implies reduction in sharpness of focus of the lenses due to a stress factor. Asterisk (*) means that the increase in FLV at the time of assessment is significant ($p < 0.05$), with some increase greater than 100% compared to the baseline measurements.

Figure 5.3. Level of lens cellular metabolism as a function of 86 and 43 J/cm^2 UVA exposures (baseline vs post-irradiation measurements).

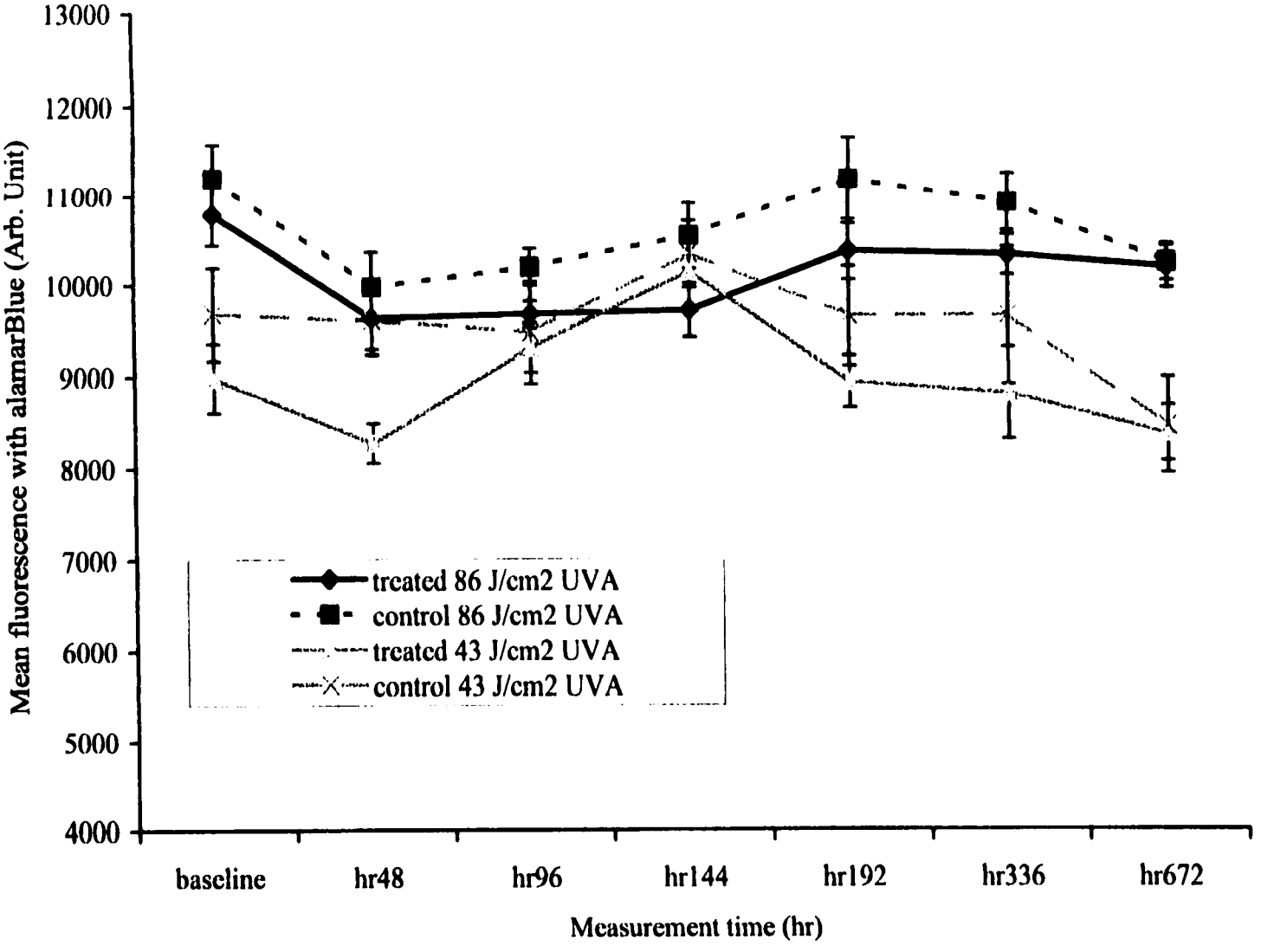

Figure 5.4. Level of lens plasma membrane integrity (esterase activity) as a function of the 86 and 43 J/cm^2 UVA exposures.

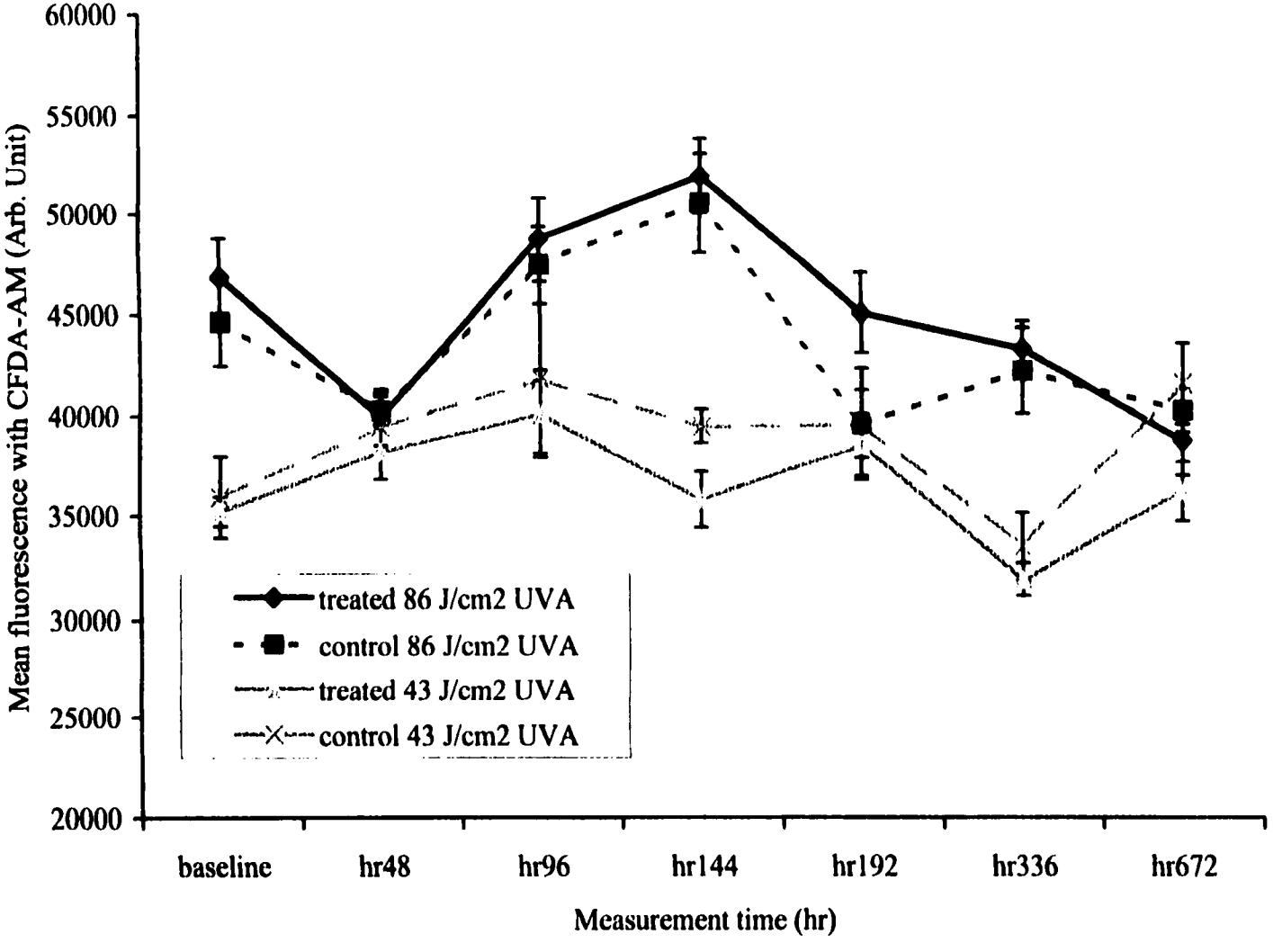

Figure 5.5. Mean focal length variability as a function of 86 and 43 J/cm^2 UVA exposures (baseline versus follow up assessment). FLV demonstrates significant increase ($p < 0.05$) in 86 J/cm^2 treated lenses beginning from 48hr (see table 6.3).

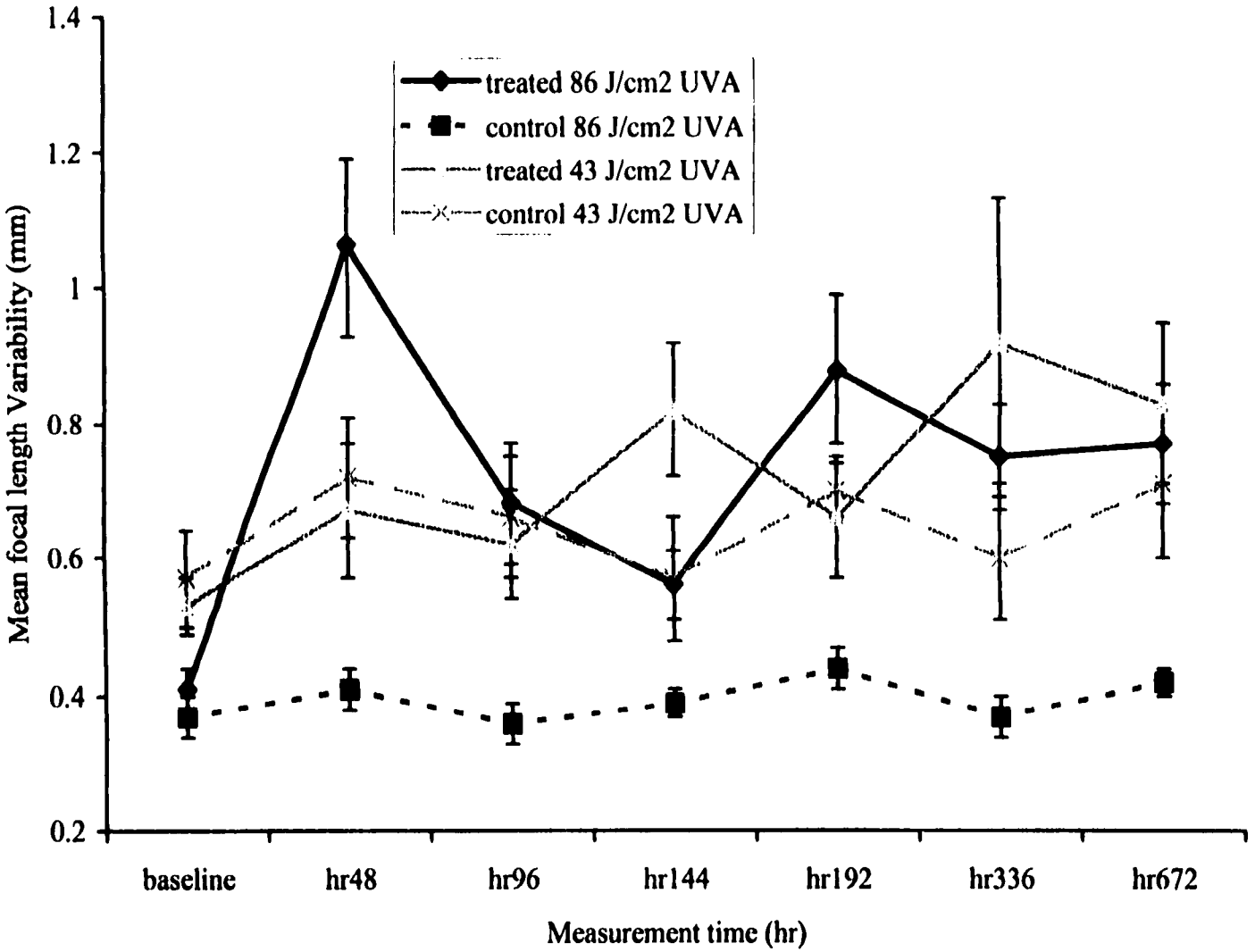

Figure 5.6. Mean focal length (AFL) as a function of 86 and 43 J/cm^2 UVA exposures, respectively (baseline versus post-irradiation assessment compared to controls).

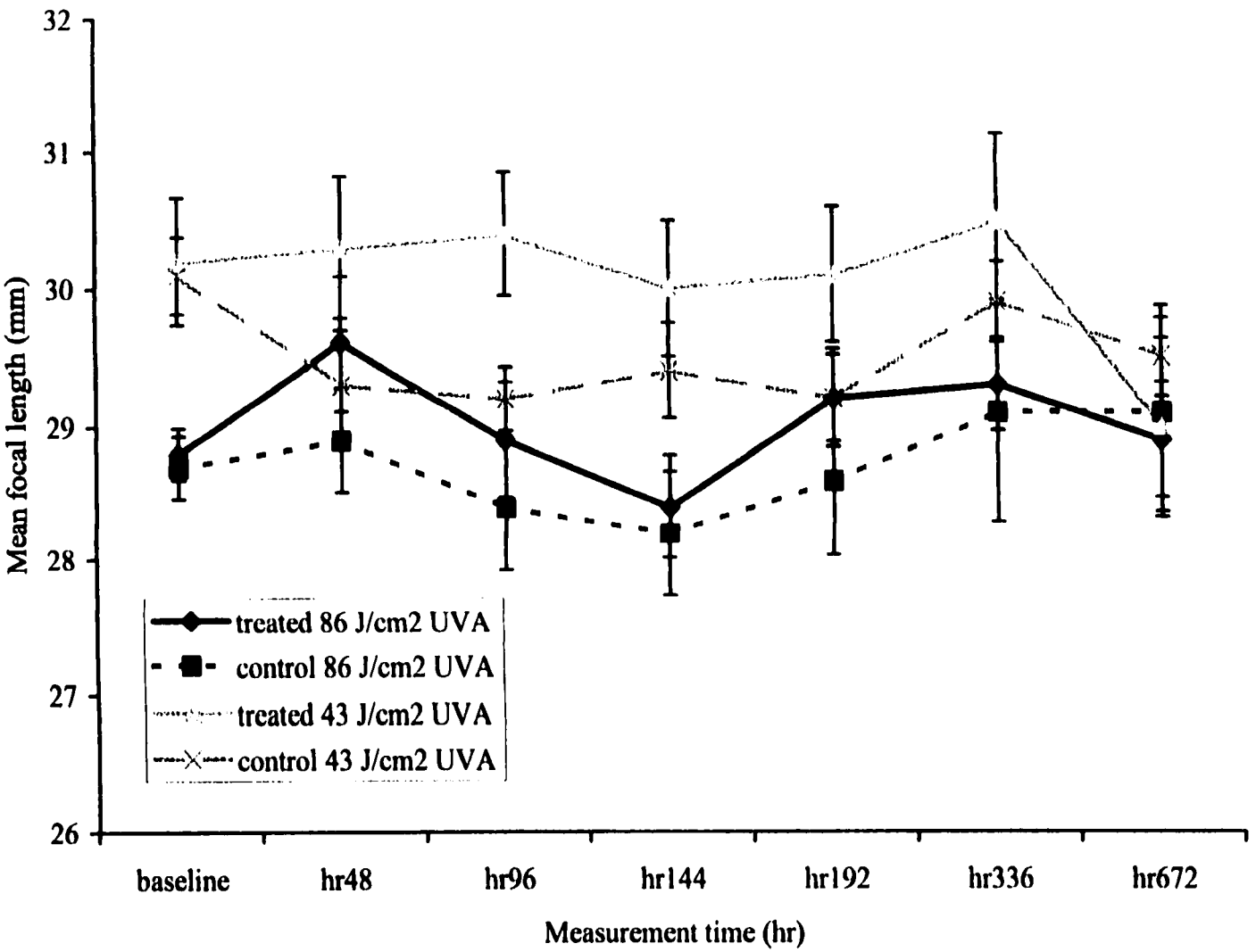

Figure 5.7. Level of lens cellular metabolism as a function of UVA/UVB synergistic exposure (baseline versus post-irradiation measurements).

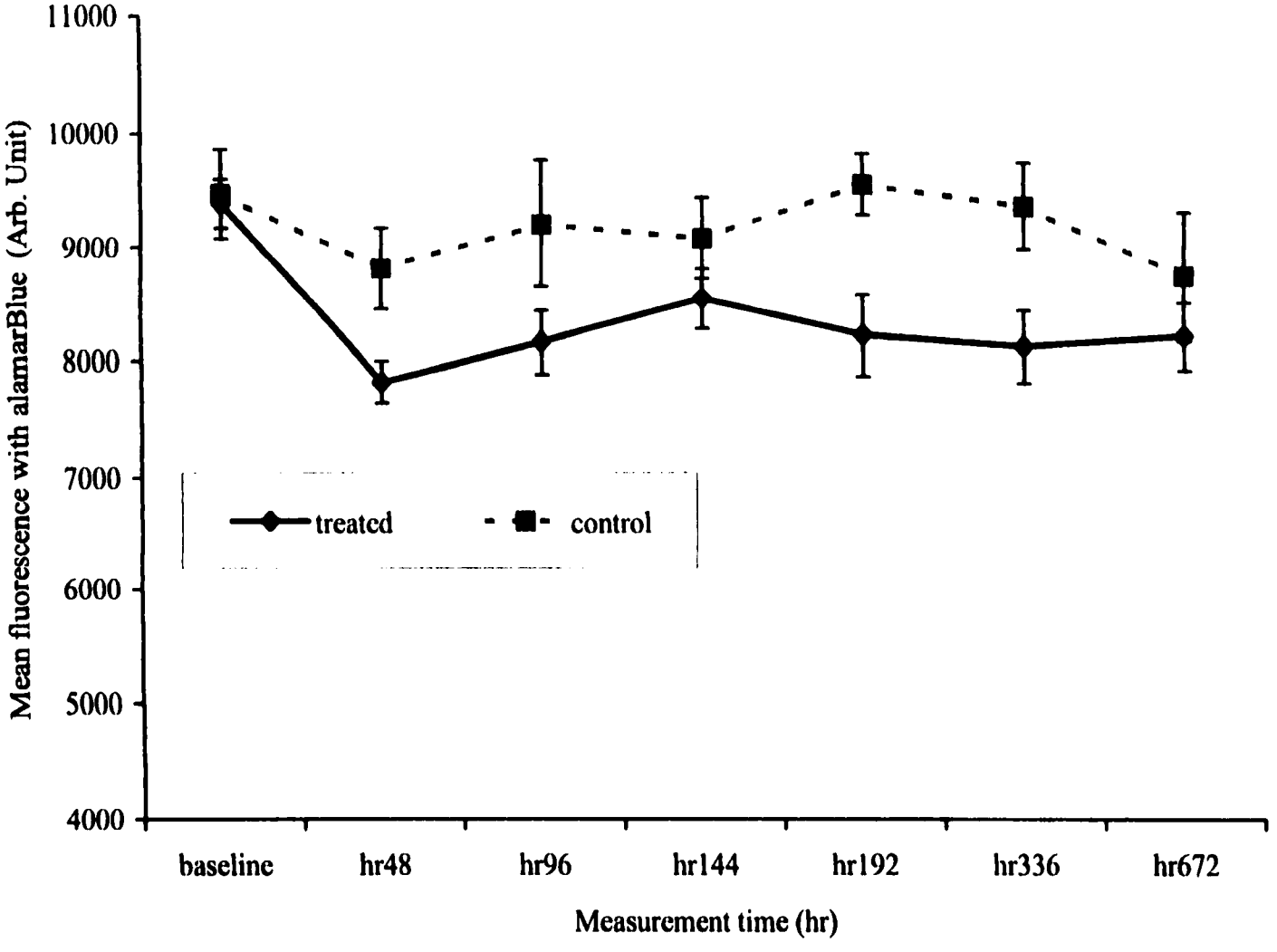

Figure 5.8. Level of lens plasma membrane integrity as a function of UVA/UVB synergistic exposure as assessed by CFDA-AM assay (baseline versus post-irradiation measurements).

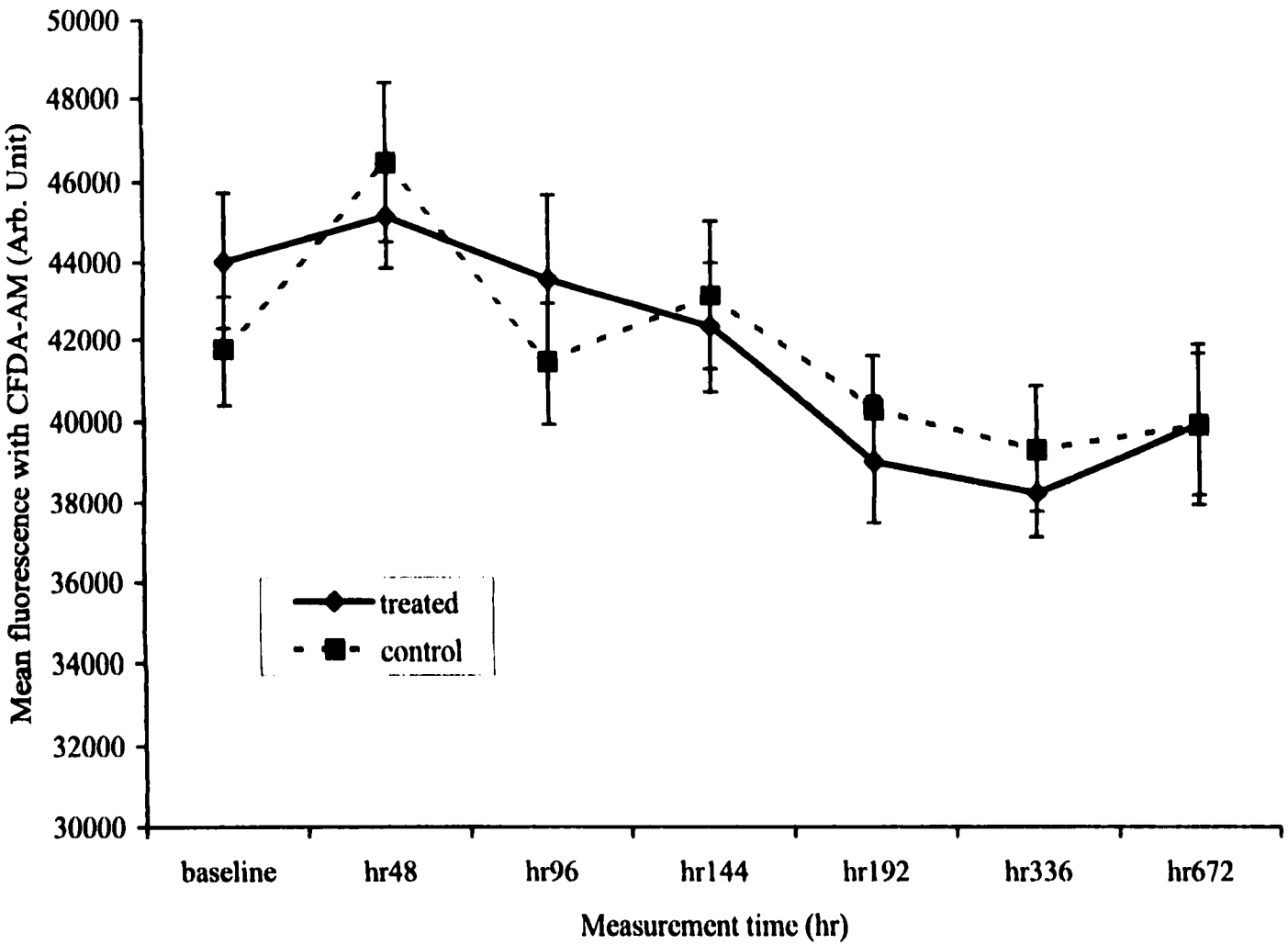

Figure 5.9. Level of sharpness of focus as a function of 15.63/0.019 J/cm^2 UVA/UVB synergistic exposure (baseline versus follow up measurements).

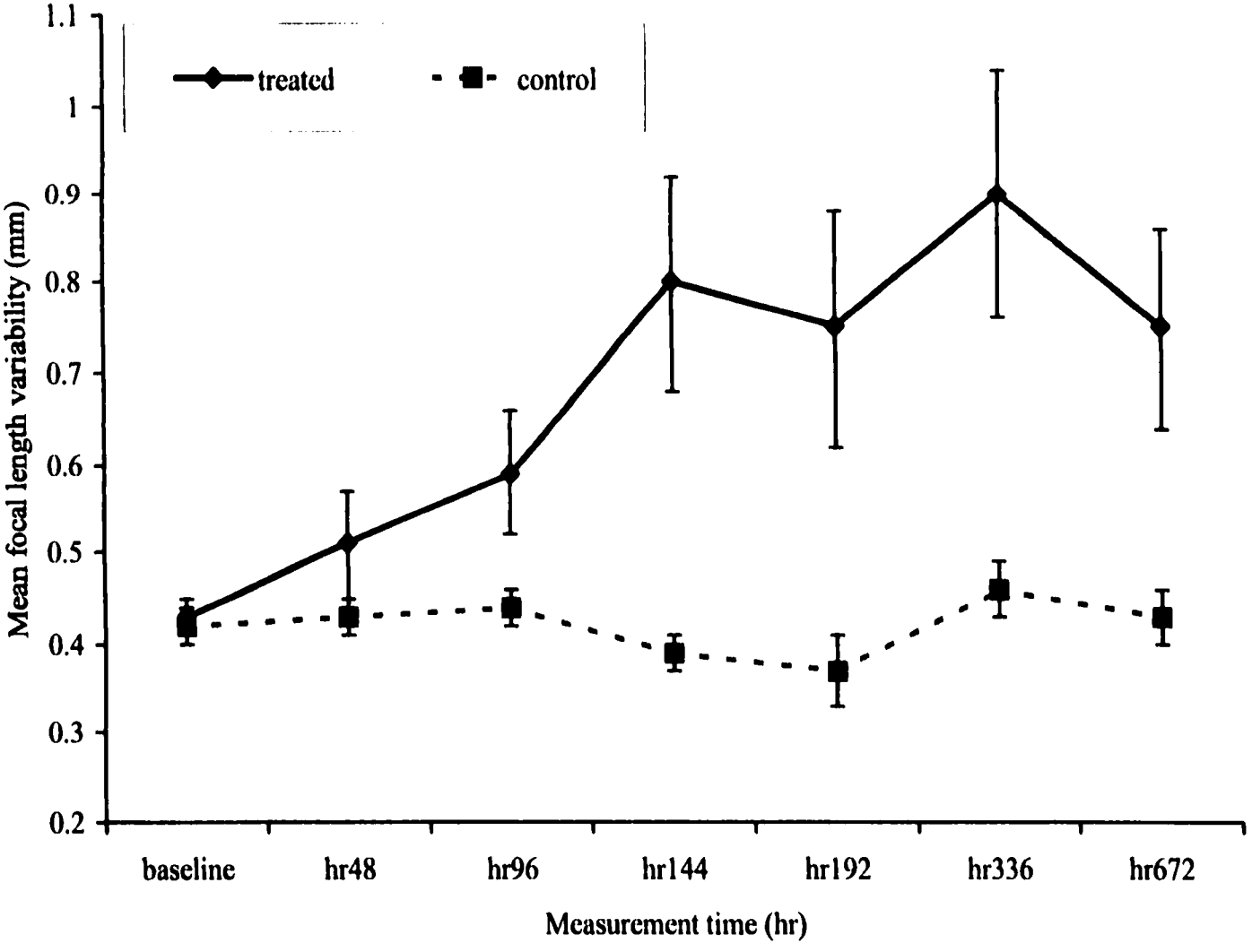

Figure 5.10. Level of mean focal length as a function of UVA/UVB synergistic exposures (baseline versus post-irradiation measurements).

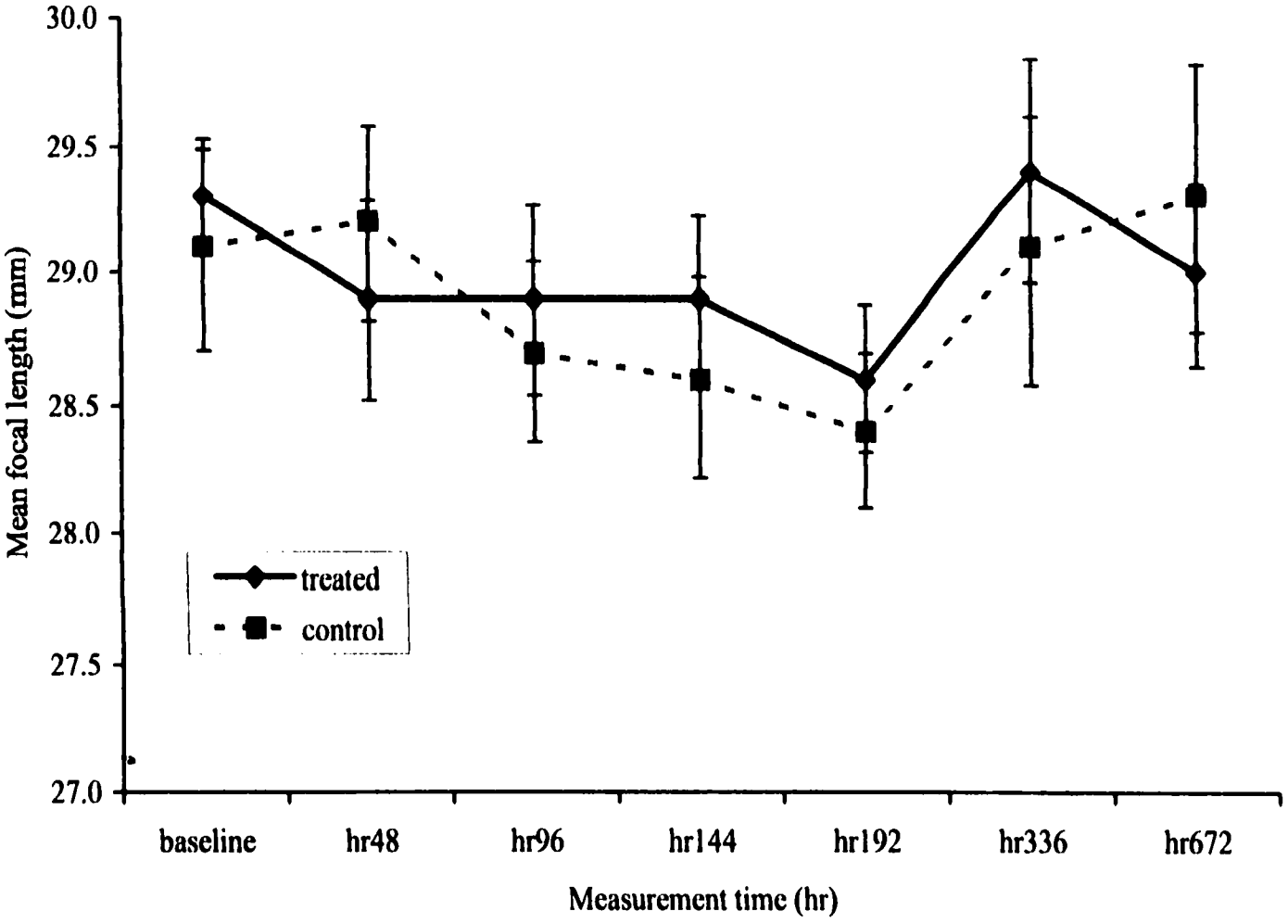

5.5 Discussion

5.5.1 Predominantly UVA Exposure

The crystalline lens is a surface tissue that continues to grow throughout life with new cells formed on the outer surface and old concentrated toward the interior (Mann, 1969). Many experimental studies have shown that exposure to UVR in the range of 290 to 400 nm, whether from sunlight or an artificial source induces photochemical changes in the crystalline lens. It is generally agreed that chronic exposure to UVR in the 290-400 nm range over a lifetime leads to the generation and increased accumulation of chromophores with an associated increase in the amount of insoluble protein within lens fibres (Zigman, 1986; Stevens and Bergmanson, 1989; Liang, 1991; Dillon et al., 1999a). Previous *in vitro* and *in vivo* experiments (van Heyningen, 1972; Zigman et al., 1991) indicated that UVR exposure converts tryptophan within the lens into an oxidised form which cross-links to other proteins. The resultant protein aggregations lead to opacities in the lens (Stevens and Bergmanson, 1989).

The results in this study show that a radiant exposure of 86 J/cm^2 UVA causes considerable damage to the cellular and optical integrity of the crystalline lens *in vitro*, some of which showed recovery and some not. The alamarBlue™ and CFDA-AM assay data show that the stress on the lens metabolic activity and esterase activity induced by the 86 J/cm^2 UVA exposure gradually dissipated through the lens repair systems in the lenses. Clearly, as shown in Table 5.3, the 86 J/cm^2 UVA exposure caused significant permanent degradation in sharpness of focus (i.e. focal length variability) in the treated lenses, but the average focal lengths of the lenses were not affected. This might not be

surprising since the variables of shape and refractive index changes may neutralise each other. However, it may indicate that focal length variability is a more sensitive indicator of UVA damage in crystalline lenses. The 43 J/cm^2 UVA radiation is shown to cause subtle reversible damage to lens cellular metabolic activity at 48 hr (Table 5.4), the esterase activity at 336 hr (Table 5.5), and the lens optics at 672hr (Table 5.6). Dovrat and Weinreb (1995) using cultured bovine lenses found partial recovery of UV damage of lens optics, and 80-90% recovery of enzyme activity in lenses irradiated with 33.6 J/cm^2 UVA, and no recovery of damage in lenses irradiated with 44.8 J/cm^2 UVA. Dovrat and Weinreb (1999) also found that 33 J/cm^2 UVA exposure caused reversible damage of bovine lens NaK-ATPase activity *in vitro*. Although the endpoints and times are somewhat different, the findings of the present study that 43 J/cm^2 UVA could induce reversible damage to the lens *in vitro* tend to agree closely with those of Dovrat and Weinreb (1999). The results of the current study and that of Dovrat and Weinreb (1995, 1999) suggest that a radiant exposure between 33 J/cm^2 and 43 J/cm^2 is the *in vitro* UVA threshold range for lens damage.

5.5.2 UVA / UVB Synergism

Tables 5.7 and 5.8 show that lens cellular metabolism and esterase activity (plasma membrane integrity) suffer significant damage due to the UVA/UVB synergism. The reduction of lens cellular metabolic activity, which began at about 48 hr post-irradiation, did not demonstrate any recovery. By comparison, damage to the lens esterase activity only occurred at 192 hr and 336 hr post-exposure. This might suggest that UV induced mitochondrial impairment, leading to reduced cellular metabolic activity, precedes

general plasma membrane damage in the lens. According to Zigman (1995), the UVA and UVB radiation that penetrates the cornea would first impinge on the lens epithelial cells. Therefore, lens anomalies would be expected to occur initially in the epithelial cells, followed by anterior outer cortical fibre damage, and subsequent anterior cortical opacity (Zigman, 1995).

The use of the infero-nasal location of cortical opacities as biomarkers of solar UVR-induced cataract in humans has been suggested (Sliney, 1986), and this was confirmed by Schein et al. (1994), who reported an association of sunlight exposure with cortical cataracts located mostly at the infero-nasal quadrant of the lens. The biochemical reason for this could be explained on the basis of a report by Blanquet and Courtois (1989) that metabolic interactions between cytoskeletal proteins differ in different regions of the lens epithelium. Thus, it could be speculated that the cytoskeleton proteins in the infero-nasal quadrant of the lens contain weak metabolic interactions, which might make UVR damage more effective at the lens infero-nasal quadrant. Alternatively, anterior eye focusing of ambient environmental ultraviolet radiation, particularly reflected rays (albedo) has been proposed as the likely reason for the more prevalent infero-nasal cortical cataract in outdoor workers (Coroneo, 1990; Cullen et al., 1997). In general, *in vitro* experimental results such as those of the current study, support UVR as a causative factor in human cataractogenesis. Anterior cortical opacity was observed 2 weeks and 4 weeks post-irradiation in some treated lenses in the current experiment as well.

The trend in the CFDA-AM and alamarBlue™ assay results (Figures 5.7 and 5.8) also suggests that alamarBlue™ is more sensitive in showing the UV toxic effect. Although not statistically significant (Table 5.8), a decrease in membrane integrity

(reduced esterase acitivity) was evident from the 96 hr data which did not seem to recover to the baseline level. That the alamarBlue™ assay results appear significant from 48 hr may not be surprising because there is the possibility that the ATP production in the mitochondria was quickly diminished due to UV damage, causing significant destabilization of epithelial cell metabolism. This possibility may be supported by the findings of Thomas et al., (1991) who found a drop in the ATP level of squirrel lenses exposed to near-UV radiation as measured by [^{31}P]NMR procedures. Also, it may be that since esterase activity is not only present in the epithelium but also in other lens components, particularly the fibres, that the CFDA-AM assay is measuring general membrane damage of the lens. This would suggest the CFDA-AM dye as a good non-toxic fluorescence indicator to use in the study of the role of UV in lens membrane aging.

Taking the assay and optical results together, the UVA/UVB synergistic degrading effect on lens cell metabolic activity and membrane integrity appears to follow a similar trend in term of the degradation of lens optics, especially as indicated by the focal length variability results. These show a significant decrease (Table 5.9), beginning at 96 hr, with no recovery tendency to the end of the study (Figure 5.9). The findings in the current study support the view that UVA involvement cannot be excluded in the formation of cataracts in humans (Zigman, 1993; Dillon, 1999). Using *in vivo* UVB exposure, Jose and Yielding (1977) proposed that the active repair mechanism noted in rat lens epithelium is through unscheduled DNA synthesis. Stuart et al., (1991) noted that DNA synthesis might not be the mechanism for recovery in *in vitro* UV exposure. Rather, it is possible that UVB damages the enzyme NaK-ATPase, allowing a water imbalance that produces temporary swelling and opacification to take place (Torriglia and Zigman, 1988). Zigman

(1991), using cultured squirrel lenses, found that predominantly UVA irradiation could damage lens epithelial NaK-ATPase activity, while Dovrat and Weinreb (1999), using cultured bovine lenses, found that UVA damage to lens epithelial NaK-ATPase activity was repairable.

Previous studies have provided information on UV-lens damage for predominantly UVB exposure (Hightower and McCready, 1992b) or predominantly UVA exposure (Zigman et al., 1992; Weinreb and Dovrat, 1996). The results of the present study indicate that both UVB and UVA exposures show similar trends of damage and recovery in terms of lens cellular and optical integrity, however, higher UVA energy is required. In conclusion, the present study demonstrates, with both cell biology and optical methods, that the synergistic effects of substantially low, sub-solar UVB and UVA exposures can adversely affect lens cellular and optical properties. Overall, this study supports the hypothesis that UVA contributes to the disruption of lens epithelial *in vivo*, and that it should be considered to be an aetiologic factor in human cataractogenesis.

Chapter 6

SUMMARY and CONCLUSIONS

Using the newly developed assay methodology and the optical scanning laser system developed by Sivak et al., (1986), this thesis has examined the suitability of the porcine crystalline lens for organ culture studies of UV-induced cataractogenesis and other lens related investigations. Contrary to Wang et al., (1997) the results in this thesis confirm that porcine lenses from commercial sources can be cultured for up to six weeks without compromising their transparency, optical or cellular integrity, with an appropriate culture medium formulation as described in this study.

In order to further address the mechanisms of UV cataractogenesis, and given the concern for animal welfare, continued *in vitro* research efforts are worthwhile. An *in vitro* UV-cataract action spectrum for the organ cultured intact lens was established using probit statistical protocol. The *in vitro* action spectrum for UV lens damage appears to follow a similar pattern to *in vivo* action spectra obtained for the cornea and lens (Pitts, Cullen and Hacker, 1977a and b). This may not be surprising, since the cornea and lens epithelium are both derived from the same embryological origin, the surface ectoderm. The characteristic of repair from UV damage in the porcine lens was also examined. In terms of UV damage and repair, the magnitude and recovery of the lesions were both wavelength and dose dependent.

The development of a new methodology warrants its testing and validation. Therefore, the feasibility of the new assay approach described in chapter two, to quantitatively measure UVB and UVA damage in cultured lenses was investigated. The

evidence as validated with the scanning laser monitor system indicates that lens cellular measures obtained with the new technique are valid.

A question that is currently a subject of debate is whether or not UVA is cataractogenic. The new assay method was employed to address this question, and to evaluate synergistic effects of UVA and UVB. Since mitochondrial function is the hallmark of cell metabolism, UVB and UVA were shown to cause a decrease in lens cellular metabolic activity. Thus, the results presented in chapters four and five suggest that UVB and UVA damage to the lens cells is through the inhibition of mitochondrial function. The results also support the view that UVA is cataractogenic, and that simultaneous subthreshold UVA and UVB exposure in combination can cause damage to the lens. The irreversibility of UV damage observed at certain radiant exposures, as indicated by the alamarBlue™ and CFDA-AM assay data, suggests that the damaged lenses are unable to replenish damaged ATPases and membrane proteins containing ion channels or transporters.

The results of this study suggest several directions of further research. New fluorescent indicator dyes are emerging; especially those that can be used to selectively quantify the apoptotic phenomenon in living cells. Thus, pathologic phenomena can be studied using the newly developed assay method, for example, to investigate if UVB and/or UVA causes lens damage by apoptosis, necrosis or a combination of both. Also, it could be possible to label DNA in cultured lens to study UV effects on lens DNA in live epithelial cells. This approach could elucidate the importance of apoptosis in relation to repair in UV-lens damage. In terms of comparative study of cellular and biochemical properties of lenses from different animal species, the new bioassay approach would be

an excellent tool. It could be speculated from the present results of the assay method that UV irradiation causes lens damage by destabilizing lens plasma protein and lipid substrate. It is known that intracellular calcium concentration (regulated by endoplasmic reticulum proteins), regulates a variety of cellular functions including secretion, contraction-relaxation, cell differentiation, cytoplasmic metabolism, apoptosis, protein synthesis and folding. The assay method could be used to study the role of endoplasmic reticulum in UV cataractogenesis, and to investigate if UV causes lens damage by directly inhibiting protein synthesis or by causing an increase in intracellular calcium (an increase in calcium content is known to inhibit lens protein synthesis [Hightower and McCready, 1997]).

Taken together, the results from this thesis are in agreement with previous *in vivo* and *in vitro* studies in finding that crystalline lens epithelial and fibre cells are important targets of UVB and UVA. The fluorometric bioassay model as now developed for lens research, is a potential addition to the ocular drug efficacy testing battery, particularly for pharmacological agents that are being developed for cataract prevention. Finally, the data in this thesis have shown that the combination of UVB and UVA can have a deleterious effect on the lens, thus confirming that preventive strategies against ultraviolet radiation should also consider the UVA waveband.

Chapter 7

APPENDICES

Appendix 7.1A. Action spectrum data arrangement for exposed lenses at 270 nm waveband. Note: under damage grade column, 'no dam', 'mod(er)' or 'sev' means no UV damage, moderate damage or severe damage, respectively.

4 sets (20 lenses) at 270 nm			
Set 1 lens #	time of lesion	damage grade	Radiant exposure J/cm2
1	48	no dam	0.0522
2	48	no dam	0.0522
3	36	mod	0.0522
4	48	mod	0.0522
5	48	no dam	0.0522
		increase by 50%	
Set 2 lens #	time of lesion		Radiant exposure J/cm2
1	36	sev	0.0783
2	36	sev	0.0783
3	48	mod	0.0783
4	48	moder	0.0783
5	24	moder	0.0783
		reduce by 25%	
Set 3 lens #	time of lesion		Radiant exposure J/cm2
1	36	sev	0.0587
2	48	no dam	0.0587
3	36	mod	0.0587
4	48	no dam	0.0587
5	48	no dam	0.0587
		increase by 10%	
Set 4 lens #	time of lesion		Radiant exposure J/cm2
1	36	sev	0.0646
2	36	mod	0.0646
3	36	mod	0.0646
4	48	no dam	0.0646
5	36	sev	0.0646

Appendix 7.2A. Action spectrum data for exposed lenses at 275 nm waveband.

5 sets (25 lenses) at 275 nm			
Set 1 lens #	time of lesion	damage grade	radiant exposure J/cm2
1	48	no dam	0.0345
2	48	no dam	0.0345
3	36	mod	0.0345
4	48	mod	0.0345
5	48	no dam	0.0345
		increase by 50%	
Set 2 lens #	time of lesion		radiant exposure J/cm2
1	48	no dam	0.0518
2	36	sev	0.0518
3	48	no dam	0.0518
4	48	no dam	0.0518
5	36	mod	0.0518
		increase by 25%	
lens # 3	time of lesion		radiant exposure J/cm2
1	36	sev	0.0647
2	24	mod	0.0647
3	36	mod	0.0647
4	24	mod	0.0647
5	36	sev	0.0647
		reduce by 10%	
lens # 4	time of lesion		radiant exposure J/cm2
1	36	sev	0.058
2	36	mod	0.058
3	36	mod	0.058
4	48	mod	0.058
5	36	sev	0.058
		reduce by 10%	
lens # 5	time of lesion		radiant exposure J/cm2
1	48	mod	0.0522
2	48	no dam	0.0522
3	48	mod	0.0522
4	48	mod	0.0522
5	36	mod	0.0522

Appendix 7.3A. Action spectrum data for exposed lenses at 280 nm waveband.

	5 sets (25 lenses) at 280 nm		
Set 1 lens #	time of lesion	damage grade	radiant exposure J/cm2
1	36	no dam	0.0253
2	36	no dam	0.0253
3	36	mod	0.0253
4	48	mod	0.0253
5	36	no dam	0.0253
		increase by 50%	
Set 2 lens #	time of lesion		radiant exposure J/cm2
1	36	sev	0.03795
2	48	mod	0.03795
3	36	mod	0.03795
4	36	sev	0.03795
5	36	mod	0.03795
		reduce by 25%	
Set 3 lens #	time of lesion		radiant exposure J/cm2
1	36	mod	0.0285
2	48	mod	0.0285
3	48	no dam	0.0285
4	48	no dam	0.0285
5	48	no dam	0.0285
		increase by 10%	
Set 4 lens #	time of lesion		radiant exposure J/cm2
1	36	mod	0.0314
2	48	no dam	0.0314
3	48	mod	0.0314
4	48	mod	0.0314
5	48	no dam	0.0314
		increase by 10%	
Set 5 lens #	time of lesion		radiant exposure J/cm2
1	36	mod	0.0345
2	48	mod	0.0345
3	48	mod	0.0345
4	48	mod	0.0345
5	36	sev	0.0345

Appendix7.4A. Action spectrum data for exposed lenses at 285 nm waveband.

	6 sets (30 lenses) at 285 nm		
Set 1 lens #	time of lesion	damage grade	radiant exposure J/cm2
1	36	sev	0.03025
2	36	sev	0.03025
3	36	sev	0.03025
4	48	mod	0.03025
5	36	sev	0.03025
Set 2 lens # (reduce by 50%)	time of lesion		radiant exposure J/cm2
1	48	no dam	0.01513
2	48	no dam	0.01513
3	48	no dam	0.01513
4	48	no dam	0.01513
5	48	no dam	0.01513
Set 3 lens # (increase by 25%)	time of lesion		radiant exposure J/cm2
1	48	no dam	0.0189
2	48	no dam	0.0189
3	48	no dam	0.0189
4	48	mod	0.0189
5	48	no dam	0.0189
Set 4 lens # (increase by 10%)	time of lesion		radiant exposure J/cm2
1	48	no dam	0.0208
2	36	no dam	0.0208
3	36	mod	0.0208
4	48	mod	0.0208
5	36	no dam	0.0208
Set 5 lens # (increase by 10%)	time of lesion		radiant exposure J/cm2
1	48	mod	0.023
2	48	no dam	0.023
3	48	no dam	0.023
4	48	no dam	0.023
5	36	mod	0.023
Set lens # (increase by 10%)	time of lesion		radiant exposure J/cm2
1	48	mod	0.0253
2	36	mod	0.0253
3	36	mod	0.0253
4	48	sev	0.0253
5	36	mod	0.0253

Appendix 7.5A. Action spectrum data for exposed lenses at 290 nm waveband.

	5 sets (25 lenses) at 290 nm		
Set 1 lens #	time of lesion	damage grade	radiant exposure J/cm2
1	36	sev	0.04
2	36	sev	0.04
3	36	sev	0.04
4	48	mod	0.04
5	36	sev	0.04
		reduce by 50%	
Set 2 lens #	time of lesion		radiant exposure J/cm2
1	48	no dam	0.02
2	48	no dam	0.02
3	48	no dam	0.02
4	48	no dam	0.02
5	48	no dam	0.02
		increase by 25%	
Set 3 lens #	time of lesion		radiant exposure J/cm2
1	48	no dam	0.025
2	48	no dam	0.025
3	48	no dam	0.025
4	48	mod	0.025
5	48	no dam	0.025
		increase by 10%	
Set 4 lens #	time of lesion		radiant exposure J/cm2
1	48	no dam	0.0275
2	36	no dam	0.0275
3	36	mod	0.0275
4	48	mod	0.0275
5	36	no dam	0.0275
		increase by 10%	
Set 5 lens #	time of lesion		radiant exposure J/cm2
1	48	mod	0.03025
2	36	mod	0.03025
3	36	mod	0.03025
4	48	sev	0.03025
5	36	mod	0.03025

Appendix 7.6A. Action spectrum data for exposed lenses at 295 nm waveband.

Set 1 lens #	6 sets (30 lenses) at 295 nm time of lesion	damage grade	radiant exposure J/cm2
1	36	sev	0.08
2	36	sev	0.08
3	36	sev	0.08
4	48	mod	0.08
5	36	sev	0.08
Set 2 lens # (reduce dose by 50%)	time of lesion		radiant exposure J/cm2
1	48	sev	0.04
2	36	mod	0.04
3	36	sev	0.04
4	48	mod	0.04
5	36	sev	0.04
Set 3 lens # (reduce dose by 50%)	time of lesion		radiant exposure J/cm2
1	48	no dam	0.02
2	48	no dam	0.02
3	48	no dam	0.02
4	48	mod	0.02
5	48	no dam	0.02
Set 4 lens # (increase dose by 25%)	time of lesion		radiant exposure J/cm2
1	48	no dam	0.025
2	36	no dam	0.025
3	36	no dam	0.025
4	48	no dam	0.025
5	36	no dam	0.025
Set 5 lens # (increase dose by 25%)	time of lesion		radiant exposure J/cm2
1	48	mod	0.03125
2	36	mod	0.03125
3	36	no dam	0.03125
4	48	sev	0.03125
5	36	no dam	0.03125
Set 6 lens # (increase dose by 25%)	time of lesion		radiant exposure J/cm2
1	48	mod	0.0391
2	36	mod	0.0391
3	36	sev	0.0391
4	48	sev	0.0391
5	36	sev	0.0391

Appendix 7.7A. Action spectrum data for exposed lenses at 300 nm waveband.

	5 sets (5 lenses per set = 25) at 300 nm		
Set 1 lens #	time of lesion	damage grade	radiant exposure J/cm2
1	48	moder	0.2
2	48	seve	0.2
3	36	moder	0.2
4	36	moder	0.2
5	48	seve	0.2
		reduce by 50%	
Set 2 lens #	time of lesion		radiant exposure J/cm2
1	48	moder	0.1
2	48	seve	0.1
3	48	moder	0.1
4	36	moder	0.1
5	48	moder	0.1
		reduce by 50%	
Set 3 lens #	time of lesion		radiant exposure J/cm2
1	48	no dama	0.05
2	48	no dama	0.05
3	48	no dama	0.05
4	48	no dama	0.05
5	48	no dama	0.05
		increase by 25%	
Set 4 lens #	time of lesion		radiant exposure J/cm2
1	48	no dama	0.0625
2	48	moder	0.0625
3	48	moder	0.0625
4	48	no dama	0.0625
5	48	no dama	0.0625
		increase by 25%	
Set 5 lens #	time of lesion		radiant exposure J/cm2
1	48	moder	0.078
2	48	moder	0.078
3	48	moder	0.078
4	48	no dama	0.078
5	48	seve	0.078

Appendix 7.8A. Action spectrum data for exposed lenses at 305 nm waveband.

	6 sets (30 lenses) at 305 nm		
Set 1 lens #	time of lesion	damage grade	radiant exposure J/cm2
1	48	no dam	0.078
2	48	no dam	0.078
3	48	no dam	0.078
4	48	moder	0.078
5	48	no dam	0.078
Set 2 lens # (Double the dose)	time of lesion		radiant exposure J/cm2
1	36	moder	0.156
2	48	seve	0.156
3	48	moder	0.156
4	36	moder	0.156
5	48	moder	0.156
Set 3 lens # (reduce dose by 25%)	time of lesion		radiant exposure J/cm2
1	48	moder	0.117
2	48	moder	0.117
3	48	moder	0.117
4	48	seve	0.117
5	48	no dama	0.117
Set 4 lens # (reduce dose by 25%)	time of lesion		radiant exposure J/cm2
1	48	no dama	0.0878
2	48	moder	0.0878
3	48	moder	0.0878
4	48	no dama	0.0878
5	48	no dama	0.0878
Set 5 lens # (increase dose by 10%)	time of lesion		radiant exposure J/cm2
1	48	no dama	0.0966
2	48	no dama	0.0966
3	48	moder	0.0966
4	48	no dama	0.0966
5	48	moder	0.0966
Set 6 lens # (increase by 10%)	time of lesion		radiant exposure J/cm2
1	36	moder	0.1063
2	48	no dam	0.1063
3	48	seve	0.1063
4	36	moder	0.1063
5	36	moder	0.1063

Appendix 7.9A. Action spectrum data for exposed lenses at 310 nm waveband.

Set 1lens #	6 sets (30 lenses) at 310 nm time of lesion	damage type	radiant exposure J/cm2
1	48	no dam	0.1063
2	48	no dam	0.1063
3	48	no dam	0.1063
4	48	moder	0.1063
5	48	no dam	0.1063
Set 2 lens # (double the dose)	time of lesion		radiant exposure J/cm2
1	48	moder	0.2126
2	48	no dam	0.2126
3	48	no dam	0.2126
4	48	no dam	0.2126
5	48	no dam	0.2126
Set 3 lens # (double the dose)	time of lesion		radiant exposure J/cm2
1	48	moder	0.4252
2	48	moder	0.4252
3	48	moder	0.4252
4	48	seve	0.4252
5	48	seve	0.4252
Set 4 lens # (reduce by 25%)	time of lesion		radiant exposure J/cm2
1	48	moder	0.3189
2	48	moder	0.3189
3	48	moder	0.3189
4	48	no dama	0.3189
5	48	moder	0.3189
Set 5 lens # (reduce by 25%)	time of lesion		radiant exposure J/cm2
1	48	no dama	0.2392
2	48	no dama	0.2392
3	48	moder	0.2392
4	48	no dama	0.2392
5	48	moder	0.2392
Set 6 lens # (increase by 10%)	time of lesion		radiant exposure J/cm2
1	36	moder	0.263
2	48	seve	0.263
3	48	no dam	0.263
4	36	moder	0.263
5	36	seve	0.263

Appendix 7.10A. Action spectrum data for exposed lenses at 315 nm waveband.

5 sets (25 lenses) at 315 nm			
set 1 lens #	time of lesion	damage grade	radiant exposure J/cm2
1	48	no dam	0.263
2	48	no dam	0.263
3	48	no dam	0.263
4	48	no dam	0.263
5	48	no dam	0.263
set 2 lens # (double the dose)	time of lesion		radiant exposure J/cm2
1	48	moder	0.526
2	48	no dam	0.526
3	48	no dam	0.526
4	48	no dam	0.526
5	48	no dam	0.526
set 3 lens # (double the dose)	time of lesion		radiant exposure J/cm2
1	36	moder	1.052
2	48	moder	1.052
3	36	moder	1.052
4	48	seve	1.052
5	48	seve	1.052
set 4 lens # (reduce by 25%)	time of lesion		radiant exposure J/cm2
1	48	no dam	0.789
2	48	moder	0.789
3	48	moder	0.789
4	48	no dama	0.789
5	48	no dam	0.789
set 5 lens # (increase by 10%)	time of lesion		radiant exposure J/cm2
1	48	seve	0.868
2	48	moder	0.868
3	48	moder	0.868
4	48	no dama	0.868
5	48	moder	0.868

Appendix 7.11A. Action spectrum data for exposed lenses at 320 nm waveband.

7 sets (35 lenses) at 320 nm			
set 1 lens #	time of lesion	damage grade	radiant exposure J/cm2
1	48	no dam	0.868
2	48	no dam	0.868
3	48	no dam	0.868
4	48	no dam	0.868
5	48	no dam	0.868
set 2 lens # (double the dose)	time of lesion		radiant exposure J/cm2
1	48	no dam	1.7358
2	48	no dam	1.7358
3	48	moder	1.7358
4	48	no dam	1.7358
5	48	no dam	1.7358
set 3 lens # (double the dose)	time of lesion		radiant exposure J/cm2
1	36	moder	3.472
2	48	no dam	3.472
3	48	no dam	3.472
4	48	no dam	3.472
5	48	no dam	3.472
set 4 lens # (double the dose)	time of lesion		radiant exposure J/cm2
1	48	seve	6.944
2	36	moder	6.944
3	48	moder	6.944
4	36	seve	6.944
5	36	seve	6.944
set 5 lens # (reduce by 25%)	time of lesion		radiant exposure J/cm2
1	48	seve	5.208
2	48	moder	5.208
3	48	moder	5.208
4	36	seve	5.208
5	48	moder	5.208
set 6 lens # (reduce by 25%)	time of lesion		radiant exposure J/cm2
1	24	conta	3.906
2	48	moder	3.906
3	48	moder	3.906
4	48	moder	3.906
5	48	moder	3.906
set 7 lens # (reduce by 10%)	time of lesion		radiant exposure J/cm2
1	48	no dam	3.515
2	48	moder	3.515
3	18	conta	3.515
4	48	moder	3.515
5	48	moder	3.515

Appendix 7.12A. Action spectrum data for exposed lenses at 325 nm waveband.

7 sets (35 lenses) at 325 nm			
set 1 lens #	time of lesion	damage grade	radiant exposure J/cm2
1	48	no dam	3.515
2	48	no dam	3.515
3	48	no dam	3.515
4	48	no dam	3.515
5	48	no dam	3.515
set 2 lens # (double the dose)	time of lesion		radiant exposure J/cm2
1	48	no dam	7.03
2	48	no dam	7.03
3	48	moder	7.03
4	48	no dam	7.03
5	48	no dam	7.03
set 3 lens # (double)	time of lesion		radiant exposure J/cm2
1	48	no dam	14.06
2	48	no dam	14.06
3	48	no dam	14.06
4	48	moder	14.06
5	48	no dam	14.06
set 4 lens # (double the dose)	time of lesion		radiant exposure J/cm2
1	48	seve	28.12
2	36	moder	28.12
3	48	moder	28.12
4	36	seve	28.12
5	36	seve	28.12
set 5 lens # (reduce by 25%)	time of lesion		radiant exposure J/cm2
1	48	moder	21.09
2	48	moder	21.09
3	48	no dam	21.09
4	36	no dam	21.09
5	48	no dam	21.09
set 6 lens # (increase by 25%)	time of lesion		radiant exposure J/cm2
1	48	seve	26.36
2	48	moder	26.36
3	48	moder	26.36
4	48	moder	26.36
5	48	moder	26.36
set 7 lens # (reduce by 10%)	time of lesion		radiant exposure J/cm2
1	48	no dam	23.724
2	48	moder	23.724
3	48	no dam	23.724
4	48	moder	23.724
5	36	seve	23.724

Appendix 7.13A. Action spectrum data for exposed lenses at 330 nm waveband.

5 sets (25 lenses) at 330 nm			
set 1 lens #	time of lesion		radiant exposure J/cm2
1	48	no dam	23.724
2	48	no dam	23.724
3	48	no dam	23.724
4	48	no dam	23.724
5	48	no dam	23.724
set 2 lens # (double dose)	time of lesion		radiant exposure J/cm2
1	24	seve	47.448
2	18	seve	47.448
3	24	seve	47.448
4	12	seve	47.448
5	12	seve	47.448
set 3 lens # (reduce by 25%)	time of lesion		radiant exposure J/cm2
1	24	seve	35.586
2	48	moder	35.586
3	30	seve	35.586
4	42	moder	35.586
5	30	moder	35.586
set 4 lens # (reduce by 25%)	time of lesion		radiant exposure J/cm2
1	48	no dam	26.689
2	36	moder	26.689
3	48	no dam	26.689
4	48	no dam	26.689
5	48	no dam	26.689
set 5 lens # (increase by 10%)	time of lesion		radiant exposure J/cm2
1	48	moder	29.358
2	48	moder	29.358
3	48	no dam	29.358
4	36	seve	29.358
5	48	moder	29.358

Appendix 7.14A. Action spectrum data for exposed lenses at 340 nm waveband.

	4 sets (20 lenses) at 340 nm		
set 1 lens #	time of lesion	damage grade	radiant exposure J/cm2
1	48	no dam	29.358
2	48	no dam	29.358
3	48	no dam	29.358
4	48	no dam	29.358
5	48	no dam	29.358
set 2 lens # (double preceding dose)	time of lesion		radiant exposure J/cm2
1	42	moder	58.72
2	36	seve	58.72
3	42	seve	58.72
4	48	moder	58.72
5	36	seve	58.72
set 3 lens # (reduce by 25%)	time of lesion		radiant exposure J/cm2
1	48	no dam	44.04
2	48	moder	44.04
3	48	no dam	44.04
4	48	no dam	44.04
5	30	moder	44.04
set 4 lens # (increase by 25%)	time of lesion		radiant exposure J/cm2
1	48	no dam	55.05
2	36	moder	55.05
3	48	moder	55.05
4	48	no dam	55.05
5	36	moder	55.05

Appendix 7.15A. Action spectrum data for exposed lenses at 350 nm waveband.

5 sets (24 lenses) at 350 nm			
set 1 lens #	time of lesion	damage type	radiant exposure J/cm2
1	48	no dam	55.05
2	48	no dam	55.05
3	48	no dam	55.05
4	48	no dam	55.05
5	48	no dam	55.05
set 2 lens # (double dose)	time of lesion		radiant exposure J/cm2
1	48	no dam	110.1
2	48	moder	110.1
3	42	moder	110.1
4	48	no dam	110.1
5	48	no dam	110.1
set 3 lens # (increase by 25%)	time of lesion		radiant exposure J/cm2
1	48	seve	137.63
2	36	moder	137.63
3	36	moder	137.63
4	48	moder	137.63
5	24	contaminated	
set 4 lens # (increase by 10%)	time of lesion		radiant exposure J/cm2
1	48	no dam	123.87
2	36	moder	123.87
3	48	moder	123.87
4	48	moder	123.87
5	48	moder	123.87
set 5 lens # (reduce by 10%)	time of lesion		radiant exposure J/cm2
1	48	no dam	111.48
2	36	seve	111.48
3	48	no dam	111.48
4	48	moder	111.48
5	48	moder	111.48

Appendix 7.16A. Action spectrum data for exposed lenses at 360 nm waveband.

	3 sets (14 lenses) at 360 nm		
set 1 lens #	time of lesion	damage grade	radiant exposure J/cm2
1	48	no dam	111.48
2	48	no dam	111.48
3	48	no dam	111.48
4	48	no dam	111.48
5	48	no dam	111.48
set 2 lens # (double the dose)	time of lesion		radiant exposure J/cm2
1	48	moder	222.96
2	36	moder	222.96
3	42	seve	222.96
4	48	seve	222.96
5	18	contaminated	
set 3 lens # (reduce by 25%)	time of lesion		radiant exposure J/cm2
1	48	no dam	167.22
2	36	moder	167.22
3	36	moder	167.22
4	48	no dam	167.22
5	36	moder	167.22

Appendix 7.17A. Action spectrum data for exposed lenses at 365 nm wavebarid.

	4 sets (19 lenses) at 365 nm		
set lens #	time of lesion	damage grade	radiant exposure J/cm2
1	48	moder	222.96
2	48	moder	222.96
3	42	sev	222.96
4	48	sev	222.96
5	30	contaminated	
set 2 lens # (reduce by 50%)	time of lesion		radiant exposure J/cm2
1	48	moder	111.48
2	48	no dam	111.48
3	42	no dam	111.48
4	48	no dam	111.48
5	48	moder	111.48
set 3 lens # (increase by 25%)	time of lesion		radiant exposure J/cm2
1	48	moder	139.35
2	48	moder	139.35
3	48	no dam	139.35
4	48	no dam	139.35
5	48	no dam	139.35
set 4 lens # (increase by 10%)	time of lesion		radiant exposure J/cm2
1	48	moder	153.29
2	36	moder	153.29
3	36	no dam	153.29
4	48	moder	153.29
5	30	no dam	153.29

Appendix 7.1B. Probit Analysis showing 95% confidence limits for effective radiant exposure at 270 nm waveband.

		95% Confidence Limits	
Probability	Dose (J/cm^2)	Lower	Upper
0.01	0.03546	N/A	0.04788
0.02	0.03801	N/A	0.04927
0.03	0.03962	N/A	0.05016
0.04	0.04084	N/A	0.05084
0.05	0.04182	N/A	0.0514
0.06	0.04266	N/A	0.05188
0.07	0.0434	N/A	0.05231
0.08	0.04406	N/A	0.05269
0.09	0.04466	N/A	0.05305
0.1	0.04521	N/A	0.05338
0.15	0.0475	N/A	0.05481
0.2	0.04932	N/A	0.05604
0.25	0.05088	N/A	0.0572
0.3	0.05228	N/A	0.05839
0.35	0.05358	N/A	0.0597
0.4	0.05481	N/A	0.06131
0.45	0.056	N/A	0.06358
0.5	0.05718	N/A	0.06754
0.55	0.05835	0.01303	0.07716
0.6	0.05954	0.04046	0.10418
0.65	0.06077	0.05054	0.15037
0.7	0.06207	0.05471	0.20551
0.75	0.06347	0.05714	0.26708
0.8	0.06503	0.05895	0.33654
0.85	0.06685	0.06057	0.41799
0.9	0.06914	0.06226	0.52083
0.91	0.06969	0.06263	0.5457
0.92	0.07029	0.06303	0.57274
0.93	0.07095	0.06345	0.60247
0.94	0.07169	0.06391	0.63568
0.95	0.07253	0.06443	0.67358
0.96	0.07352	0.06502	0.71812
0.97	0.07473	0.06574	0.77289
0.98	0.07635	0.06666	0.84571
0.99	0.07889	0.06809	0.96053

Appendix 7.2B. Probit analysis showing 95% confidence limits for effective radiant exposure at 275 nm waveband.

		95% Confidence limits	
Probability	Dose (J/cm^2)	Lower	Upper
0.01	0.01056	N/A	0.02907
0.02	0.01426	N/A	0.03119
0.03	0.01661	N/A	0.03256
0.04	0.01838	N/A	0.03359
0.05	0.01982	N/A	0.03443
0.06	0.02104	N/A	0.03516
0.07	0.02211	N/A	0.0358
0.08	0.02307	N/A	0.03637
0.09	0.02395	N/A	0.0369
0.1	0.02475	N/A	0.03739
0.15	0.02808	N/A	0.03944
0.2	0.03072	N/A	0.04113
0.25	0.03299	N/A	0.04264
0.3	0.03503	N/A	0.04406
0.35	0.03692	N/A	0.04546
0.4	0.03871	N/A	0.04689
0.45	0.04045	N/A	0.04841
0.5	0.04215	0.00331	0.05012
0.55	0.04386	0.0121	0.05214
0.6	0.0456	0.02051	0.05471
0.65	0.04739	0.02833	0.05825
0.7	0.04928	0.03516	0.06339
0.75	0.05132	0.04064	0.07082
0.8	0.05359	0.04485	0.08099
0.85	0.05623	0.04826	0.09435
0.9	0.05956	0.05143	0.11226
0.91	0.06036	0.0521	0.11669
0.92	0.06124	0.05279	0.12153
0.93	0.0622	0.05352	0.12688
0.94	0.06327	0.05431	0.13289
0.95	0.06449	0.05518	0.13978
0.96	0.06593	0.05617	0.1479
0.97	0.0677	0.05734	0.15792
0.98	0.07005	0.05884	0.1713
0.99	0.07375	0.06114	0.19246

Appendix 7.3B. Probit analysis showing 95% confidence limits for effective radiant exposure at 280 nm waveband.

		95% Confidence limits	
Probability	Dose (J/cm^2)	Lower	Upper
0.01	0.01737	N/A	0.02308
0.02	0.01859	N/A	0.0238
0.03	0.01936	N/A	0.02426
0.04	0.01994	N/A	0.02461
0.05	0.02042	N/A	0.02489
0.06	0.02082	N/A	0.02514
0.07	0.02117	N/A	0.02536
0.08	0.02149	N/A	0.02555
0.09	0.02177	N/A	0.02573
0.1	0.02204	N/A	0.0259
0.15	0.02313	N/A	0.02661
0.2	0.024	0.00131	0.0272
0.25	0.02475	0.005	0.02774
0.3	0.02542	0.00828	0.02826
0.35	0.02604	0.01127	0.02878
0.4	0.02663	0.01405	0.02933
0.45	0.0272	0.01666	0.02995
0.5	0.02776	0.01912	0.03067
0.55	0.02832	0.02139	0.03157
0.6	0.02889	0.02344	0.03275
0.65	0.02948	0.0252	0.03432
0.7	0.0301	0.02665	0.0364
0.75	0.03077	0.02781	0.03903
0.8	0.03152	0.02878	0.04228
0.85	0.03239	0.02967	0.04631
0.9	0.03348	0.0306	0.05159
0.91	0.03375	0.0308	0.05288
0.92	0.03404	0.03101	0.05429
0.93	0.03435	0.03124	0.05585
0.94	0.0347	0.03149	0.0576
0.95	0.03511	0.03177	0.0596
0.96	0.03558	0.03208	0.06196
0.97	0.03616	0.03246	0.06486
0.98	0.03693	0.03296	0.06874
0.99	0.03815	0.03371	0.07488

Appendix 7.4B. Probit analysis showing 95% confidence limits for effective radiant exposure at 285 nm waveband.

		95% Confidence limits	
Probability	Dose (J/cm^2)	Lower	Upper
0.01	0.01548	0.00072	0.01835
0.02	0.01623	0.00319	0.01884
0.03	0.01671	0.00475	0.01916
0.04	0.01707	0.00592	0.0194
0.05	0.01737	0.00687	0.0196
0.06	0.01762	0.00768	0.01977
0.07	0.01783	0.00838	0.01993
0.08	0.01803	0.00901	0.02007
0.09	0.01821	0.00957	0.0202
0.1	0.01837	0.0101	0.02032
0.15	0.01905	0.01223	0.02084
0.2	0.01959	0.01388	0.02131
0.25	0.02006	0.01525	0.02175
0.3	0.02047	0.01643	0.0222
0.35	0.02086	0.01745	0.02269
0.4	0.02122	0.01834	0.02324
0.45	0.02158	0.01911	0.02385
0.5	0.02193	0.01977	0.02455
0.55	0.02227	0.02034	0.02535
0.6	0.02263	0.02084	0.02624
0.65	0.02299	0.02128	0.02723
0.7	0.02338	0.02169	0.02833
0.75	0.0238	0.02208	0.02956
0.8	0.02426	0.02248	0.03098
0.85	0.0248	0.0229	0.03267
0.9	0.02548	0.0234	0.03483
0.91	0.02564	0.02352	0.03536
0.92	0.02582	0.02364	0.03593
0.93	0.02602	0.02378	0.03656
0.94	0.02624	0.02393	0.03727
0.95	0.02649	0.02409	0.03808
0.96	0.02678	0.02429	0.03903
0.97	0.02714	0.02453	0.04021
0.98	0.02762	0.02484	0.04177
0.99	0.02838	0.02532	0.04425

Appendix 7.5B. Probit analysis showing 95% confidence limits for effective radiant exposure at 290 nm waveband.

		95% Confidence limits	
Probability	Dose (J/cm^2)	Lower	Upper
0.01	0.0227	0.00004	0.02501
0.02	0.02323	0.00321	0.02533
0.03	0.02356	0.00521	0.02555
0.04	0.02381	0.00671	0.02571
0.05	0.02402	0.00793	0.02585
0.06	0.02419	0.00897	0.02597
0.07	0.02435	0.00987	0.02608
0.08	0.02448	0.01068	0.02617
0.09	0.02461	0.01141	0.02626
0.1	0.02472	0.01209	0.02635
0.15	0.0252	0.01485	0.02673
0.2	0.02557	0.017	0.02707
0.25	0.0259	0.0188	0.02742
0.3	0.02619	0.02034	0.0278
0.35	0.02646	0.0217	0.02823
0.4	0.02671	0.02287	0.02874
0.45	0.02696	0.02387	0.02938
0.5	0.0272	0.02469	0.03017
0.55	0.02745	0.02535	0.03112
0.6	0.02769	0.02587	0.03223
0.65	0.02795	0.02631	0.03349
0.7	0.02822	0.02667	0.03491
0.75	0.02851	0.027	0.0365
0.8	0.02883	0.02732	0.03833
0.85	0.02921	0.02764	0.0405
0.9	0.02968	0.028	0.04328
0.91	0.0298	0.02809	0.04396
0.92	0.02992	0.02817	0.04469
0.93	0.03006	0.02827	0.0455
0.94	0.03021	0.02837	0.04641
0.95	0.03039	0.02849	0.04745
0.96	0.03059	0.02862	0.04867
0.97	0.03084	0.02879	0.05018
0.98	0.03118	0.029	0.05218
0.99	0.0317	0.02932	0.05535

Appendix 7.6B. Probit analysis showing 95% confidence limits for effective radiant exposure at 295 nm waveband.

		95% Confidence limits	
Probability	Dose (J/cm2)	Lower	Upper
0.01	0.01607	N/A	0.02186
0.02	0.01764	0.00003	0.02296
0.03	0.01864	0.00238	0.02368
0.04	0.01939	0.00413	0.02423
0.05	0.02	0.00555	0.02468
0.06	0.02052	0.00675	0.02507
0.07	0.02098	0.0078	0.02542
0.08	0.02139	0.00873	0.02574
0.09	0.02176	0.00957	0.02604
0.1	0.0221	0.01035	0.02631
0.15	0.02351	0.0135	0.0275
0.2	0.02463	0.01592	0.02852
0.25	0.0256	0.01793	0.02947
0.3	0.02646	0.01966	0.0304
0.35	0.02727	0.02118	0.03134
0.4	0.02803	0.02253	0.03232
0.45	0.02876	0.02376	0.03335
0.5	0.02949	0.02487	0.03446
0.55	0.03021	0.0259	0.03566
0.6	0.03095	0.02685	0.03696
0.65	0.03171	0.02776	0.03839
0.7	0.03251	0.02864	0.03997
0.75	0.03338	0.02951	0.04176
0.8	0.03434	0.03041	0.04382
0.85	0.03547	0.03138	0.04629
0.9	0.03688	0.03253	0.04948
0.91	0.03722	0.0328	0.05026
0.92	0.03759	0.03309	0.05111
0.93	0.038	0.0334	0.05205
0.94	0.03845	0.03374	0.0531
0.95	0.03897	0.03412	0.05431
0.96	0.03958	0.03457	0.05574
0.97	0.04034	0.03511	0.0575
0.98	0.04133	0.03582	0.05985
0.99	0.0429	0.03691	0.06358

Appendix 7.7B. Probit analysis showing 95% confidence limits for effective radiant exposure at 300 nm waveband.

		95% Confidence limits	
Probability	Dose (J/cm^2)	Lower	Upper
0.01	0.04273	N/A	0.05576
0.02	0.04587	N/A	0.05777
0.03	0.04786	N/A	0.05908
0.04	0.04936	N/A	0.0601
0.05	0.05058	N/A	0.06094
0.06	0.05161	N/A	0.06168
0.07	0.05252	N/A	0.06235
0.08	0.05334	N/A	0.06296
0.09	0.05408	N/A	0.06353
0.1	0.05476	N/A	0.06406
0.15	0.05759	0.0127	0.06646
0.2	0.05983	0.02291	0.06868
0.25	0.06175	0.03132	0.07093
0.3	0.06348	0.03845	0.07337
0.35	0.06509	0.04452	0.07617
0.4	0.06661	0.04966	0.07945
0.45	0.06808	0.05394	0.08331
0.5	0.06952	0.05746	0.08781
0.55	0.07097	0.06035	0.09293
0.6	0.07244	0.06276	0.09866
0.65	0.07396	0.06484	0.105
0.7	0.07557	0.06671	0.112
0.75	0.07729	0.06846	0.11982
0.8	0.07922	0.07019	0.12875
0.85	0.08146	0.07202	0.13935
0.9	0.08429	0.07412	0.15288
0.91	0.08497	0.0746	0.15618
0.92	0.08571	0.07512	0.15976
0.93	0.08652	0.07568	0.16371
0.94	0.08743	0.07629	0.16813
0.95	0.08847	0.07698	0.17319
0.96	0.08969	0.07778	0.17914
0.97	0.09119	0.07875	0.18647
0.98	0.09318	0.08001	0.19624
0.99	0.09632	0.08196	0.21167

Appendix 7.8B. Probit analysis showing 95% confidence limits for effective radiant exposure at 305 nm waveband.

		95% Confidence limits	
Probability	Dose (J/cm^2)	Lower	Upper
0.01	0.04643	N/A	0.07058
0.02	0.05221	N/A	0.07397
0.03	0.05588	N/A	0.07615
0.04	0.05864	N/A	0.0778
0.05	0.06088	N/A	0.07916
0.06	0.06279	N/A	0.08033
0.07	0.06447	N/A	0.08137
0.08	0.06596	N/A	0.08231
0.09	0.06733	N/A	0.08317
0.1	0.06858	N/A	0.08397
0.15	0.07378	N/A	0.08741
0.2	0.07791	N/A	0.09033
0.25	0.08145	0.01119	0.09307
0.3	0.08464	0.02672	0.09584
0.35	0.08759	0.04068	0.09883
0.4	0.09038	0.05329	0.1023
0.45	0.09309	0.0645	0.10665
0.5	0.09576	0.07406	0.1124
0.55	0.09842	0.08173	0.12005
0.6	0.10113	0.08758	0.12976
0.65	0.10393	0.09205	0.14138
0.7	0.10687	0.09566	0.15472
0.75	0.11006	0.09881	0.16985
0.8	0.1136	0.10181	0.18722
0.85	0.11773	0.10491	0.20786
0.9	0.12293	0.10848	0.23417
0.91	0.12418	0.1093	0.24056
0.92	0.12555	0.11018	0.24752
0.93	0.12705	0.11114	0.25518
0.94	0.12872	0.1122	0.26375
0.95	0.13063	0.11339	0.27354
0.96	0.13287	0.11477	0.28506
0.97	0.13563	0.11644	0.29924
0.98	0.1393	0.11864	0.31812
0.99	0.14508	0.12205	0.34793

Appendix 7.9B. Probit analysis showing 95% confidence limits for effective radiant exposure at 310 nm waveband.

		95% Confidence limits	
Probability	Dose (J/cm^2)	Lower	Upper
0.01	0.00481	N/A	0.11035
0.02	0.03161	N/A	0.12705
0.03	0.04862	N/A	0.13778
0.04	0.06141	N/A	0.14594
0.05	0.07182	N/A	0.15265
0.06	0.08067	N/A	0.15841
0.07	0.08844	N/A	0.16351
0.08	0.09539	N/A	0.16813
0.09	0.10172	N/A	0.17236
0.1	0.10754	N/A	0.1763
0.15	0.13164	N/A	0.19313
0.2	0.15079	N/A	0.20735
0.25	0.16722	N/A	0.2205
0.3	0.18198	0.01394	0.23346
0.35	0.19565	0.0545	0.24694
0.4	0.20863	0.09104	0.26167
0.45	0.22118	0.12382	0.27849
0.5	0.23354	0.15278	0.29835
0.55	0.24589	0.17784	0.3221
0.6	0.25845	0.19922	0.35034
0.65	0.27142	0.21752	0.3833
0.7	0.2851	0.23363	0.42123
0.75	0.29985	0.24848	0.46469
0.8	0.31629	0.26299	0.5151
0.85	0.33544	0.27822	0.57557
0.9	0.35954	0.29581	0.6532
0.91	0.36536	0.29988	0.67213
0.92	0.37168	0.30425	0.69275
0.93	0.37864	0.30899	0.71549
0.94	0.3864	0.31421	0.74095
0.95	0.39526	0.32009	0.77006
0.96	0.40567	0.32692	0.80436
0.97	0.41846	0.3352	0.84662
0.98	0.43546	0.34606	0.90295
0.99	0.46226	0.36291	0.992

Appendix 7.10B. Probit analysis showing 95% confidence limits for effective radiant exposure at 315 nm waveband.

		95% Confidence limits	
Probability	Dose (J/cm^2)	Lower	Upper
0.01	0.3147	N/A	0.52288
0.02	0.36484	N/A	0.55512
0.03	0.39664	N/A	0.57592
0.04	0.42057	N/A	0.5918
0.05	0.44004	N/A	0.60489
0.06	0.4566	N/A	0.61618
0.07	0.47113	N/A	0.6262
0.08	0.48414	N/A	0.63528
0.09	0.49596	N/A	0.64365
0.1	0.50685	N/A	0.65144
0.15	0.55193	0.0137	0.68495
0.2	0.58776	0.12429	0.71352
0.25	0.6185	0.21713	0.74007
0.3	0.6461	0.29819	0.76622
0.35	0.67168	0.37058	0.79317
0.4	0.69595	0.43599	0.82203
0.45	0.71943	0.49528	0.85395
0.5	0.74254	0.54887	0.89013
0.55	0.76566	0.59698	0.93178
0.6	0.78914	0.63994	0.98002
0.65	0.81341	0.67835	1.03588
0.7	0.83899	0.71315	1.10043
0.75	0.86659	0.74555	1.17524
0.8	0.89733	0.77701	1.26316
0.85	0.93316	0.80946	1.36987
0.9	0.97824	0.84609	1.50833
0.91	0.98913	0.85445	1.54226
0.92	1.00095	0.86336	1.57929
0.93	1.01396	0.87298	1.62019
0.94	1.02849	0.88353	1.66606
0.95	1.04505	0.89533	1.7186
0.96	1.06452	0.90895	1.78058
0.97	1.08844	0.92537	1.85709
0.98	1.12025	0.94676	1.95925
0.99	1.17039	0.97968	2.12105

Appendix 7.11B. Probit analysis showing 95% confidence limits for effective radiant exposure at 320 nm waveband.

		95% Confidence limits	
Probability	Dose (J/cm2)	Lower	Upper
0.01	0.66101	N/A	1.78336
0.02	0.95057	N/A	1.97495
0.03	1.13429	N/A	2.09845
0.04	1.27249	N/A	2.19263
0.05	1.38491	N/A	2.27021
0.06	1.4806	N/A	2.33704
0.07	1.56449	N/A	2.39633
0.08	1.63961	N/A	2.45004
0.09	1.70793	N/A	2.49946
0.1	1.77082	N/A	2.54548
0.15	2.03119	N/A	2.74283
0.2	2.23812	0.20734	2.91029
0.25	2.41565	0.65159	3.06499
0.3	2.57508	1.0383	3.21617
0.35	2.72282	1.38254	3.37036
0.4	2.863	1.69271	3.53315
0.45	2.99863	1.97357	3.70988
0.5	3.13211	2.22804	3.90576
0.55	3.26559	2.45843	4.12571
0.6	3.40122	2.66741	4.37433
0.65	3.54141	2.8586	4.6561
0.7	3.68914	3.03668	4.97645
0.75	3.84857	3.2074	5.34362
0.8	4.0261	3.37787	5.77211
0.85	4.23304	3.55808	6.29006
0.9	4.49341	3.76594	6.96064
0.91	4.55629	3.81388	7.12487
0.92	4.62461	3.86517	7.30408
0.93	4.69973	3.92071	7.50198
0.94	4.78363	3.98181	7.72394
0.95	4.87932	4.05045	7.97813
0.96	4.99173	4.12985	8.278
0.97	5.12994	4.22593	8.6482
0.98	5.31365	4.35147	9.14248
0.99	5.60321	4.54549	9.9254

Appendix 7.12B. Probit analysis showing 95% confidence limits for effective radiant exposure at 325 nm waveband.

		95% Confidence limits	
Probability	Dose (J/cm^2)	Lower	Upper
0.01	1.07015	N/A	8.25383
0.02	3.13642	N/A	9.68281
0.03	4.4474	N/A	10.6011
0.04	5.4336	N/A	11.2994
0.05	6.23579	N/A	11.8732
0.06	6.91859	N/A	12.3663
0.07	7.51727	N/A	12.8027
0.08	8.05331	N/A	13.197
0.09	8.54082	N/A	13.559
0.1	8.98958	N/A	13.8954
0.15	10.84755	N/A	15.3268
0.2	12.3242	2.24655	16.5246
0.25	13.59104	4.75092	17.6131
0.3	14.7287	6.93409	18.6564
0.35	15.78291	8.88357	19.6967
0.4	16.78325	10.6501	20.7673
0.45	17.75109	12.265	21.8973
0.5	18.70359	13.7496	23.114
0.55	19.65609	15.1213	24.4437
0.6	20.62393	16.3979	25.9119
0.65	21.62427	17.6007	27.5463
0.7	22.67848	18.7556	29.3812
0.75	23.81614	19.8957	31.4676
0.8	25.08298	21.0647	33.8914
0.85	26.55963	22.3295	36.8146
0.9	28.4176	23.8178	40.5956
0.91	28.86635	24.1646	41.5215
0.92	29.35386	24.5369	42.5319
0.93	29.88991	24.9414	43.6476
0.94	30.48859	25.3879	44.8991
0.95	31.17138	25.891	46.3324
0.96	31.97358	26.475	48.0235
0.97	32.95978	27.1841	50.1114
0.98	34.27076	28.1139	52.8996
0.99	36.33703	29.5567	57.3169

Appendix 7.13B. Probit analysis showing 95% confidence limits for effective radiant exposure at 330 nm waveband.

		95% Confidence limits	
Probability	Dose (J/cm^2)	Lower	Upper
0.01	24.35196	N/A	26.3457
0.02	24.78068	N/A	26.607
0.03	25.05268	N/A	26.7787
0.04	25.2573	N/A	26.9119
0.05	25.42374	N/A	27.0234
0.06	25.56541	N/A	27.1209
0.07	25.68963	N/A	27.2089
0.08	25.80085	N/A	27.2899
0.09	25.902	0.59915	27.3657
0.1	25.9951	1.82182	27.4375
0.15	26.3806	6.85591	27.7629
0.2	26.68698	10.8067	28.0717
0.25	26.94982	14.1325	28.4003
0.3	27.18587	17.0296	28.7848
0.35	27.4046	19.5786	29.2769
0.4	27.61215	21.7832	29.9579
0.45	27.81296	23.5905	30.9424
0.5	28.01059	24.9488	32.3317
0.55	28.20822	25.8943	34.1338
0.6	28.40903	26.5435	36.2764
0.65	28.61658	27.0112	38.6943
0.7	28.83531	27.3743	41.3722
0.75	29.07135	27.6796	44.3486
0.8	29.3342	27.9573	47.7253
0.85	29.64058	28.2316	51.7105
0.9	30.02607	28.5325	56.7692
0.91	30.11918	28.6001	57.996
0.92	30.22033	28.672	59.3305
0.93	30.33155	28.7492	60.7995
0.94	30.45577	28.8334	62.4422
0.95	30.59744	28.9274	64.3178
0.96	30.76388	29.0353	66.5239
0.97	30.9685	29.1649	69.2392
0.98	31.2405	29.3328	72.853
0.99	31.66922	29.5897	78.5564

Appendix 7.14B. Probit analysis showing 95% confidence limits for effective radiant exposure at 340 nm waveband.

		95% Confidence limits	
Probability	Dose (J/cm^2)	Lower	Upper
0.01	28.49927	N/A	39.0539
0.02	30.81554	N/A	40.4776
0.03	32.28513	N/A	41.3964
0.04	33.39065	N/A	42.0976
0.05	34.28991	N/A	42.6757
0.06	35.05532	N/A	43.174
0.07	35.72643	N/A	43.6165
0.08	36.32733	N/A	44.0175
0.09	36.87383	N/A	44.3868
0.1	37.37688	N/A	44.731
0.15	39.45964	N/A	46.2099
0.2	41.11496	6.72233	47.471
0.25	42.53507	12.7623	48.6444
0.3	43.81037	18.0804	49.804
0.35	44.99213	22.8785	51.0085
0.4	46.11351	27.2656	52.3173
0.45	47.19845	31.2925	53.8012
0.5	48.26619	34.9683	55.5489
0.55	49.33393	38.2731	57.6676
0.6	50.41887	41.1798	60.2717
0.65	51.54025	43.6848	63.4626
0.7	52.72201	45.8299	67.3201
0.75	53.99731	47.6988	71.929
0.8	55.41742	49.3985	77.4426
0.85	57.07274	51.0528	84.1963
0.9	59.1555	52.8339	92.9943
0.91	59.65855	53.2308	95.1526
0.92	60.20505	53.6509	97.5084
0.93	60.80595	54.1012	100.11
0.94	61.47706	54.5917	103.029
0.95	62.24247	55.1374	106.371
0.96	63.14173	55.7628	110.313
0.97	64.24725	56.5125	115.179
0.98	65.71684	57.4827	121.673
0.99	68.03311	58.9665	131.955

Appendix 7.15B. Probit analysis showing 95% confidence limits for effective radiant exposure at 350 nm waveband.

		95% Confidence limits	
Probability	Dose (J/cm2)	Lower	Upper
0.01	82.43693	N/A	N/A
0.02	85.81541	N/A	N/A
0.03	87.95895	N/A	N/A
0.04	89.57145	N/A	N/A
0.05	90.8831	N/A	N/A
0.06	91.99951	N/A	N/A
0.07	92.97839	N/A	N/A
0.08	93.85486	N/A	N/A
0.09	94.65197	N/A	N/A
0.1	95.38572	N/A	N/A
0.15	98.42362	N/A	N/A
0.2	100.83804	N/A	N/A
0.25	102.9094	N/A	N/A
0.3	104.76955	N/A	N/A
0.35	106.49325	N/A	N/A
0.4	108.12887	N/A	N/A
0.45	109.71136	N/A	N/A
0.5	111.26876	N/A	N/A
0.55	112.82615	N/A	N/A
0.6	114.40864	N/A	N/A
0.65	116.04427	N/A	N/A
0.7	117.76797	N/A	N/A
0.75	119.62811	N/A	N/A
0.8	121.69948	N/A	N/A
0.85	124.1139	N/A	N/A
0.9	127.1518	N/A	N/A
0.91	127.88554	N/A	N/A
0.92	128.68265	N/A	N/A
0.93	129.55912	N/A	N/A
0.94	130.538	N/A	N/A
0.95	131.65442	N/A	N/A
0.96	132.96606	N/A	N/A
0.97	134.57856	N/A	N/A
0.98	136.7221	N/A	N/A
0.99	140.10059	N/A	N/A

Appendix 7.16B. Probit analysis showing 95% confidence limits for effective radiant exposure at 360 nm waveband.

		95% Confidence limits	
Probability	Dose (J/cm2)	Lower	Upper
0.01	134.48255	N/A	N/A
0.02	137.94481	N/A	N/A
0.03	140.14151	N/A	N/A
0.04	141.794	N/A	N/A
0.05	143.13817	N/A	N/A
0.06	144.28228	N/A	N/A
0.07	145.28543	N/A	N/A
0.08	146.18364	N/A	N/A
0.09	147.00052	N/A	N/A
0.1	147.75246	N/A	N/A
0.15	150.86569	N/A	N/A
0.2	153.33999	N/A	N/A
0.25	155.46272	N/A	N/A
0.3	157.369	N/A	N/A
0.35	159.13545	N/A	N/A
0.4	160.81164	N/A	N/A
0.45	162.43337	N/A	N/A
0.5	164.02939	N/A	N/A
0.55	165.62541	N/A	N/A
0.6	167.24714	N/A	N/A
0.65	168.92333	N/A	N/A
0.7	170.68978	N/A	N/A
0.75	172.59605	N/A	N/A
0.8	174.71878	N/A	N/A
0.85	177.19308	N/A	N/A
0.9	180.30632	N/A	N/A
0.91	181.05826	N/A	N/A
0.92	181.87514	N/A	N/A
0.93	182.77335	N/A	N/A
0.94	183.7765	N/A	N/A
0.95	184.9206	N/A	N/A
0.96	186.26478	N/A	N/A
0.97	187.91727	N/A	N/A
0.98	190.11396	N/A	N/A
0.99	193.57623	N/A	N/A

Appendix 7.17B. Probit analysis showing 95% confidence limits for effective radiant exposure at 365 nm waveband.

		95% Confidence limits	
Probability	Dose (J/cm^2)	Lower	Upper
0.01	25.91159	N/A	N/A
0.02	38.95138	N/A	N/A
0.03	47.22471	N/A	N/A
0.04	53.44841	N/A	N/A
0.05	58.51092	N/A	N/A
0.06	62.8199	N/A	N/A
0.07	66.59804	N/A	N/A
0.08	69.98091	N/A	N/A
0.09	73.0575	N/A	N/A
0.1	75.8895	N/A	N/A
0.15	87.61474	N/A	N/A
0.2	96.9336	N/A	N/A
0.25	104.92834	N/A	N/A
0.3	112.10787	N/A	N/A
0.35	118.76078	N/A	N/A
0.4	125.07373	N/A	N/A
0.45	131.18159	N/A	N/A
0.5	137.19261	N/A	N/A
0.55	143.20363	N/A	N/A
0.6	149.31149	N/A	N/A
0.65	155.62444	N/A	N/A
0.7	162.27734	N/A	N/A
0.75	169.45687	N/A	N/A
0.8	177.45162	N/A	N/A
0.85	186.77047	N/A	N/A
0.9	198.49572	N/A	N/A
0.91	201.32772	N/A	N/A
0.92	204.40431	N/A	N/A
0.93	207.78718	N/A	N/A
0.94	211.56531	N/A	N/A
0.95	215.8743	N/A	N/A
0.96	220.9368	N/A	N/A
0.97	227.16051	N/A	N/A
0.98	235.43383	N/A	N/A
0.99	248.47363	N/A	N/A

REFERENCES

Acetoxymethyl (AM) Esters and Diacetates. (1998). Product information sheet. Molecular Probes Incorporation. Eugene, Oregon, USA.

Ahmed, S. A., Gogal, R. M., and Walsh, J. E. (1994). A new rapid and simple non-radioactive assay to monitor and determine the proliferation of lymphocytes: an alternative to [^{3}H] thymidine incorporation assay. *J Immunol Methods.* **170**, 211-24.

AlamarBlue™ Assay (1999). Package insert. Medicorp Incorporation. Montreal, Quebec, Canada (U.S. Patent No. 5,501,959).

Al Farran, M. F. (1990). Visual outcome and complications after cataract extraction in Saudi Arabia. *Brit. J. Ophthalmol.* **74**, 141-143.

Alyea, F. N., Cunnold, D. M. and Prinn, R. G. (1975). Stratospheric ozone destruction by aircraft-induced nitrogen oxides. *Science.* **188,** 117-121.

Andley, U. P., Lewis, R. M., Redan, J. R., and Kochevar, I. E. (1994). Action spectrum for cytotoxicity in the UVA and UVB wavelength region in cultured lens epithelial cells. *Invest. Ophthalmol. Vis. Sci.* **35**, 367-73.

Andley, U. P. and Weber, J. G. (1995). Ultraviolet action spectra for photobiological effects in cultured human lens epithelial cells. *Photochem. Photobiol.* **62**, 840-46.

Anon (1979). Stratospheric ozone depletion by halocarbons: chemistry and transport. Panel on stratospheric chemistry and transport – Committee on impacts of stratospheric change (H. I. Schiff, chairman). National Academy of Sciences. Washington, D.C., U.S.A.

Aquilina, J. A., Carver, J. A., and Truscott, R. J. W. (1997). Oxidation products of 3-hydroxykynurenine bind to lens proteins: relevance to nuclear cataract. *Exp. Eye Res.* **64,** 727-35.

Austin, J., Butchart, N. and Shine, K. P. (1992). Possibility of an arctic ozone hole in a doubled-CO_2 climate. *Nature.* **360,** 221-225.

Babizhayev, M. A., Deyev, A. I., and Linberg, L. F. (1988) Lipid peroxidation as a possible cause of cataract. *Mechanisms of Ageing and Development.* **44,** 69-89).

Bachem, A. (1956). Ophthalmic ultraviolet action spectra. *Am. J. Ophthalmol.* **41,** 969-975.

Badr, I. A. (1993). The scope of cataract problem in the Middle East and the Mediterranean. *Int. Ophthalmol.* **17,** 150-160.

Barker, F. M. II. (1979). The transmittance of electromagnetic spectrum from 200 to 2500 nm through the optical tissues of the eye of the pigmented rabbit. MS thesis. University of Houston, Houston, Texas, U.S.A.

Barron, B. C., Yu, N. T. and Kuck, J. F. R. (1987). Tryptophan Raman/457.9-nm-excited fluorescence of intact guinea pig lenses in aging and ultraviolet light. *Invest. Ophthalmol. Vis. Res.* **28,** 815-821

Bassnett, S and Beebe, D. C. (1992). Coincident loss of mitochondria and nuclei during lens fibre cell differentiation. *Dev. Dyn.* **194,** 85-93.

Bassnett, S., Kuszak, J. R, Reinisch, L, Brown, H. G, Beebe, D. C. (1994). Intercellular communication between epithelial and fiber cells of the eye lens. *J. Cell. Sci.* **107,** 799-811.

Baum, J. and Pitts, D. G. (1997). Posterior sucapsular cataract following intense ultraviolet radiation exposure: a case report. *Eye.* **11,** 661-662.

Beauchemin, M. L. (1974). The fine structure of the pig's retina. *Albrecht v. Graefes Arch. Klin. Exp. Ophthalmol.* **190,** 27-45.

Begue, W. J. and Moran, J. W. (1979). Hygromycin B tissue residue analysis in swine. Tissue residue analysis, Experiment No. TIU807802. Elli Lilly & Co. Greenfield, Indiana, U.S.A.

Bergmanson, J. P. G. and Söderberg, P. G. (1995). The significance of ultraviolet radiation for eye diseases. A review with comments on the efficacy of UV-blocking contact lenses. *Ophthal. Physiol. Opt.* **15,** 83-91.

Bhuyan, K. C., Bhuyan, D. K., Kuck (Jr), J. F. R., Kuck, K. D., Kern, H. L. (1983). Increased lipid peroxidation and altered membrane functions in Emory mouse cataract. *Curr. Eye Res.* **2,** 597-606.

Blanquet, P. R., and Courtois, Y. (1989). Differential assemblage of the basal membrane-cytoskeleton complex in bovine epithelial lens cells. *Exp. Eye Res.* **48,** 187-207.

Blumthaler, M. and Ambach, W. (1990). Indication of increasing solar Ultraviolet-B radiation flux in Alpine regions. *Science.* **248,** 206-208.

Boettner, E. A., and Wolter, J. R. (1962). Transmission of the ocular media. *Invest. Ophthalmol.* **1,** 776-783.

Boisvenue, R. J., Handy, P. R. and Hendrix, J. (1978). Hygromycin B tissue residue depletion study in growing pigs. Experiment No. TIU80/701, Lilly Research Laboratories, Eli Lilly and Co., Greenfield, Indiana, U.S.A.

Borkman, R. F. and Lerman, S. (1977). Evidence for a free radical mechanism in aging and UV-irradiated ocular lenses. *Exp. Eye Res.* **25**, 303-309

Bowman, K. P. (1988). Global trends in total ozone. *Science.* **239**, 48-50.

Brilliant, L. B., Grasset, N. C., Porkhrel, R. P., Kolstad, A., Lepkowski, J. M., Brilliant, G. E., Hawks, W. N. and Pararajasegaram, R. (1983). Associations among cataract prevalence, sunlight hours and altitude in the Himalayas. *Am. J. Epidemiol.* **118**, 250-64.

Brown, H. G., Pappas, G. D, Ireland, M. E., and Kuszak, J. R. (1990). Ultrastructural, biochemical, and immunologic evidence of receptor-mediated endocytosis in the crystalline lens. *Invest. Ophthalmol. Vis. Sci.* **31**, 2579-2592.

Brown, K. S. (1999). The ozone layer: burnt by the sun down under. *Science.* **285 (5434),** 1647-49.

Burge, W. E., Wickwire, G. C. and Schamp, H. M. (1937). Cause of calcification of the crystalline lens. *Arch. Ophthalmol.* **17**, 234-240.

Cavonius, C. R., Elgin, S. and Robbins, D. O. (1974). Thresholds for damage to the human retina by white light. *Exp. Eye Res.* **19**, 543-548.

Cenedella, R. J. (1996). Cholesterol and cataracts. *Surv. Ophthalmol.* **40**, 320-27.

Chartterjee, A.., Milton, R. C. and Thyle, S. (1982). Prevalence and etiology of cataract in Punjab. *Brit. J. Ophthalmol.* **66**, 35-42.

Chou, B. R. (1982). Spectral Transmittance of the ocular media of the thirteen-lined ground squirrel. MSc thesis. University of Waterloo, Waterloo, Ontario, Canada.

Chou, B. R. and Cullen, A. P. (1984). Spectral transmittance of the ocular media of the thirteen-lined ground squirrel (*Spermophilus tridecemlineatus*). Can. J. Zool. **62,** 825-830.

Clark, J. H. (1935). The effect of ultraviolet radiation on lens protein in the presence of salts and the relation of radiation to industrial and senile cataract. *Am. J. Physiol.* **113,** 538-547.

Commission Internationale de l'Eclairage. (1987). Ch 845-01: Radiation, quantities and units. In *CIE Publication No. 17.4, International lighting vocabulary.* Pp. 1-40. Bureau Central de la Commission Electrotechnique Internationale: Geneve.

Cooper, G. F. and Robson, J. G. (1969). The yellow colour of the lens of man and other primates. *J. Physiol.* **203,** 411-417.

Coroneo, M. T. (1990). Albedo concentration in the anterior eye: a phenomenon that locates some solar diseases. *Ophthalmic Surgery.* **21,** 60-66.

Creighton, M. O., Trevithick, J. R., Sanford, S. E. and Duke, T. W. (1982). Modelling cortical cataractogenesis. IV. Induction by hygromycin B in vivo (swine) and in vitro (rat lens). *Exp. Eye Res.* **34,** 467-476.

Cullen, A. P. (1980). Additive effects of ultraviolet radiation on the eye. *Am. J. Optom. Physiol. Opt.* **57,** 808-814.

Cullen, A. P., Monteith-McMaster, C. and Sivak, J. G. (1994). Lenticular changes in rainbow trout following chronic exposure to UV Radiation. *Curr. Eye Res.* **13,** 731-737.

Cullen, A. P., Oriowo, O. M., and Voisin, A. C. (1997). Anterior eye focusing of peripheral ultraviolet and visible radiation albedo. *Clin. Exp. Optom.* **80,** 80-86.

Delamere, N. A. and Dean, W. L. (1993). Distribution of lens sodium-potasium adenosine triphosphatase. *Invest. Ophthalmol. Vis. Sci.* **34**, 2159-63.

Dickson, D. and Marshall, E. (1989). Europe recognizes the ozone threat. *Science.* **243,** 1279.

Dillon, J. (1999). Sunlight exposure and cataract. *J.A.M.A.* **281**, 229.

Dillon, J., Ortwerth, B. J., Chignell, C. F., and Reszka, K. J. (1999a). Electron paramagnetic resonance and spin trapping investigations of the photoreactivity of human lens proteins. *Photochem. Photobiol.* **69**, 259-264.

Dillon, J., Zheng, L., Merrian, J.C. and Gaillard, E.R. (1999b). The optical properties of the anterior segment of the eye: implications for cortical cataract. *Exp. Eye Res.* **68,** 785-795.

Dolin, P. J. (1994). Ultraviolet radiation and cataract: a review of the epidemiological evidence. *Br. J. Ophthalmol.* **78,** 478-482.

Dorfman-Hecht, J. E. (1993). Acute effects of the organophosphate pesticide NUVAN™ on the optical and biochemical properties of cultured atlantic salmon (Salmo salar) lenses. MSc thesis. University of Waterloo, Waterloo, Ontario, Canada.

Dovrat, A. and Weinreb, O. (1995). Recovery of lens optics and epithelial enzymes after ultraviolet A radiation. *Invest. Ophthalmol. Vis. Sci.* **36,** 2417-2424.

Dovrat, A. and Weinreb, O. (1999). Effects of UV-A radiation on lens epithelial NaK-ATPase in organ culture. *Invest. Ophthalmol. Vis. Sci.* **40,** 1616-1620.

Duke-Elder, W. S. (1926). The pathological action of light upon the eye. Part II. Action upon the lens: theory of the genesis of cataract . *Lancet.* **1,** 1188-91.

Duke-Elder, W. S. and Duke-Elder, P. M. (1929). A histological study on the action of short-waved light upon the eye, with a note on "inclusion bodies". *Br. J. Ophthalmol.* **13**, 1-37.

Duke-Elder, W. S. (1958). The Eye in Evolution. In *System of Ophthalmology*. **vol. 1**, Pp. 474-507, Henry Kimpton: London, U.K.

Duke-Elder, S., and McFaul, P. A. (1972). Injuries: Abiotic lesions. In *System of Ophthalmology*. **vol. XIV (part 2),** Pp. 912-932, Henry Kimpton: London, U.K.

Elliott, M. (1993). The contribution of the crystalline lens to residual astigmatism. MSc thesis. University of Waterloo, Waterloo, Canada.

El-Sayed, G. N., and Cenedella, R. J. (1987). Relationship of cholesterologenesis to DNA synthesis and proliferation by lens epithelial cells in culture. *Exp. Eye Res.* **45,** 443-451.

Finney D. J. (1971). Probit analysis. Cambridge University Press: Cambridge, UK.

Foster, A. (1999). Cataract – a global perspective: output, outcome and outlay. *Eye*. **13,** 449-453.

Frederick, J. E. and Lubin, D. (1988). Possible long-term changes in biologically active ultraviolet radiation reaching the ground. *Photochem. Photobiol.* **47,** 571-578.

Frederick, J. E., Snell, H. E., and Haywood, E. K. (1989). Solar ultraviolet radiation at the Earth's surface. *Photochem. Photobiol.* **50,** 443-450.

Frederick, J. E. and Alberts, A. D. (1992). The natural UVA radiation in environment. In *Biological responses to Ultraviolet-A radiation* (Urbach, F. Ed.). Valdenmar Publishing: Overland Park, KS, U.S.A.

Fröhlich, C. and Brusa, R. W. (1981). Solar radiation and its variation in time. *Solar Physics* **74**, 209-215.

Geeraets, W. J., Williams, R. C., Ghosh, M., Ham, W. T. Jr., Guerry, D. III., Schmidt, F. and Ruffin, R. (1963). Light reflectance from the ocular fundus: A means of estimating susceptibility to retinal burns. *Arch. Ophthalmol.* **69**, 612-617.

Giblin, F. J. (1998). In vivo models for nuclear cataract: hyperbaric oxygen, UVA light, and GSHPx knockout mouse. *Exp. Eye Res.* **67 (Suppl. 1)**, S. 32.

Gibson, J. A., Rosenthal, A. R. and Lavery, J. (1985). A study of the prevalence of eye disease in the elderly in an English community. *Tran. Ophthalmol. Soc. UK.* **104**, 196-203.

Gille, J. C., Smythe, C. M. and Heath, D. F. (1984). Observed ozone response to variations in solar ultraviolet radiation. *Science.* **225**, 315-317.

Girao, H., Mota, C., and Pereira, P. (1999). Cholesterol may act as an antioxidant in lens membranes. *Curr. Eye Res.* **18**, 448-454.

Goegan, P., Johnson, G., and Vincent, R. (1995). Effects of serum protein and colloid on the Alamar blue assay in cell cultures. *Toxicology in Vitro.* **9**, 257-266.

Green, A. E. S., Sawada, T., and Shettle, E. P. (1974). The middle ultraviolet reaching the ground. *Photochem. Photobiol.* **19**, 251-259.

Grover, D. and Zigman, S. (1972). Coloration of human lenses by near-ultraviolet photo-oxidized tryptophan. *Exp. Eye Res.* **13**, 70-76.

Hanthamrongwit, M., Reid, W. H., Coutney, J. M. and Grant, M. H. (1994). 5-Carboxyfluorescein diacetate as a probe for measuring the growth of keratinocytes. *Hum. Exp. Toxicol.* **13**, 423-427.

Harding, C. V., Reddan, J. R., Unakar, N. J., and Bagchi, M. (1971). The control of cell division in the ocular lens. *Int. Rev. Cyto.* **31**, 215-300.

Harding, J. (1991). Cataract: Biochemistry, Epidemiology, and Pharmacology. Chapman & Hall: London, UK.

Harding, J. J. (1992). Physiology, biochemistry, pathogenesis, and epidemiology of cataract. *Curr. Opin. Ophthalmol.* **3**, 3-12.

Harding, J. J. (1997). *Biochemistry of the eye.* Pp.94-134. Chapman and Hall: London, U.K.

Harding, J. J. (1999). Can cataract be prevented?. *Eye.* **13**, 454-456.

Haugland, R. P. (1996). Handbook of fluorescent probes and research chemicals. Molecular Probes Inc., Eugene, Oregon, U.S.A.

Hess, C. (1907). Versuche über die Einwirkung ultravioletten Lichtes auf die Linse. *Arch. f. Augenheilk.* **57**, 185-196.

Hietanem, M. (1991). Ocular exposure to solar ultraviolet and visible radiation at high altitudes. *Scan. J. Work Health.* **17**, 398-403.

Hightower K. R., McCready J. (1992a). Mechanisms involved in cataract development following near-ultraviolet radiation of cultured lenses. *Cur. Eye Res.* **11**, 679-689.

Hightower, K. R., McCready, J. (1992b). Physiological effects of UVB irradiation on cultured rabbit lens. *Invest. Ophthalmol. Vis. Sci.* **33**, 1783-1787.

Hightower, K. R., Reddan, J. R., McCready, J. P. and Dziedzic, D. C. (1994a). Lens epithelium: a primary target of UVB irradiation. *Exp. Eye Res.* **59**, 557-564.

Hightower, K. R., McCready, J. P. and Borchman, D. (1994b). Membrane damage in UV-irradiated lenses. *Photochem. Photobiol.* **59**, 485-490.

Hightower, K. R., McCready, J. (1997). The role of calcium in UVB-induced damage in irradiated ocular lens. *Photochem Photobiol.* **65,** 155-160.

Hiller, R., Sperduto, R. D. and Ederer F. (1983). Epidemiologic associations with cataracts in the 1971-1972 National Health and Nutritional Examination Survey. *Am. J. Epidemiol.* **118,** 239-249.

Hogan, M. J., Alvarado, J. A., and Weddell, J. E. (1971). Histology of the human eye, an atlas and textbook. W.B. Saunders & Co: Philadelphia, U.S.A.

Hoyer, H. E. (1982). Scanning electron-microscopic study of lens fibres of the pig. *Cell Tissue.* **224,** 225-232.

Jacob, T. J. C. (1999). The relationship between cataract, cell swelling and volume regulation. *Prog. Ret. Eye Res.* **18,** 223-233.

Jose, J. G. (1982). DNA repair synthesis in lens epithelial cells by 300 nm radiation. *Invest. Ophthalmol.* **22 (Suppl.),** 198.

Jose, J. G. (1986). Posterior cataracts induction by UVB radiation in albino mice. *Exp. Eye Res.* **42,** 11-20.

Jose, J. G. and Yielding, K. L. (1977). "Unscheduled" DNA synthesis in lens epithelium following ultraviolet irradiation.. *Exp. Eye Res.* **24,** 113-119.

Jose, J. G. and Pitts, D. G. (1985). Wavelength dependence of cataracts in albino mice following chronic exposure. *Exp. Eye Res.* **41,** 545-563.

Kahn, H. A., Leibowitz, H. A., Ganley, J. P., Kini, M. M., Colton, T., Nickerson, R. S. and Dawber, T. R. (1977a). The Framigham eye study I. Outline and major prevalence findings. *Am. J. Epidemiol.* **106,** 17-32.

Kahn, H. A., Leibowitz, H. A., Ganley, J. P., Kini, M. M., Colton, T., Nickerson, R. S. and Dawber, T. R. (1977b). The Framigham eye study II. Association of ophthalmic pathology with single variables previously measured in the Framigham heart study. *Am. J. Epidemiol.* **106,** 33-41.

Karim, A. K. A., Jacob, T. J. C. and Thompson, G. A. (1989). The human lens epithelium; morphological and ultrastructural changes associated with steroid therapy. *Exp. Eye Res.* **48,** 215-224.

Kerr, J. B. and McElroy, C. T. (1993). Evidence for large upward trends of UVB radiation linked to ozone depletion. *Science.* **262**, 1032-1034.

Kerr, J. B. (1997). Observed dependences of atmospheric UV radiation and trends. In *Solar ultraviolet radiation modelling, measurements and effects. NATO ASI series* (Zerefos, C. S. and Bais, A.F. eds). **I 52**, 259-265.

Kinoshita, J. H. and Masurat, T. (1957). Studies of glutathione in bovine lens. *Arch. Ophthalmol.* **57,** 266-274.

Kinsey, V. E. (1948). Spectral transmission of the eye to ultraviolet radiation. *Arch. Ophthalmol.* **39**, 508-513.

Kise, K., Kosaka, H., Nakabayashi, M., Kishida, K., Shiga, T. and Tano, Y. (1994). Reactive oxygen species involved in phenazine-methosulfate-induced rat lens opacification. An experimental model of cataract. *Ophthalmic Res.* **26,** 41-50.

Kuszak, J. R., Sivak, J. G., and Weerheim, J. A. (1991). Lens optical quality is a direct function of lens sutural architecture. *Invest. Ophthalmol. Vis. Sci.* **32,** 2119-2129.

Larson, E. M., Doughman, D. J., Gregerson, D. S., and Obritsch, W. F. (1997). A new, simple, non-radioactive, nontoxic in vitro assay to monitor corneal endothelial cell viability. *Invest. Ophthalmol. Vis. Sci.* **38,** 1929-1933.

Lembares, A., Hu, X-H. and Kalmus G. W. (1997). Absorption spectra of corneas in the far ultraviolet region. *Invest. Ophthalmol. Vis. Sci.* **38,** 1283-1287.

Lerman, S., Kuck, J. F. Jr., Borkman, R. F., and Saker, E. (1976). Induction, acceleration and prevention (in vitro) of an aging parameter in the ocular lens. *Ophthalmic Res.* **8,** 213-226.

Lerman, S. and Borkman, R. F. (1978). Photochemistry and lens aging. *Interdisciplinary Topics in Gerontology.* **13,** 154-182.

Liang, J. N. (1991). Photooxidation of the nonenzymatic browning products in calf lens α-crystallin. *Ophthalmic Res.* **23,** 259-264.

Linetsky, M. and Orthwerth, B. J. (1995). The generation of hydrogen peroxide by the UVA irradiation of human lens proteins. *Photochem. Photobiol.* **62,** 87-93.

Livingston, P. M., Guest, C. S. Stanislavsky, Y., Lee, S., Bayley, S., Walker, C., McKean, C. and Taylor, H. R. (1994). A population based estimate of cataract prevalence: The Melbourne Visual Impairment Project Experience. *In Cataract pathogenesis: results of epidemiological studies and experimental models* (O. Hockwin and K. Sasaki Eds). *Dev. Ophthalmol.* Kager: Basel. **26,** 1-6.

Maisel, H. (1985). The ocular lens - structure, function, and pathology. Marcel Dekker Inc.: New York, U.S.A.

Malakoff, D. (1999). Animal research: Groups sue to tighten oversight of rodents. *Science.* **283 (5403),** 767-769.

Mann, I. (1969). The development of the human eye. Pp. 46-67. Grune and Stratton: New York. U.S.A.

Martin, E. K. (1912). The effects of ultraviolet rays upon the eye. *Proc. Roy. Soc. Ser B. Biological Sciences.* **85,** 319-334.

Mayman, C. I., Miller, D. and Tijerina, M. L. (1979). In vitro production of steroid cataract in bovine lens. II: Measurement of sodium-potassium adenosine triphosphatase activity. *Acta Ophthalmol.* **57,** 1107-1116.

McKenzie, R., Connor, B. and Bodeker, G. (1999). Increased summertime UV radiation in New Zealand in response to ozone loss. *Science.* **285 (5434),** 1709-1711.

Mecherikunnel, A. T., Gatlin, J. A. and Richmond, J. C. (1983). Data on total and spectral solar irradiance. *Applied Optics.* **22,** 1354-1359.

Meister, A. (1992). On the antioxidant effects of ascorbic acid and glutathione. *Biochem. Pharmacol.* **44,** 1905-1915.

Miller, D., Mayman, C. I. and Tijerina, M. L. (1979). In vitro production of steroid cataract in bovine lens. I: Measurement of optical changes. *Acta Ophthalmol.* **57,** 1101-1106.

Mitchell B. D. and Lepowski J. M. (1986). The epidemiology of cataract in Nepal. *Hum. Biol.* **58,** 975-990.

Molina, M. J. and Rowland, F. S. (1974). Stratospheric sink for chlorofluoromethanes: chlorine atom-catalyzed destruction of ozone. *Nature.* **249,** 810-812.

Montreal Protocol on Substances that Deplete the Ozone Layer. (1987). United Nations Environment Program (UNEP), No. 87-6106. Final Act 1987. Environment Protection Agency, Washington, D. C., U.S.A

Moses, R. A. (1981). *In Adler's physiology of the eye. Clinical application.* Pp. 38. The C.V. Mosby Company: St. Louis. Missouri, U.S.A.

Motluk, C. and Cullen, A. P. (1994). The quest for a non-cytotoxic, non-phototoxic solvent for in vitro studies of crystalline lens phototoxicity. School of Optometry, University of Waterloo. 1994. (unpublished).

Newell, F. W. (1992). *In Ophthalmology: principles and concepts.* pp. 23-31. Mosby-Year Book: St. Louis, U.S.A.

O'Connor, S., McNamara, L., Swerdin, M. and Van Buskirk, R. G. (1991). Multifluorescent assays reveal mechanisms underlying cytotoxicity – phase I CFTA compounds. *In Vitro Toxicology.* **4,** 197-206.

Oriowo, O. M. (1996). Risk factors for retinal phototoxicity in aphakic and pseudophakic patients: a review and case report. *The South African Optometrist.* **55,** 41-47.

Oriowo, O. M., Chou, B. R. and Cullen, A. P. (1997). Glassblowers' ocular health and safety: optical radiation hazards and eye protection assessment. *Ophthal. Physiol. Opt.* **17,** 216-224.

Pagé, B., Pagé, M. and Noel, C. (1993). A new fluorometric assay for cytotoxicity measurements in vitro. *Int. J. Oncol.* **3,** 473-476.

Parrish, J. A., Anderson, R. R., Urbach, F. and Pitts, D. G. (1978). UV-A: biological effects of ultraviolet radiation with emphasis on human responses to longwave ultraviolet. Plenum Press: NY, U.S.A.

Paterson, C. A. and Delamere, N. A. (1992). The Lens. In *Adler's Physiology of the Eye: Clinical Application* (W. M. Hart Ed.), pp. 348-390. Mosby-Year Book: St. Louis, Missouri, U.S.A.

Pathak, M. A. (1986). Immediate and delayed pigmentary and other cutaneous responses to solar UVA radiation (320-400 nm). In *The biological effects of UVA radiation* (F. Urbach and R.W. Gange Eds). pp. 156-167. Praeger: New York, U.S.A.

Pearson, A. A. and Weleber, R.G. (1972). The development of the eye. University of Oregon Health Sciences Center. Portland, Oregon, U.S.A.

Piatigorsky, J. (1981). Lens differentiation in vertebrates. A review of cellular and molecular features. *Differentiation.* **19,** 134-153.

Pirie, A. (1971). Formation of N-formylkynurenine in proteins from lens and other sources by exposure to sunlight. *Biochem. J.* **125,** 203-208.

Pitts, D. G. (1978). The ocular effects of ultraviolet radiation. *Am. J. Optom. Physiol. Opt.* **55,**19-35.

Pitts, D. G. (1988). Should ocular exposure to solar UVR be a concern? In *Vision Science Symposium. A tribute to Gordon G. Heath.* Pp. 145-162. Indiana University, U.S.A.

Pitts, D. G. (1990). Sunlight as an ultraviolet source. *Optom. Vis. Sci.* **67,** 401-406.

Pitts, D. G. (1993). The ocular effects of ultraviolet radiation. In *Environmental Vision: interaction of the eye, vision and the environment* (D.G. Pitts and R. N. Kleinstein Eds). Pp. 151-220. Butterworth-Heinemann: Boston, U.S.A.

Pitts, D. G., and Cullen, A.P., Hacker, P.D. and Parr, W.H. (1977a). Ocular ultraviolet effects from 295 to 400 nm in the rabbit eye. US Dept of Health, Education and Welfare. NIOSH Publication No. 77-175. Cincinnati, OH, USA.

Pitts, D. G., and Cullen, A.P. and Hacker, P.D. (1977b). Ocular effects of ultraviolet radiation from 295 to 365 nm. *Invest. Ophthalmol. Vis. Sci.* **16,** 932- 939.

Pitts, D.G., Cullen, A.P. and Hacker, P.D. (1977c). Ocular effects of near ultraviolet radiation: Literature review. *Am. J. Optom. Physiol. Opt.* **54,** 542-549.

Prevent Blindness America (1996). The National Society to Prevent Blindness. Schamburg, Illinois, U.S.A.

Rafferty, N. S., Rafferty, K. A. and Zigman, S. (1997). Comparative response to UV irradiation of cytoskeletal elements in rabbit and skate lens epithelial cells. *Curr. Eye Res.* **16,** 310-319.

Reddy, V. N. (1971). Metabolism of glutathione in the lens. *Exp. Eye Res.* **11,** 310-328.

Reddy, V. N., Giblin, F. J. and Matsuda, H. (1980). In *Red blood cell and lens metabolism* (S.K. Srivastava Ed). pp 139. Elsevier-North Holland: New York, U.S.A.

Reddy, V. N., and Giblin, F. J. (1984). Metabolism and function of glutathione in the lens. *Ciba Foundation Symposium.* **106,** 65-87. Pitman: London. U.K.

Ritter (1801) cited by **Tousey, R.** (1961). Solar spectroscopy in the far ultraviolet. *J. Opt. Soc Am.* **51,** 384-395.

Roorda, A. and Glasser, A. (1999). In vitro wavefront aberration measurements of isolated crystalline lenses. In *Optical Society of America (ILS-XV: 15th Interdisciplinary Laser Science Conference.* Santa Clara, California, U.S.A.

Rosenthal, F. S., Safran, M. and Taylor, H. R. (1985). The ocular dose of ultraviolet radiation from sunlight exposure. *Photochem. Photobiol.* **42,** 163-171.

Rosenthal, F. S., Phoon, C. and Bakalia, A. E. and Taylor, H. R. (1988). The ocular dose of ultraviolet radiation to outdoor workers. *Invest. Ophthalmol. Vis. Sci.* **29,** 649-656.

Rosner, B. (1990). *Fundamentals of biostatitics.* Duxbury Press: Belmont, CA, U.S.A.

Saar, I., Neumann, E. and Gershon, D. (1989). Effects of gentamycin and chloramphenicol on the transparency of cultured rat lenses. *Ophthalmic Res.* **21,** 118-122.

Sanford, S. E. and Dukes, T. W. (1979). Acquired bilateral cortical cataracts in mature sows. *J. Am. Vet. Med. Assoc.* **173,** 852-853.

Sanford, S. E., Dukes, T. W., Creighton, M. O. and Trevithick, J. R. (1981). Cortical cataracts induced by hygromycin B in swine. *J. Am. Vet. Med. Assoc.* **42,** 1534-1537.

Sarkar, C. P. and Cenedella, R. J. (1982). Gangliosides in normal and cataractous lenses of several species. *Biochim. Biophys. Acta.* **711,** 503-508.

Schirmer, K., Chan, G. J., Greenberg, B. M., Dixon, D. G. and Bols, N. C. (1997). Methodology for demonstrating and measuring the phototoxicity of fluoranthene to fish cells in culture. *Toxicology in Vitro.* **11,** 107-119.

Schirmer, K., Chan, G. J., Greenberg, B. M., Dixon, D. G. and Bols, N. C. (1998). Ability of 16 priority PAHs to be photocytotoxic to a cell line from the rainbow trout gill. *Toxicology.* **127,** 143-155.

Schein, O.D., West, S., Munoz, B., Vitale, S., Maguire, M., Taylor, H. R. and Bressler, N. M. (1994). Cortical lenticular opacification: distribution and location in longitudinal study. *Invest. Ophthalmol. Vis. Sci.* **35,** 363-366.

Scotto, J., Fears, T. R. and Gori, G. B. (1976). Ultraviolet exposure patterns. *Env. Res.* **12,** 228-237.

Seidman-Ripley, J. and Huang, J. (1993). Monograph series on aging-related diseases: I. Cataract (senile). *Chronic Diseases in Canada.* **14(1),** 4-15.

Sen, P. C. and Pfeiffer, D. R. (1982). Characterization of partially purified (N^+ +K^+)-ATPase from porcine lens. *Biochimica et Biophysica Acta.* **693,** 34-44.

Sivak, J. G. and Kreuzer, R. O. (1983). Spherical aberration of the crystalline lens. *Vision Res.* **23,** 59-70.

Sivak, J. G., Gershon, D., Dovrat, A. and Weerheim, J. (1986). Computer assisted scanning laser monitor of optical quality of the excised crystalline lens. *Vision Res.* **26,** 1873-1879.

Sivak, J. G., Yoshimura, M., Weerheim, J. and Dovrat, A. (1990). Effect hydrogen peroxide, DL-Propranolol, and prednisolone on bovine lens optical function in culture. *Invest. Ophthalmol. Vis. Sci.* **31,** 954-963.

Sivak, J. G., Herbert, K. L. and Segal, L. (1994). Ocular organ culture as a measure of ocular irritancy: the effect of surfactants. *Toxicology Methods.* **4,** 56-65.

Sliney, D. H. (1986). Physical factors in cataractogenesis: Ambient ultraviolet radiation and temperature. *Invest. Ophthalmol. Vis. Sci.* **27,** 781-789.

Söderberg, P. G. (1990). Experimental cataract induced by ultraviolet radiation. *Acta Ophthalmol.* 68 (Suppl 196).

Spector, A. (1984). Oxidation and cataract. In *Human cataract formation. CIBA Foundation Symposium.* **106,** 48-64. Pitman: London. U.K.

Steele, A. (1990). Cataract surgery (Editorial). *B. J. Ophthalmol.* **74,** 130.

Stevens, M. A. and Bergmanson, J. P. G. (1989). Does sunlight cause premature aging of the crystalline lens? *J. Am. Optom. Assoc.* **60,** 660-663.

Stewart-DeHaan, P. J., Dzialoszynski, T. and Trevithick, J. R. (1999). Modelling cortical cataractogenesis XXIV: uptake by the lens of glutathione injected into the rat. *Molecular Vision.* **5,** 37.

Stuart, D. D., Sivak, J. G., Cullen, A. P., Weerheim, J. A. and Monteith, C. A. (1991). UV-B radiation and the optical properties of cultured bovine lenses. *Curr. Eye. Res.* **10,** 177-184.

Stuart, D. D. and Doughty, M. J. (1996). In vitro UVB irradiation of the bovine crystalline lens causes cell damage and reduction in leucine aminopeptidase activity in lens epithelium. *J. Photochem. Photobiol. (Biology).* **32,** 81-87.

Taylor, H. R. (1995). Ocular effects of UVB exposure. *Doc. Ophthalmol.* **88,** 285-293.

Taylor, A., Brown, M. J., Daims, M. A., Cohen, J. (1983). Localization of leucine aminopeptidase in normal hog lens by immunofluorescence and activity assays. *Invest. Ophthalmol. Vis. Sci.* **24,** 1172-1180.

Taylor, H. R., West, S. K., Rosenthal, F. S., Muñoz, B., Newland, H. S., Abbey, H. and Emmett E. A. (1988). Effect of ultraviolet radiation on cataract formation. *N. Engl. J. Med.* **319,** 1429-1433.

The Italian-American Cataract Study Group. (1991). Risk factors for age-related cortical, nuclear and posterior subcapsular cataracts. *Am. J. Epidemiol.* **133,** 541-553.

Thomas, D. M., Schepler, K. L. (1980). Raman spectra of normal and ultraviolet-induced cataractous rabbit lens. *Invest.Ophthalmol. Vis. Sci.* **19,** 904-912.

Thomas, D. M., Papadopoulou, O., Mahendroo, P. R. and Zigman, S. (1991). Phosphorous-31 NMR study of the effects of UV on squirrel lenses. *Invest. Ophthalmol. Vis. Sci.* **32 (Suppl.),** 748.

Thylefors, B. (1995). The role of international ophthalmology in blindness prevention. Editorial. *Am. J. Ophthalmol.* **119,** 229-230.

Thylefors, B. (1998). A global initiative for the elimination of avoidable blindness. *Community Eye Health (Intl. Centre for Eye Health) Journal.* **11 (25).**

Torriglia, A. and Zigman, S. (1988). The effect of near-UV light on Na-K-ATPase of the rat lens. Curr. Eye Res. **7,** 539-542.

Trevithick, J. R., Chaudun, E., Muel, A. S., Courtois, Y. and Counis, M. F. (1987). Effect of X-irradiation and vitamin C on DNA degradation and endogenous DNase in embryonic chick lens cells. *Curr. Eye Res.* **6,** 1275-1281.

Urban, R. C. and Cotlier, E. (1986). Corticosteroid-induced cataracts. *Surv. Ophthalmol.* **31,** 102-110.

Van Heyningen, R. (1971). Fluorescent derivatives of 3-hydroxykynurenine in the lens of man, baboons, and the grey squirrel. *Biochem. J.* **123,** 30-31.

Van Heyningen, R. (1972). The human lens, part 1: a comparison of cataracts extracted in Oxford (England) and Shikarpur (W. Pakistan). *Exp. Eye Res.* **13,** 136-147.

Van Horn, D. L. Hanna, C. Schultz, R. O. (1970). Corneal cryo-preservation: ultrastructural and viability changes. *Arch. Ophthalmol.* **84,** 655-667.

Verhoeff, F. H., Bell, L. and Walker, C. B. (1916). The pathological effects of radiant energy on the eye: An experimental investigation with a systematic review of the literature. *Proc. Am. Acad. Arts Sci.* **51,** 630-818.

Vérétout, F., Delaye, M., and Tardieu, A. (1989). Molecular basis of eye lens transparency. Osmotic pressure and X-ray analysis of α-crystallin solutions. *J. Mol. Biol.* **205,** 713-728.

Vestre, W. A. (1984). Porcine ophthalmology. *Veterinary Clinic North American (Large animal practice).* **6 (3),** 667-676.

Wang G- M, Raghavachari, N. and Lou, M. F. (1997). Relationship of protein-glutathione mixed disulfide and thiotransferase in H_2O_2-induced cataract in cultured pig lens. *Exp. Eye Res.* **64,** 693-700.

Wanko, T., and Gavin, M. A. (1958). The fine structure of the lens epithelium. *Arch. Ophthalmol.* **60,** 868-879.

Wardle, D. I., Kerr, J. B., McElroy, C. T. and Francis, D. R. (1997). Ozone science: a Canadian perspective on the changing ozone layer. Montreal Protocol 1987-1997. Environment Canada. University of Toronto Press: Toronto, Canada.

Wheater, P. R., Burkitt, H.G. and Daniels, V.G. (1993). Functional histology: a text and colour atlas. pp. 20-385. Churchill Livingstone: New York, U.S.A.

Weerheim, J. A. and Sivak, J. G. (1992). Scanning laser measure of optical quality of the cultured crystalline lens. *Ophthal. Physiol. Opt.* **12,** 72-79.

Weinreb, O. and Dovrat, A. (1996). Transglutaminase involvement in UV-A damage to the eye lens. *Exp. Eye Res.* **63,** 591-597.

Weiss , L. (1988). Cell and tissue biology – A textbook of histology. pp.1-92. Urban and Schwarzenberg Inc.: Baltimore, U.S.A.

West, S. K. and Valmadrid, C. T. (1995). Epidemiology of risk factors for age related cataract. *Surv. Ophthalmol.* **39,** 323-334.

West, S. K., Duncan, D. D., Muñoz, B, Rubin, G. S., Fried, L. P., Bandeen-Roche, K. and Schein, O. D. (1998). Sunlight exposure and risk of lens opacities in a population-based study. The Salisbury Eye Evaluation Project. *J.A.M.A.* **280,** 714-718.

Widmark, J. (1889). Üeber den Einfluss des Lichtes auf die vorderen Medien des Auges. *Skand. Arch. F. Physiol.* **1,** 265-330.

Widmark, J. (1892). Üeber die Durchdringlichkeit der Augenmedien für ultraviolette strahlen. *Skand. Arch. F. Physiol.* **3,** 14-46.

Widmark, J. (1893). Üeber Blendung des Netzhaut. *Scand. Arch. F. Physiol.* **4,** 281-295.

Widmark, J. (1901). Üeber den Einfluss des Lichtes auf die Linse. *Mitteil. Aus d. Augenklin. d. Carol. Med.-chir., Inst. Zu Stockholm.* **3,** 135.

Worgul, J. C., Merrian, G. R. and Medvedovsky, C. (1989). Cortical cataract development: An expression of primary damage to the lens epithelium. *Lens Eye Tox. Res.* **6,** 559-571.

Wu, K. -Y., Wang, H. -Z. and Hong, S. -J. (1998). Calcium-induced changes on crystallins in organ cultured porcine lens. *Kao Hsiung I Ko Hsueh Tsa Chih (Kaohsiung J. Med. Sci.).* **14,** 569-576.

Yap, M. and Wong, E. (1992). The chinese eye in perspective. Part I. Causes of blindness in chinese. *J. Intern. Fed. of Asian and Pacific Associations of Optometrists.* **(December 92),** pp.6. Vision Asian – Pacific.

Young, R. W. (1991). Age related cataract. Oxford University Press: New York, U.S.A.

Young, R. W. (1993). Optometry and the preservation of visual health. *Optom. Vis. Sci.* **70,** 255-262.

Zelenka, P. S. (1984). Lens lipids. *Curr. Eye Res.* **3,** 1337-1359.

Zerihun, N. (1994). Ophthalmology in Illubabor Region, South Western Ethiopia. *Community Eye Health (Intl. Centre for Eye Health) Journal.* **7(13),** 9-11.

Zigman, S. (1977). Near UV light and cataracts. *Photobiol. Photochem.* **26,** 437-441.

Zigman, S. (1981). Photochemical mechanisms in cataract formation. In *Mechanisms of Cataract Formation in the Human Lens* (G. Duncan Ed). pp. 117-149. Academic Press: London, U.K.

Zigman, S. (1983). The role of sunlight in human cataract formation. *Surv. Ophthalmol.* **27,** 317-326.

Zigman, S. (1985). Photobiology of the lens. In *The ocular lens: structure, function and pathology* (H. Maisel Ed). pp. 301-347. Marcel Dekker, Inc: New York, U.S.A.

Zigman, S. (1986). Recent research on near-UV radiation and the eye. In *The biological effect of UVA radiation.* (F. Urbarch and R. W. Gange Eds). Pp. 252-262. Praeger: New York, U.S.A.

Zigman, S. (1993). Ocular light damage – annual review. *Photobiol. Photochem.* **57,** 1060-1068.

Zigman, S. (1995). Environmental near UV radiation and cataracts. *Optom. Vis. Sci.* **72,** 899-901.

Zigman, S., Griess G., Yulo, T. and Schultz, J. (1973). Ocular protein alterations by near UV light. *Exp. Eye Res.* **15,** 255-264.

Zigman, S. and Vaughan, T. (1974). Near-ultraviolet light effects on the lenses and retinas of mice. *Invest. Ophthalmol. Vis. Sci.* **13,** 462-465.

Zigman, S., Groff, J., Yulo, T. and Griess G. (1976). Light extinction and protein in lens. *Exp. Eye Res.* **23,** 555-567.

Zigman, S., Groff, J. and Yulo, T. (1977). Enhancement of non-tryptophan fluorescence of human lens proteins after near-UV light exposure. *Photobiol. Photochem.* **26,** 505-509.

Zigman, S., Datiles, M. and Torczynski, E. (1979). Sunlight and human cataracts. *Invest. Ophthalmol. Vis. Sci.* **18,** 462-467.

Zigman, S., Paxhia, T., McDaniel, T., Lou, M. F. and Yu, N. -T. (1991). Effect of chronic near-ultraviolet radiation on the gray squirrel lens in vivo. *Invest. Ophthalmol. Vis. Sci.* **32,** 1723-1732.

Zigman, S., Paxhia, T., McDaniel, T. and Schultz, J. (1992). New mechanisms for UV-induced cataract. In *Biologic effects of light.* (M. F. Holick and A. M. Kligman Eds), pp. 245-252. de Gruyter & Co: Berlin, NY, U.S.A.

Zubay, G. L. (1988). Biochemistry. pp. 970. Macmillan Publishing Co: New York, NY, USA.